TECHNIQUES TO REDUCE MULTIPLE-ACCESS INTERFERENCE IN MULTI-CARRIER CDMA SYSTEMS

by

S. Sureshkumar

SUBMITTED IN PARTIAL FULFILLMENT OF THE
REQUIREMENTS FOR THE DEGREE OF
DOCTOR OF PHILOSOPHY
AT
THE UNIVERSITY OF MANITOBA
WINNIPEG, MANITOBA
AUGUST, 2005

© Copyright by S. Sureshkumar, 2005

THE UNIVERSITY OF MANITOBA

FACULTY OF GRADUATE STUDIES

*****

COPYRIGHT PERMISSION

Techniques to Reduce Multiple-Access Interference in Multi-Carrier CDMA Systems

BY

S. Sureshkumar

A Thesis/Practicum submitted to the Faculty of Graduate Studies of The University of Manitoba in partial fulfillment of the requirement of the degree

Of

Doctor of Philosophy

S. Sureshkumar © 2005

Permission has been granted to the Library of the University of Manitoba to lend or sell copies of this thesis/practicum, to the National Library of Canada to microfilm this thesis and to lend or sell copies of the film, and to University Microfilms Inc. to publish an abstract of this thesis/practicum.

This reproduction or copy of this thesis has been made available by authority of the copyright owner solely for the purpose of private study and research, and may only be reproduced and copied as permitted by copyright laws or with express written authorization from the copyright owner.

To my mother, Rajes, Dilu and Harshi.

Acknowledgements

I cordially express my sincere gratefulness to Professor Ed Shwedyk, my advisor, for his endless support and guidance throughout my studies. Your technical expertise and moral encouragement have always been a grate source of motivation to me. My express gratitude goes to my co-advisor, Dr. Ha H. Nguyen. It has been a great privilege working with you these past years. I don't know how you manage to balance everything on your plate, but you, nevertheless, always made time for me and supported me in every respect. I would like to thank Professors M. Pawlak, P. Yahampath and N. Popplewell for serving on my dissertation committee and for their valuable comments and suggestions on my research work.

I would like to thank the Canadian People for their funding support and the Natural Science and Engineering Research Council of Canada (NSERC) for administrating the funds. I greatly appreciate the financial support from an NSERC operating grant, the Department of Electrical and Computer Engineering, University of Manitoba, which made my dream come true.

I would like to thank my parents-in-laws, brother-in-law and my friends for their encouragement and their love.

Finally, I would like to express my deepest love and gratitude to my mother, wife and kids for their understanding, support, encouragement and sacrifices. I thank Dilu and Harshi for allowing me to put their lives on hold for many years to complete my degree and always being there for me. Most importantly, I give thanks to Rajes, for her neverending love, great understanding, patience, support and for boosting my morale in hard times throughout this long journey. Without her, this research work and dissertation would have not been possible. To them I dedicate this dissertation.

Abstract

For future high data rate wireless applications, multi-carrier code division multiple access (CDMA) has emerged as the most promising multiple access scheme due to its numerous advantages over single-carrier CDMA (SC-CDMA). However, the performance of multi-carrier CDMA systems similar to the conventional SC-CDMA systems is limited by the multiple access interference (MAI). Therefore, it is important to suppress the MAI in multi-carrier CDMA systems. This dissertation focuses mainly on techniques to reduce the MAI. In literature, two multi-carrier CDMA systems namely MC-CDMA and multi-carrier direct sequence CDMA (MC-DS-CDMA) have been proposed. In this dissertation both schemes are considered.

In the first part of this dissertation, assuming the signature sequences are random sequences, the impact of the carrier spacing and the chip waveforms on the performance of asynchronous MC-DS-CDMA systems is analyzed, for a given system bandwidth. The family of band-limited chip waveforms is considered. The average MAI at the output of the receiver is taken as the performance measurement. The analysis demonstrates that there exists an optimal carrier spacing for a given chip waveform which gives the minimum MAI. Motivated by this observation, a method to jointly design the chip waveform and the carrier spacing to achieve the minimum MAI is presented.

In the second part, an adaptive carrier interferometry scheme is proposed for synchronous MC-CDMA systems. By exploiting the additional degree of freedom in selecting the amplitudes of the subcarriers in accordance with the channel condition, the proposed scheme attains a significant performance gain over the conventional carrier interferometry MC-CDMA systems in which a constant amplitude is set for all the carriers. Two adaptation strategies, namely local adaptation and global adaptation, are proposed for estimating the appropriate subcarrier amplitudes at the receiver in

the proposed systems. A further advantage of the proposed scheme is that it reduces the peak-to-average power ratio (PAPR) problem present in the conventional carrier interferometry MC-CDMA systems.

Finally, in the last part of this dissertation, a synchronous MC-DS-CDMA system especially for downlink, called phase offset assisted MC-DS-CDMA is proposed. Two phase offset assignment schemes are introduced: i) the Carrier-Based phase offset, in which a carefully chosen phase offset is introduced in each carrier to minimize the MAI and ii) the User-Based phase offset, in which each user is assigned a different phase offset. However, in contrast to the Carrier-Based phase offset, the same phase offset is used in all the carriers. It is shown both schemes achieve approximately a 50% reduction in MAI level.

Contents

List of Tables

List of Figures

List of Symbols and Abbreviations

$\mathbf{A}$	The carrier amplitude matrix
$\mathbf{a}_k$	The kth user's carrier amplitude vector
$a_{k,m}$	The kth user's mth carrier amplitude
B_T	The system bandwidth
B_c	The subcarrier bandwidth
$\mathbf{b}(i)$	The ith information bit vector
$b_k(i)$	The kth user's ith information bit
$b_{k,m}(i)$	The kth user's mth carrier ith information bit
c	The normalized carrier spacing
$\mathbf{c}_k$	The kth user's signature sequence vector
$c_k(n)$	The kth user's signature sequence
E_b	The energy per bit
$\overline{E}_b$	The average energy per bit
E_c	The energy per chip
F	The bandwidth-bit duration product
f_m	The mth carrier frequency
$G(f)$	The power spectral density of the chip waveform
$\mathbf{H}$	The channel matrix
$\mathbf{H}_k$	The kth user's channel matrix
$h_{k,m}$	The kth user's mth carrier channel gain
$h_{k,m}(t)$	The kth user's complex low-pass mth carrier channel impulse response
$\mathbf{I}$	The identity matrix
$I_{k,m}^{(1)}$, $I_{k,m}^{(2)}$, $I_{k,m}^{(3)}$	The mth carrier interference parameters of the kth user
$\widehat{I}_k$	The average MAI of the kth user

$i_{k,m}^{(1)}(t)$, $i_{k,m}^{(2)}(t)$, $i_{k,m}^{(3)}(t)$	The mth carrier interference signals of the kth user
J	The total average MAI variance
K	The number of users in the system
M	The number of carriers in the system
N	The processing gain of the system
$N_0/2$	The two-sided power spectral density of white noise
$\mathbf{n}$	The noise vector
$n(t)$	The additive white gaussian noise
$\mathbf{P}$	The carrier phase offset matrix
$P(f)$	The fourier transform of the chip waveform $p(t)$
P_k	The kth user's carrier phase offset matrix
$p(t)$	The chip waveform
$\mathbf{R}$	The received correlation matrix
$\mathbf{R}_k$	The interference-plus-noise correlation matrix corresponding to the kth user
$\mathbf{r}$	The received vector
$r(t)$	The received signal
$s_k(t)$	The signature waveform of the kth user
T	The bit duration after serial-to-parallel conversion
T_b	The bit duration
T_c	The chip duration of multi-carrier CDMA systems
T_d	The maximum delay spread of the channel
$T_{s,c}$	The chip duration of SC-CDMA systems
$\mathbf{U}$, $\mathbf{V}$, $\widetilde{\mathbf{V}}$	The unitary matrices
$u(t)$	The transmitted signal
$\mathbf{W}$	The weight matrix of the receive filters
$\mathbf{w}_k$	The weight vector of the receive filter/combiner of the kth user
$w_{k,m}$	The mth branch weight of the receiver filter/combiner of the kth user
$X(f)$	The normalized elementary density function
x_i	The coefficient of the polynomial expansion of the elementary density function $X(f)$

$y_k(t)$	The transmitted signal of the kth user
Z_k	The decision statistic of the kth user
$Z_{k,m}$	The output of the mth branch correlater of the kth user
$z_{k,m}(t)$	The kth user's signal at the output of the chip-matched filter on the mth branch
ξ	The total transmitted power
ξ_k	The maximum transmitted power of the kth user
μ	The Lagrange multiplier
$\boldsymbol{\alpha}$	The fading amplitude vector
α_m	The mth carrier fading amplitude
$\alpha_{k,m}$	The kth user's mth carrier fading amplitude
β	The roll-off factor
Δ	The carrier spacing
$\mathbf{\Sigma}$	The matrix of the singular values of the channel matrix $\mathbf{H}$
σ^2	The noise variance
υ_n, ε_n	The nth eigenvalues
λ	The mean value of the Rayleigh random variable
φ_m	The overall phase shift of the mth carrier signal
$\varphi_{k,m}$	The overall phase shift of the kth user's mth carrier signal
τ_k	The delay of the kth user's signal
θ_k	The kth user's phase offset
$\theta_{k,m}$	The kth user's mth carrier phase offset
$\rho_{k,j}$	The time-phase correlation between the kth and jth user's signature waveforms
$\widetilde{\rho}_{k,j}$	The time correlation between the kth and jth user's spreading sequences
$\chi_l(\beta, c, X(f))$	The inter-carrier interferences from the same user
$\kappa_l(\beta, c, X(f))$	The inter-carrier interferences from the other users
$\gamma(\beta, c, X(f))$	The average interference parameter/average MAI
ACI-MC-CDMA	Adaptive carrier interferometry multi-carrier code division multiple access
AWGN	Additive white Gaussian noise

BER	Bit error rate
CDMA	Code division multiple access
CF	Crest factor
CI	Carrier interferometry
CI-MC-CDMA	Carrier interferometry multi-carrier code division multiple access
DS-CDMA	Direct sequence code division multiple access
FDMA	Frequency division multiple access
MAI	Multiple access interference
MC-CDMA	Multi-carrier code division multiple access
MC-DS-CDMA	Multi-carrier direct sequence code division multiple access
MMSE	Minimum mean-square error
MSE	Mean-square error
PAPR	Peak-to-average power ratio
PSD	Power spectral density
RMS	Root-mean-square
SC-CDMA	Single-carrier code division multiple access
SINR	Signal-to-interference-plus-noise ratio
SNR	Signal-to-noise ratio
TDMA	Time division multiple access
TMSE	Total mean squared error
TSC	Total squared correlation
TSINR	Total signal-to-interference-plus-noise ratio

Chapter 1

Introduction and Organization of the Dissertation

Multiple access schemes enable a large number of users to share a common transmission medium to transmit information to a receiver at the same time. As an example, in a mobile cellular communication system, multiple users are allowed to access the same frequency spectrum at the same time by means of a multiple access scheme. Frequency spectrum is a scarce resource and one cannot afford to have only a single user to use this resource exclusively at a given time. In this example, the frequency spectrum (i.e. some range of frequencies allocated by the service provider) is the common medium and the users are the cellular telephone customers. In general, there are three different types of multiple access schemes, time division multiple access (TDMA), frequency division multiple access (FDMA) and code division multiple access (CDMA).

The FDMA system divides the available frequency bands into disjoint subbands and each subband is allocated to carry simultaneously a specific user's information in time. In TDMA systems, the entire available frequency bandwidth is used by a user for a short period of time. A symbol time duration is divided into time slots, and these slots are periodically allocated to the same user. Both schemes do not allow users to share the same frequency band or the time slot at the same time. This tends to be inefficient because a certain percentage of available slots, assigned to a user may not carry information, which limits the number of simultaneous users in the channel. Although it limits the number of users in the system, both access systems have the

attractive feature is that there is no interference between the users.

In CDMA systems, all users share the same frequency and can transmit at the same time. The users are distinguishable from each other by means of a user-specific spreading sequence. The sequences used should have low cross-correlations in order to keep the multiple access interference (MAI) from the other active users within the system low. The most popular implementation of CDMA is called direct sequence (DS) CDMA (DS-CDMA). In a DS-CDMA system, each user is assigned a spreading sequence, which is multiplied by a chip waveform with duration of T_c, to form the user's signature waveform. Then each user sends his/her data stream by modulating his/her own signature waveform with a single carrier frequency as in a single-user communication system.

DS-CDMA has been used in second generation (2G) wireless communication systems like IS-95 and also in 3G wireless communication systems known as IMT-2000 due to it's capability to support capacity increase, provision of security and interference rejection [1], [2]. However, to satisfy the increasing demand for high data rate transmissions and multimedia services in future mobile communications (4G), a larger spreading bandwidth is required for DS-CDMA. From a practical point of view, the need of wider bandwidth requires a contiguous frequency spectrum, which can be difficult to obtain, in some cases. To cope up with these demands, recently, multi-carrier CDMA has been chosen for radio transmission technology of IMT-2000 in the proposal of cdma2000 [3].

The multi-carrier CDMA system comprises of M subcarriers, such that the overall system bandwidth (B_T) is identical to that of the single-carrier CDMA (SC-CDMA), as depicted in Fig. 1.1. In other words, the entire system bandwidth is divided into M equal width frequency bands, and thus each subcarrier is modulated by a spreading sequence which yields a narrowband[1] DS-CDMA waveform. The user utilizes all the subcarrier frequencies simultaneously.

A result of the entire bandwidth being divided equally among the subcarriers is

[1]One uses the term narrowband to refer to a spreading bandwidth of a subchannel that is (much) less than the bandwidth of a conventional single carrier DS-CDMA.

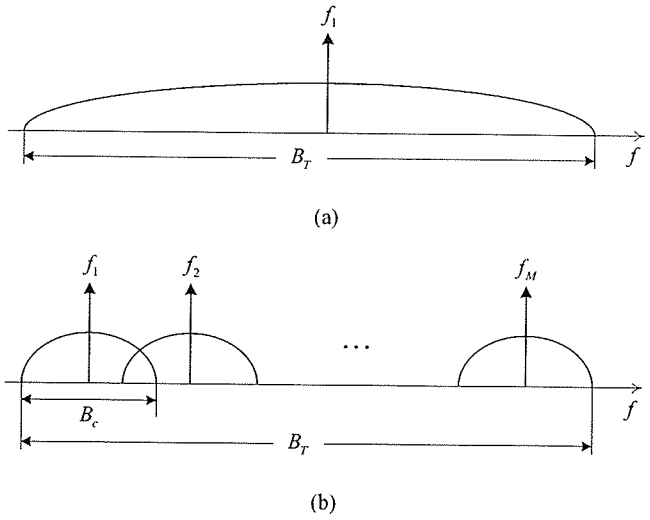

Figure 1.1: Power spectral density (PSD) of (a) single-carrier CDMA and (b) multi-carrier CDMA systems.

that the multi-carrier CDMA system requires a lower chip rate. This allows multi-carrier systems to support high data rate services over hostile, i.e., fading radio channels. In addition, by allowing the subcarriers to overlap, the multi-carrier CDMA system can achieve a higher spectral efficiency (see Fig. 1.1(b)). Moreover, if the bandwidth of a subcarrier is selected to be approximately equal to the coherence bandwidth of the channel (i.e., the multi-carrier chip duration is greater than or equal to the multipath delay spread of the channel), then each subcarrier will tend to fade non-selectively (i.e., flat) [4–10]. Furthermore, a multi-carrier system requires a lower speed, parallel type of signal processing, in contrast to a fast serial type of signal processing in SC-CDMA. Another interesting property of multi-carrier CDMA system is that the modulation and demodulation operation can be easily implemented with the aid of the Fast Fourier Transform (FFT) [4].

The current literature on multi-carrier CDMA may be classified into two general groups, depending upon whether time domain or frequency domain spreading is employed. In the former case, known as MC-DS-CDMA, transmitted symbols are multiplied by low-rate spreading sequences in time, yielding conventional, narrow band DS waveforms. The complete DS-CDMA waveforms are then transmitted at different

carrier frequencies [9–13], such that the net bandwidth allocation is equal to that of a SC-CDMA system using a higher rate spreading sequence. With frequency domain spreading, however, the spreading sequence is serial-to-parallel converted such that each chip modulates a different carrier frequency, and thus, the data symbol is transmitted in parallel [6, 7, 14]. Such systems are commonly referred to as MC-CDMA systems.

Both groups of multi-carrier CDMA systems show a similar capability to mitigate the effect of fading. The time spreading group will, in general, employ a smaller number of carriers relative to the frequency spreading group, and thus, be lower in complexity. This dissertation considers both groups of multi-carrier CDMA systems.

Although the multi-carrier CDMA system has desirable properties, it's system performance, as in the SC-CDMA system, is degraded due to MAI in addition to the background noise. The objective of this dissertation is to develop MAI minimization techniques for multi-carrier CDMA systems. The motivations for this research is given in each individual chapter. In this chapter only a general picture about problems discussed in this dissertation is given. More detailed introductions are presented in the subsequent individual chapters.

1.1 Organization of the Dissertation

This dissertation is organized as follows. Chapter 2 investigates the impact of carrier spacing on MAI performance, in an MC-DS-CDMA system, for a given chip waveform. Similar to [13] this study also concentrates on band-limited chip waveforms as most practical systems are essentially band-limited. Throughout it is assumed that the signature sequences are random signature sequences. This assumption implies, that the MAI level depends only on the carrier spacing and the chip waveform shape. It is shown that there exists an optimal carrier spacing, which gives the minimum MAI, for a given chip waveform. Furthermore, a method to jointly design the chip waveform and the carrier spacing to achieve the minimum MAI is presented. The methodology uses a polynomial to synthesize the elementary density function, which characterizes the band-limited chip waveform. It is shown that using a simple

polynomial representation (only a few terms) for the elementary density functions the proposed chip waveforms and carrier spacings considerably reduce the MAI compared to the existing chip waveforms, particularly the commonly used raised cosine waveform, for large value of roll-off factors.

In chapter 3, an adaptive carrier interferometry scheme is proposed for MC-CDMA systems, where it is assumed that there is a feedback channel between the receiver and the transmitter. By exploiting the additional degree of freedom in selecting the amplitudes of the subcarriers in accordance with the channel condition, the proposed scheme attains a significant performance gain over the conventional carrier interferometry MC-CDMA (CI-MC-CDMA) [15] systems in which a constant amplitude is set for all the carriers. Two adaptation strategies, namely local adaptation and global adaptation, are considered for estimating the appropriate subcarrier amplitudes at the receiver in the proposed systems. Both single-user adaptation, in which the interferers do not adapt, and multiuser adaptation, in which all users adapt are investigated. A further advantage of the proposed scheme is that it reduces the peak-to-average power ratio (PAPR) problem present in conventional CI-MC-CDMA [15] systems.

In Chapter 4, a novel MC-DS-CDMA system especially for downlink is proposed. It is called phase offset assisted MC-DS-CDMA. Introduced are two phase offset assignment schemes. The first is Carrier-Based phase offset, where a carefully chosen phase offset is introduced in each carrier to minimize the MAI. In this scheme, when the total number of users in the system is less than twice the number of carriers, then a different phase offset can be assigned for each user. However, when the total number of users in the system becomes more than twice the number of carriers, the same phase offset needs to be assigned to several users. In contrast, the second is User-Based phase offset, where each user is assigned a different phase offset. However, unlike Carrier-Based phase offset, the same phase offset is used in all the carriers. It is shown that both schemes achieve approximately 50% reduction in MAI level over existing MC-DS-CDMA systems. Furthermore, the tradeoff between both schemes also presented in this chapter.

Finally Chapter 5 draws conclusions and gives suggestions for future study.

Chapter 2

Chip Waveforms and Carrier Spacing for MC-DS-CDMA

The current literature on multi-carrier CDMA can be classified into two general groups, depending upon whether time domain or frequency domain spreading is employed. The system considered in this chapter belongs to the time spreading group, known as MC-DS-CDMA. As mentioned before, the performance of the MC-DS-CDMA systems degrades mainly due to MAI. Accordingly, it is important to identify the system parameters that characterize the MAI in MC-DS-CDMA systems. In general, the following system parameters will affect the MAI in MC-DS-CDMA systems [13]: (i) the number of carriers and the carrier spacing between two adjacent carriers, (ii) the spreading sequences, and (iii) the shape of the chip waveform employed. Here, the question of interest is: for a given channel bandwidth and number of users, how to choose these parameters efficiently, such that the MAI is minimum.

Different carrier spacings have been used for MC-DS-CDMA systems. For systems using time-limited chip waveforms in [16], the distance between the two adjacent carriers equals the bit rate (after serial-to-parallel conversion), whereas it equals the chip rate for the systems considered in [9, 11, 17]. For MC-DS-CDMA systems using a band-limited chip waveform, there is yet another popular choice of carrier spacing such that the spectrum of two adjacent carriers do not overlap [10]. A general carrier spacing for MC-DS-CDMA systems using a time-limited chip waveform (rectangular chip waveform) is also considered in [12, 18, 19], where it is shown that the optimal carrier spacing is very close to the chip rate. Regarding the effect of the number

of carriers on MAI, it was observed that increasing the number of carriers reduces the MAI level but there is a lower limit to this reduction. However, none of the above mentioned studies have studied the effect of carrier spacing on the MAI in MC-DS-CDMA systems with band-limited chip waveforms.

The chip waveform has been noted to be an important system parameter for conventional SC-CDMA systems. The effect of both time-limited and band-limited chip waveforms on MAI level in SC-CDMA has been investigated in [20–22]. In contrast, for most of the MC-DS-CDMA systems found in the literature, either a time-limited rectangular waveform or a band-limited raised cosine waveform is generally employed [9–12, 17–19]. However, recently, the influence of the different band-limited and time-limited chip waveforms on the MAI performance of MC-DS-CDMA was studied in [13] and [23] respectively. In both papers the carrier spacing is assumed to be equal to the chip rate. In [13], it was shown that the commonly used raised cosine chip waveform has the poorest MAI compared to the other band-limited chip waveforms.

Although the search for good signature sequences could improve the performance of MC-DS-CDMA systems [24], random binary signature sequences have been widely used to analyze the MAI in MC-DS-CDMA systems [10–13, 16–19]. Some reasons for using random signature sequences are as follows [25]. First, random signature sequences are often used in an attempt to match certain characteristics of extremely complex signature sequences with a very long period. Second, random signature sequence models may serve as substitutes for deterministic models when there is little or no information about the structure of the signature sequences to be used. Finally, for a system with a large number of users and very long signature sequences, the use of random signature sequences helps to obtain computable closed-form expressions for the system analysis.

To investigate the impact of the carrier spacing on MAI performance, in an asynchronous MC-DS-CDMA systems, for a given chip waveform, is the goal of this chapter. Similar to [13] this study also concentrates on the band-limited chip waveforms since most practical systems are essentially band-limited. The performance criterion

is the *average MAI* at the output of a correlation receiver. Throughout it is assumed that the signature sequences are random signature sequences. This assumption implies, that the MAI level depends only on the carrier spacing and the chip waveform shape. Finally, a method to jointly design the chip waveform and the carrier spacing to achieve the minimum MAI is presented. The methodology uses a polynomial to synthesize the elementary density function, which characterizes the band-limited chip waveform.

This chapter is organized as follows. Section 2.1 describes the model of the MC-DS-CDMA system under consideration. Multiple access interference analysis is carried out in Section 2.2. Section 2.3 investigates the impact of the carrier spacing and the chip waveforms on the MAI performance. A method to jointly design the chip waveform and the carrier spacing to achieve the minimum average MAI is presented in Section 2.4. Finally, Section 2.5 summarizes the chapter.

2.1 System Model

Consider an asynchronous band-limited MC-DS-CDMA system with M subcarriers and K users. The transmitter of the kth user is shown in Fig. 2.1, which is similar to the one described in [13]. At the transmitter, each user's bit stream with bit duration T_b is serial-to-parallel converted into M lower-rate streams. The serial-to-parallel output bit is a lower-rate sequence of duration $T = MT_b$. Let $b_{k,m}(i)$ be the kth user's bit stream, which is transmitted over the mth carrier during the ith bit duration. Each bit stream is spread by a random signature sequence $c_k(n)$ of chip duration T_c. Both $b_{k,m}(i)$ and $c_k(n)$ are modeled as sequences of independent and identically distributed (i.i.d) random variables taking values in $\{-1, +1\}$ with equal probability. Furthermore, for each bit duration T, there are N chips. Thus

$$T = NT_c = MT_b \tag{2.1}$$

and $i = \lfloor n/N \rfloor$.

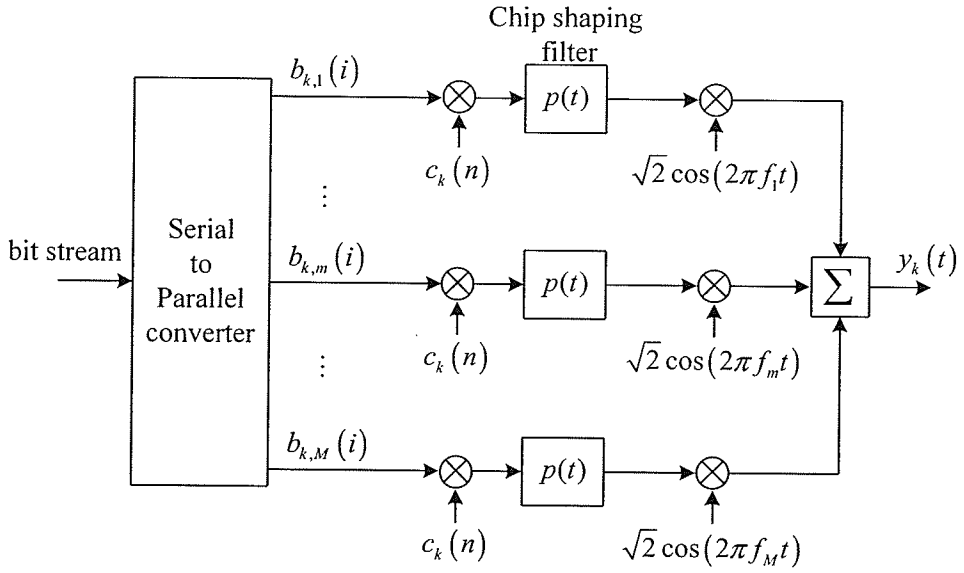

Figure 2.1: The transmitter of the kth user in an MC-DS-CDMA system.

The transmitted signal of the kth user can be expressed as

$$y_k(t) = \sqrt{2E_c} \sum_{n=-\infty}^{\infty} \sum_{m=1}^{M} b_{k,m}(\lfloor n/N \rfloor) c_k(n) p(t - nT_c) \cos(2\pi f_m t) \qquad (2.2)$$

where E_c represents the energy per chip, while f_m represents the carrier frequency of the mth subcarrier. The chip waveform $p(t)$ is band-limited and it is normalized to have unit energy, i.e., $\int_{-\infty}^{\infty} p^2(t)dt = 1$. Let $P(f) = \mathcal{F}\{p(t)\}$, where $\mathcal{F}$ denotes the Fourier transform. It is assumed that $P(f)$ is limited to $[-B_c/2, B_c/2]$ and $G(f) = |P(f)|^2$ satisfies the Nyquist criterion with a roll-off factor β $(0 \leq \beta \leq 1)$. This implies that $B_c = (1+\beta)/T_c$ and the general expression for $G(f)$ corresponding to $p(t)$ is as follows [13]:

$$G(f) = \begin{cases} T_c, & 0 \leq |f| \leq \frac{(1-\beta)}{2T_c} \\ T_c \left[1 - X\left(\frac{-|f|2T_c+1}{\beta}\right)\right], & \frac{(1-\beta)}{2T_c} \leq |f| \leq \frac{1}{2T_c} \\ T_c X\left(\frac{|f|2T_c-1}{\beta}\right), & \frac{1}{2T_c} \leq |f| \leq \frac{(1+\beta)}{2T_c} \\ 0 & \frac{(1+\beta)}{2T_c} \leq |f| \end{cases} \qquad (2.3)$$

where the *normalized elementary density function* $X(f)$ is any continuous function of f defined over $0 \leq f \leq 1$ that satisfies the following conditions: $0 \leq X(f) \leq 1$ for $f \in [0, 1]$; $X(0) = 0.5$ and $X(1) = 0$.

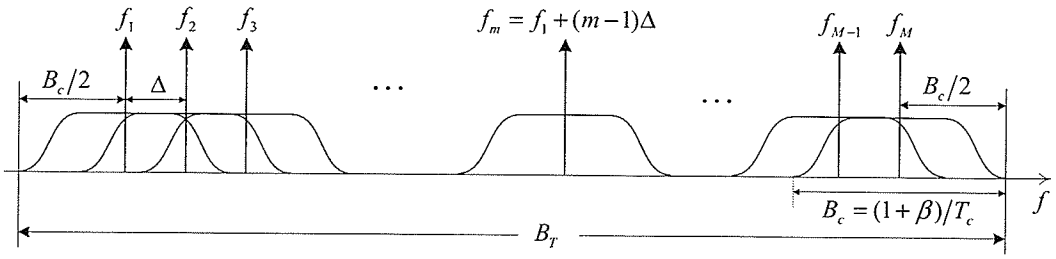

Figure 2.2: The generalized PSD of a band-limited MC-DS-CDMA system.

The generic power spectral density (PSD) of a band-limited MC-DS-CDMA system is shown in Fig. 2.2, where B_T is the total bandwidth of the system and $B_c = (1+\beta)/T_c$ represents the passband bandwidth of each subcarrier. Unlike [13], this chapter considers a variable carrier spacing, $\Delta = cB_c$, between successive carriers, where the *normalized carrier spacing* c is allowed to vary between 0 and 1. Hereafter in this chapter, the *normalized carrier spacing* is referred to as *carrier spacing*. Finally, the subcarrier frequencies in Fig. 2.2 are arranged according to

$$f_m = f_1 + (m-1)\Delta, \quad m = 1, 2, \ldots, M. \tag{2.4}$$

Then, according to Fig. 2.2, the system's total bandwidth, the carrier spacing c and the bandwidth of the subcarriers are related by

$$B_T = [(M-1)c + 1]B_c. \tag{2.5}$$

It follows from (2.1) and (2.5) that the processing gain N of the system can be expressed as

$$N = \frac{MF}{(1+\beta)[c(M-1)+1]} \tag{2.6}$$

where $F = B_T T_b$ is a parameter characterizing the bandwidth-bit duration product of the system. Thus, for given B_T, T_b and M, the processing gain N depends on β and c.

The channel model can either be additive white Gaussian noise (AWGN) or slowly varying frequency-selective Rayleigh fading with maximum delay spread T_d. Let

$T_{s,c}$ be the chip period of the single-carrier system, which is related to the system bandwidth by $T_{s,c} = (1+\beta)/B_T$. Then the number of resolvable paths of the fading channel is [10]

$$L = \left\lfloor \frac{T_d}{T_{s,c}} \right\rfloor + 1 \tag{2.7}$$

It was shown in [10], [17] that if the number of carriers M is chosen to be the same as the number of resolvable paths, i.e., $M = L$, then the subchannels for MC-DS-CDMA systems become frequency nonselective. It follows that the complex low-pass impulse response of the kth user's subchannels can be modeled as

$$h_{k,m}(t) = h_{k,m}\delta(t) = \alpha_{k,m}e^{j\psi_{k,m}}\delta(t), \quad m = 1, 2, \cdots, M \tag{2.8}$$

where $\alpha_{k,m}$ and $\psi_{k,m}$ are the fading amplitude and the phase of the mth subchannel, respectively. The fading amplitudes are generally correlated, but after the information bits are properly interleaved they can be assumed to be i.i.d. Rayleigh random variables with $E\{\alpha_{k,m}^2\} = 1$. Note that if $\alpha_{k,m}$ is set to be a constant one and $\psi_{k,m}$ is set to zero, then (2.8) models an AWGN channel.

The received signal can be written as

$$\begin{aligned} r(t) &= \sqrt{2E_c}\sum_{k=1}^{K}\sum_{m=1}^{M}\sum_{n=-\infty}^{\infty}\alpha_{k,m}b_{k,m}(\lfloor n/N \rfloor)c_k(n) \\ &\quad \cdot p(t - nT_c - \tau_k)\cos(2\pi f_m t + \varphi_{k,m}) + n(t). \end{aligned} \tag{2.9}$$

In (2.9), the propagation delay τ_k and the overall phase shift $\varphi_{k,m}$ are i.i.d uniform random variables over $[0, T]$ and $[0, 2\pi]$ respectively; and $n(t)$ is additive white Gaussian noise with two-sided power spectral density of $N_0/2$.

The receiver for user k employs a bank of M chip matched filters, each detects the bits transmitted on a particular carrier. The received signal is coherently demodulated and low-passed for each subcarrier to obtain the transmitted signal of each subcarrier. Here the low-pass filter is used to remove the double frequency terms. Then the low-pass filter output is passed through a filter matched to the chip waveform. The output of each chip matched filter is sampled every T_c seconds and then correlated with the corresponding spreading sequence to generate the decision statistic. The lth branch of the receiver for user k is illustrated in Fig. 2.3.

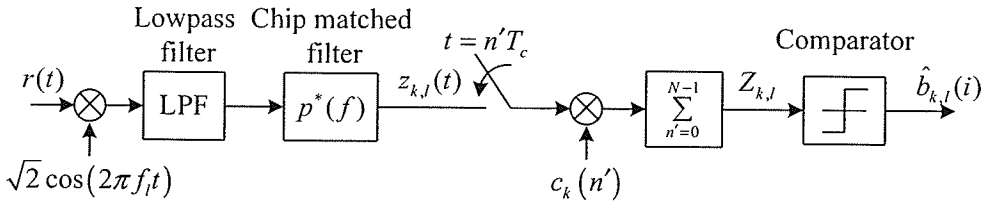

Figure 2.3: The lth branch of the kth user's receiver.

2.2 Interference Analysis

Consider the detection of the bit stream associated with the lth subcarrier of user $k = 1$. It is assumed that the carrier, code and bit are perfectly synchronized. Since only relative delays and phases are important one can set $\tau_1 = 0$ and $\varphi_{1,l} = 0$. The signal at the output of the matched filter, $z_{1,l}(t)$, in Fig. 2.3 can be written as

$$\begin{aligned} z_{1,l}(t) &= \sqrt{E_c}\sum_{k=1}^{K}\sum_{n=-\infty}^{\infty}\sum_{m=1}^{M}\alpha_{k,m}b_{k,m}(\lfloor n/N\rfloor)c_k(n) \\ &\quad \cdot\int_{-\infty}^{\infty} p(t-nT_c-\tau_k+u)p(u)\cos\left(2\pi(f_m-f_l)(t+u)+\varphi_{k,m}\right)du+\eta(t) \\ &= d_{1,l}(t)+i_{1,l}^{(1)}(t)+i_{1,l}^{(2)}(t)+i_{1,l}^{(3)}(t)+\eta(t). \end{aligned} \tag{2.10}$$

The output is composed of $d_{1,l}(t)$ the desired signal, three interference terms $i_{1,l}^{(1)}$, $i_{1,l}^{(2)}$, $i_{1,l}^{(3)}$ which comprise the MAI and a component $\eta(t)$ due to the input AWGN. $d_{1,l}(t)$ (corresponding to $k = 1, m = l$), is given by

$$\begin{aligned} d_{1,l}(t) &= \sqrt{E_c}\alpha_{1,l}\sum_{n=-\infty}^{\infty} b_{1,l}(\lfloor n/N\rfloor)c_1(n)\int_{-\infty}^{\infty} p(t-nT_c+u)p(u)du \\ &= \sqrt{E_c}\alpha_{1,l}\sum_{n=-\infty}^{\infty} b_{1,l}(\lfloor n/N\rfloor)c_1(n)g(t-nT_c). \end{aligned} \tag{2.11}$$

The function $g(t)$ in (2.11) is defined as

$$g(t) = \mathcal{F}^{-1}\{G(f)\} = p(t) * p(-t) \tag{2.12}$$

where $*$ denotes the convolution operation. $\eta(t)$ is the AWGN component and defined by

$$\eta(t) = \mathcal{L}_p\left\{n(t)\sqrt{2}\cos\left(2\pi f_l t\right)\right\} \tag{2.13}$$

where $\mathcal{L}_p$ represents a lowpass filtering operation that eliminates double frequency terms.

The other three terms in (2.10) account for the following types of interference:

(a) The interference from the other carriers of the first user (corresponding to $k = 1$, $m \neq l$) is given by

$$i_{1,l}^{(1)}(t) = \sqrt{E_c} \sum_{\substack{m=1 \\ m \neq l}}^{M} \sum_{n=-\infty}^{\infty} \alpha_{1,m} b_{1,m}(\lfloor n/N \rfloor) c_1(n) \cdot \int_{-\infty}^{\infty} p(t - nT_c + u) p(u) \cos(2\pi\Delta(m-l)(t+u) + \varphi_{1,m}) du. \quad (2.14)$$

(b) The interference from the same carrier of the other $(K-1)$ users (corresponding to $k \neq 1, m = l$) which can be expressed as follows:

$$i_{1,l}^{(2)}(t) = \sqrt{E_c} \sum_{k=2}^{K} \sum_{n=-\infty}^{\infty} \alpha_{k,l} b_{k,l}(\lfloor n/N \rfloor) c_k(n) \cdot \int_{-\infty}^{\infty} p(t - nT_c - \tau_k + u) p(u) \cos(\varphi_{k,l}) du. \quad (2.15)$$

Note that $i_{1,l}^{(2)}(t)$ can be treated as the MAI in a SC-CDMA system (with carrier frequency f_l).

(c) The third term in (2.10) is the interference from all other carriers of the $(K-1)$ users (corresponding to $k \neq 1, m \neq l$) and can be written as

$$i_{1,l}^{(3)}(t) = \sqrt{E_c} \sum_{k=2}^{K} \sum_{\substack{m=1 \\ m \neq l}}^{M} \sum_{n=-\infty}^{\infty} \alpha_{k,m} b_{k,m}(\lfloor n/N \rfloor) c_k(n) \cdot \int_{-\infty}^{\infty} p(t - nT_c - \tau_k + u) p(u) \cos(2\pi\Delta(m-l)(t+u) + \varphi_{k,m}) du. \quad (2.16)$$

The decision statistic for the transmitted bit $b_{1,l}(0)$ is obtained by sampling $z_{1,l}(t)$ at the chip rate and correlating the results with the corresponding signature sequence. This decision statistic can be written as

$$\begin{aligned} Z_{1,l} &= \sum_{n'=0}^{N-1} c_1(n') z_{1,l}(n' T_c) \\ &= D_{1,l} + I_{1,l}^{(1)} + I_{1,l}^{(2)} + I_{1,l}^{(3)} + \eta \end{aligned} \quad (2.17)$$

where

$$D_{1,l} = \sum_{n'=0}^{N-1} c_1(n')d_{1,l}(n'T_c) = N\sqrt{E_c}\alpha_{1,l}b_{1,l}(0) \tag{2.18}$$

$$I_{1,l}^{(j)} = \sum_{n'=0}^{N-1} c_1(n')i_{1,l}^{(j)}(n'T_c), \quad j = 1, 2, 3 \tag{2.19}$$

and

$$\eta = \sum_{n'=0}^{N-1} c_1(n')\eta(n'T_c). \tag{2.20}$$

Note that property $g(n' - n)T_c = 0$ for $n' \neq n$ has been used to obtain the expression for $D_{1,l}$ in (2.18).

Since $I_{1,l}^{(1)}$, $I_{1,l}^{(2)}$, $I_{1,l}^{(3)}$ and η are uncorrelated and have zero means, the variance of $Z_{1,l}$ conditioned on $b_{1,l}(0)$ and $\alpha_{1,l}$ (for the case of fading channel) can be written as

$$\text{var}\left\{Z_{1,l}|b_{1,l}(0), \alpha_{1,l}\right\} = \sum_{j=1}^{3} \text{var}\left\{I_{1,l}^{(j)}\right\} + \text{var}\left\{\eta\right\}. \tag{2.21}$$

Using the results in [10], [13], and [17] one has

$$\text{var}\left\{I_{1,l}^{(1)}\right\} = \frac{NE_c}{2}\chi_l(\beta, c, X(f)) \tag{2.22}$$

$$\text{var}\left\{I_{1,l}^{(2)}\right\} + \text{var}\left\{I_{1,l}^{(3)}\right\} = \frac{NE_c(K-1)}{2}\kappa_l(\beta, c, X(f)) \tag{2.23}$$

and

$$\text{var}\left\{\eta\right\} = \frac{NN_0}{2} \tag{2.24}$$

where

$$\chi_l(\beta, c, X(f)) = \sum_{\substack{m=1 \\ m\neq l}}^{M} \sum_{r=-\infty}^{\infty} \left| \int_{-\infty}^{\infty} \sqrt{\tilde{G}_{l,m}(f)} e^{-j2\pi f r T_c} df \right|^2 \tag{2.25}$$

$$\kappa_l(\beta, c, X(f)) = \frac{1}{T_c} \sum_{m=1}^{M} \int_{-\infty}^{\infty} \tilde{G}_{l,m}(f) df \tag{2.26}$$

are interpreted as inter-carrier interferences from the same user and different users, respectively, where $\tilde{G}_{l,m}(f) = G(f)G(f - c|m - l|B_c)$.

Note that $G(f)$ depends on both $X(f)$ and β as in (2.3). Furthermore, in (2.25) and (2.26), the number of subcarriers overlapped with the subcarrier l is determined by the carrier spacing c. From the PSD drawn in Fig. 2.2, and the facts that $0 \leq c \leq 1$, and $G(f)$ is an even function limited to $[-B_c/2, B_c/2]$, one can write $\chi_l(\beta, c, X(f))$ and $\kappa_l(\beta, c, X(f))$ as follows:

$$\chi_l(\beta, c, X(f)) = 2 \sum_{\substack{m=\Lambda^-(l,c) \\ m \neq l}}^{\Lambda^+(l,c)} \sum_{r=-\infty}^{\infty} \left| \int_{L(l,m,c)}^{\frac{B_c}{2}} \sqrt{\tilde{G}_{l,m}(f)} e^{-j2\pi f r T_c} df \right|^2 \tag{2.27}$$

$$\kappa_l(\beta, c, X(f)) = \frac{2}{T_c} \sum_{m=\Lambda^-(l,c)}^{\Lambda^+(l,c)} \int_{L(l,m,c)}^{\frac{B_c}{2}} \tilde{G}_{l,m}(f)\, df \tag{2.28}$$

where $L(l, m, c) = cB_c|m - l|/2$; $\Lambda^-(l, c)$ and $\Lambda^+(l, c)$ indicate the lowest and the highest subcarriers that are overlapped with the lth subcarrier. These two subcarriers can be determined as follows:

$$\Lambda^-(l,c) = \begin{cases} 1, & l - \lceil \frac{1}{c} \rceil + 1 \leq 1 \\ l - \lceil \frac{1}{c} \rceil + 1, & l - \lceil \frac{1}{c} \rceil + 1 > 1 \end{cases},$$

$$\Lambda^+(l,c) = \begin{cases} M, & l + \lceil \frac{1}{c} \rceil - 1 \geq M \\ l + \lceil \frac{1}{c} \rceil - 1, & l + \lceil \frac{1}{c} \rceil - 1 < M \end{cases}. \tag{2.29}$$

The signal-to-interference plus noise ratio (SINR) at the input of the comparator of the lth subcarrier in Fig. 2.3 is given by [13]

$$\begin{aligned} \text{SINR}_l &= \frac{[E\{Z_{1,l}|b_{1,l}(0), \alpha_{1,l}\}]^2}{\text{var}\{Z_{1,l}|b_{1,l}(0), \alpha_{1,l}\}} \\ &= \frac{N^2 E_c \alpha_{1,l}^2}{\sum_{j=1}^{3} \text{var}\left\{I_{1,l}^{(j)}\right\} + \frac{NN_0}{2}} \\ &= \underbrace{\alpha_{1,l}^2 \left[\left(\frac{2E_b}{N_0} \right)^{-1} + \frac{(K-1)}{2} J_l(\beta, c, X(f)) \right]^{-1}}_{\overline{\text{SINR}}_l} \end{aligned} \tag{2.30}$$

where $E_b = NE_c$ is the energy per bit, $J_l(\beta, c, X(f))$ is the normalized interference parameter [13], given by

$$J_l(\beta, c, X(f)) = \frac{1}{N}\left[\frac{\chi_l(\beta, c, X(f))}{(K-1)} + \kappa_l(\beta, c, X(f))\right] \tag{2.31}$$

and $\overline{\text{SINR}_l}$ is the SINR that corresponds to an AWGN channel, i.e., when $\alpha_{1,l} = 1$.

It can be seen from (2.30) that when the signal to background noise ratio (E_b/N_0) and the number of users K are fixed, the performance of the system is determined by $J_l(\beta, c, X(f))$, which in turn depends on the particular carrier under consideration, the roll-off factor, the carrier spacing and the shape of the chip waveform. To take all the carriers into account, define the following average interference parameter (*average MAI*) [13]

$$\begin{aligned}\gamma(\beta, c, X(f)) &= \frac{1}{M}\sum_{l=1}^{M} J_l(\beta, c, X(f)) \\ &= \frac{1}{MN}\left[\underbrace{\sum_{l=1}^{M}\frac{\chi_l(\beta, c, X(f))}{(K-1)}}_{\chi} + \underbrace{\sum_{l=1}^{M}\kappa_l(\beta, c, X(f))}_{\kappa}\right]\end{aligned} \tag{2.32}$$

where in (2.32) the processing gain N is defined by (2.6), which depends on the roll-off factor and the carrier spacing. It can be observed from (2.32), that for a fixed B_T and T_b, a specific chip waveform and a given K and β, the MAI mainly depends on the carrier spacing.

In general, it is sensible to use the chip waveform and the carrier spacing that minimizes the above average MAI in order to improve the SINR performance. Furthermore, the inter-carrier interference from the same user (the first term in (2.32)) can be neglected when K is large. In this case the average MAI is well approximated [13] as

$$\gamma(\beta, c, X(f)) \approx \widehat{\gamma}(\beta, c, X(f)) = \frac{1}{MN}\sum_{l=1}^{M}\kappa_l(\beta, c, X(f)). \tag{2.33}$$

Having defined the average MAI, the next section demonstrates the impact of the carrier spacing for a given chip waveform on the MAI performance.

2.3 The Impact of a Chip Waveform and Carrier Spacing

This section investigates the impact of carrier spacing on the MAI performance with different chip waveforms corresponding to the following elementary density functions, defined over $f \in [0, 1]$:

(1) The raised cosine pulse: $X(f) = \frac{1}{2}\left[1 - \sin\left(\frac{\pi f}{2}\right)\right]$

(2) The "Better than Nyquist" pulse [26]: $X(f) = \frac{1}{2}\left[2 - \exp\left(\ln 2f\right)\right]$

(3) The cosine pulse [13]: $X(f) = \frac{1}{2}\cos\left(\frac{\pi f}{2}\right)$

Other chip waveforms [27, 28] were investigated. Their performance was similar and hence only the above chip waveforms are considered here. In this investigation, the transmission rate and the system bandwidth are fixed so that the bandwidth-bit duration product defined by $F = T_b B_T$ is constant. Based on the system parameters given in [3], for all systems under comparison, the parameter F is set to 256. All the numerical results presented in this section are obtained using MATLAB.

Figures 2.4-(a) and 2.4-(b) show the inter-carrier interference from the same user, χ, and inter-carrier interference from other users, κ, respectively. The results were obtained using the raised cosine chip waveform with $\beta = 0.5$ and $M = 4$[1]. Observe from Fig. 2.4-(a) that χ reduces as the number of users increases. As pointed out in Section 2.2, it can be seen from these two figures that $\kappa > \chi$ and the difference becomes larger for larger values of K. Thus, it is reasonable to use (2.33) to quantify the average MAI. Furthermore, note that from Fig. 2.4-(b) when carrier spacing increases up to 0.8 that κ decreases and is approximately constant over the range of $c \in [0.8, 1.0]$. This is because the inter-carrier interference from other users due to other subcarriers decreases significantly as c increases and becomes zero when $c = 1$. However, there will be interference at the same carrier from other users.

---

[1]Note that one can choose any value for M. However, it will be shown later in this section that there is a negligible reduction in MAI for larger M. Therefore for all the examples considered in this section a good choice for M is 4.

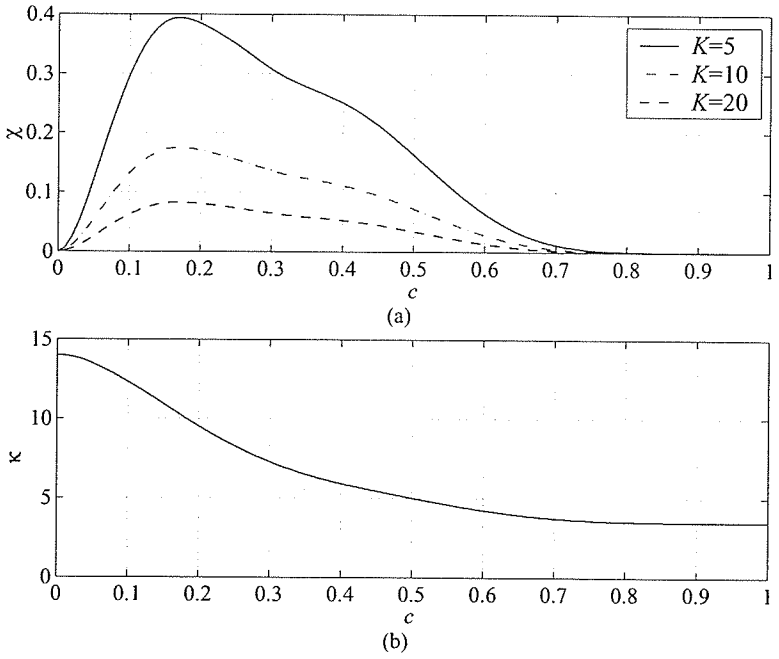

Figure 2.4: The inter-carrier interference from (a) same user and (b) other users: $M = 4$ $F = 256$ and $\beta = 0.5$.

For fixed $M = 4$ and $K = 20$, Figures 2.5 to 2.7 illustrate the impact of the carrier spacing on MAI levels, $\widehat{\gamma}(\beta, c, X(f))$, of each chip waveform for different roll-off factors. The MAI changes due to the variation of carrier spacing, in Fig. 2.6, with roll-off factor $\beta = 0.5$ can be explained by the results obtained from Fig. 2.8 (processing gain versus carrier spacing) and Fig. 2.4-(b) (inter-carrier interference from other users versus carrier spacing). For a carrier spacing between 0 and 0.1, the MAI increases, because the processing gain decreases faster than that the decrease in interference (recall that MAI is inversely proportional to processing gain). In contrast, roughly, between 0.1 and 0.7, both processing gain and the interference reduce approximately at the same rate. Hence the MAI reduces. After 0.7, the decreasing rate of the interference is less than that of processing gain, while result in the MAI increasing.

For the three chip waveforms, Fig. 2.9 shows that regardless of the roll-off factor, β, the carrier spacing, c, should be less than one to minimize MAI. Furthermore, it

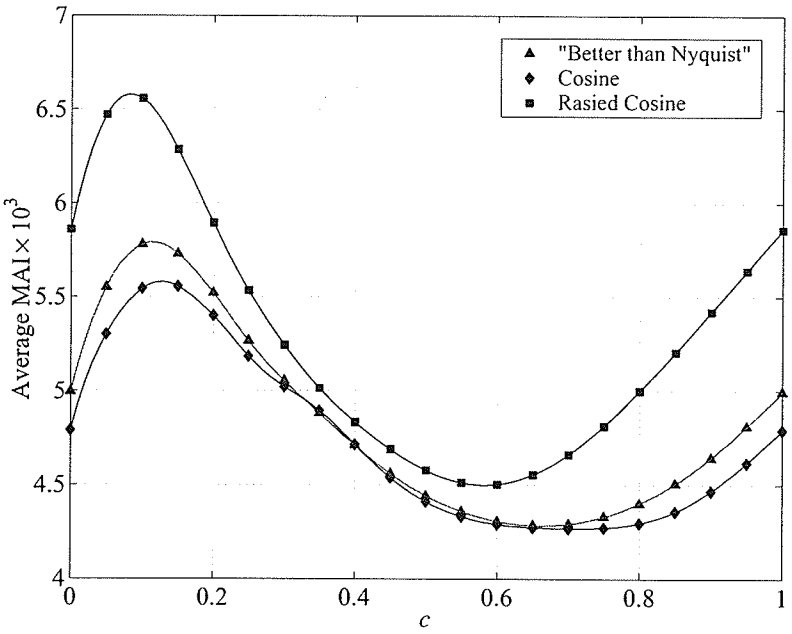

Figure 2.5: Influence of the carrier spacing on MAI levels using different chip waveforms: $\beta = 1.0$.

can be seen that the optimal carrier spacings are almost the same when $\beta < 0.5$. The optimal carrier spacing for $\beta \geq 0.5$ is, however, different. By observing the figure, one may speculate that there is a possibility to get minimum MAI when c is greater than one. But this is not the case. When $c \geq 1$, the interference from the other carriers of the 1st user and the interference from other carriers of (K-1) users is zero, with only the interference from the same carrier of the $(K-1)$ users, present. This interference is independent of c. However, because the processing gain decreases as c increases, the resulting MAI increases.

Finally, the effect of the number of carriers M on the MAI level is illustrated in Fig. 2.10, for the raised cosine chip waveform with $\beta = 0.5$. As seen from Fig. 2.10, the MAI reduces as the number of carriers increases. However, there is a limit to the MAI reduction achievable by increasing the number of carrier M, especially for a larger carrier spacing. It is also observed that, though for all the chip waveforms considered the MAI level reduces as the number of carriers increases, the optimal

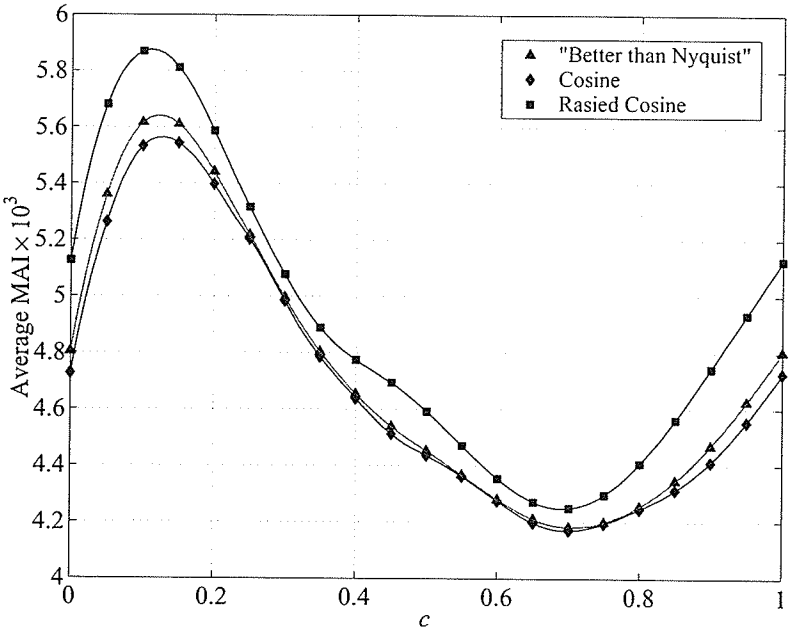

Figure 2.6: Influence of the carrier spacing on MAI levels using different chip waveforms: $\beta = 0.5$.

carrier spacing remains unchanged with the number of carriers.

In this section, one has investigated the impact of carrier spacing on MAI in an MC-DS-CDMA system with different chip waveforms. It was demonstrated that, there exists an optimal carrier spacing, which gives the minimum MAI, for a given chip waveform. Motivated by this observation, a methodology to jointly design the chip waveform and the carrier spacing which minimizes MAI is presented in the next section.

2.4 The Joint Optimization of the Chip Waveform and Carrier Spacing

Ideally, one would like to jointly design the chip waveform and the carrier spacing that maximizes the average SINR among the M carriers. However, such an optimization problem appears to be intractable. Instead, one tries to optimize the chip waveform and the carrier spacing jointly that minimizes the average MAI defined by (2.33).

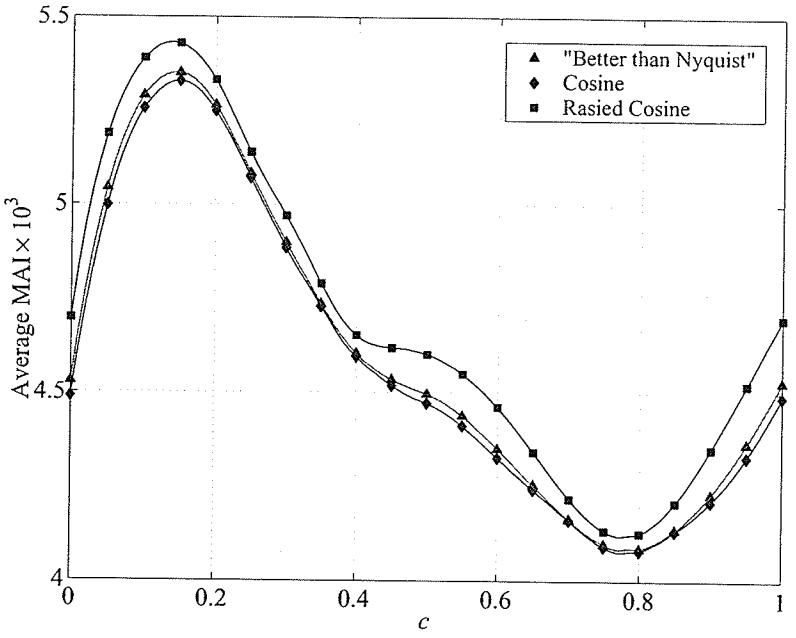

Figure 2.7: Influence of the carrier spacing on MAI levels using different chip waveforms: $\beta = 0.3$.

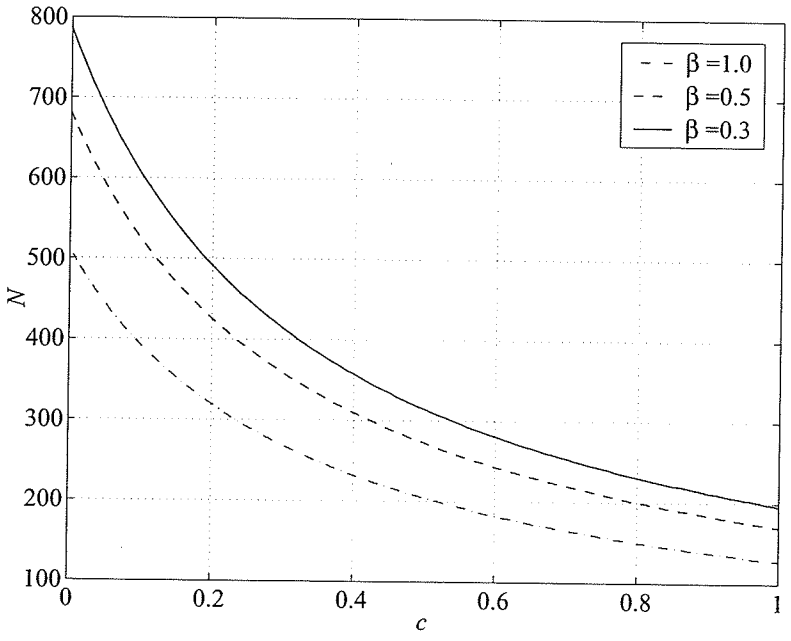

Figure 2.8: Influence of the carrier spacing on processing gain.

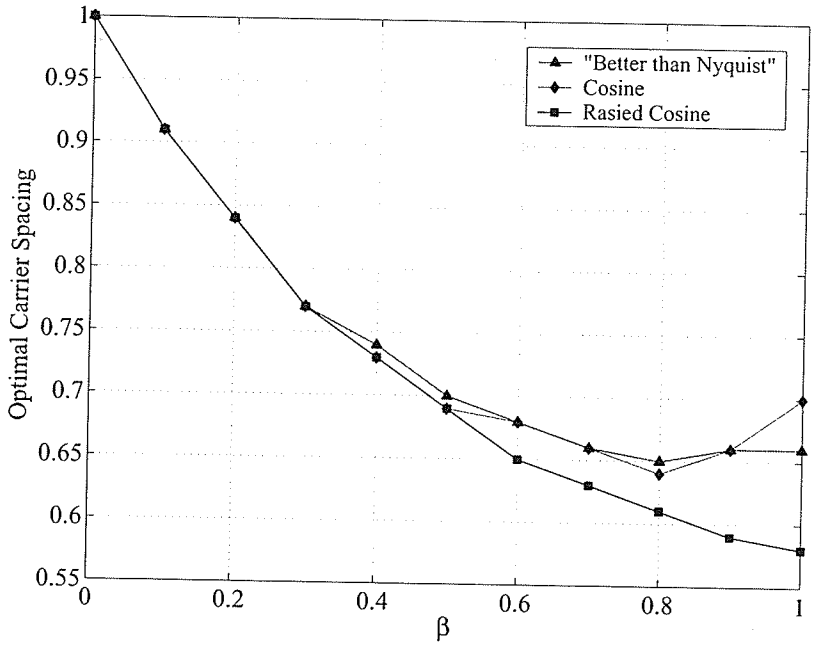

Figure 2.9: Influence of the roll-off factor β on optimum carrier spacing using different chip waveforms.

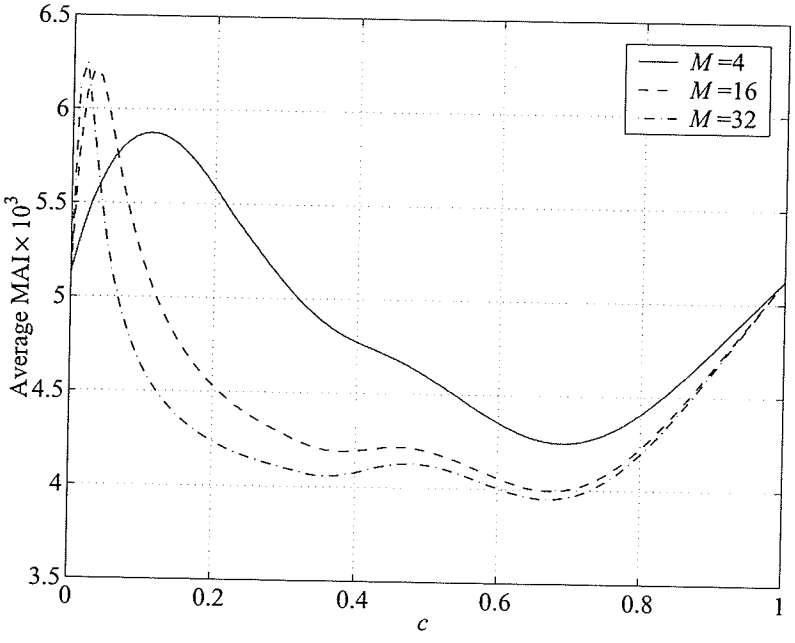

Figure 2.10: Influence of the number of carriers M on MAI levels using raised cosine chip waveform: $\beta = 0.5$.

This problem to jointly design the chip waveform and the carrier spacing for MC-DS-CDMA systems can be formulated as follows.

Problem 1: Consider an MC-DS-CDMA system equipped with a correlation receiver in each subchannel. Given the transmission rate $(1/T_b)$, the total bandwidth B_T (or equivalently F), the number of users K and the roll-off factor β, find the optimal elementary density function $X(f)$ and optimal carrier spacing c that minimizes $\widehat{\gamma}(\beta, c, X(f))$ subject to the following constraints. (i) $X(0) = 0.5$, $X(1) = 0$ and (ii) $0 \leq c \leq 1$.

Given the complexity of the objective and constraint functions, it is difficult to solve for $X(f)$ and c directly. Instead, the elementary density function $X(f)$ is approximated with an Lth-order polynomial as follows:

$$X(f) = \sum_{i=0}^{L} x_i f^i. \tag{2.34}$$

Using the expansion in (2.34), the problem of finding the chip waveform and carrier spacing jointly to minimize (2.33) reduces to a finite-dimensional optimization problem in $(L+2)$ unknowns $\{\{x_i\}_{i=0}^{L}, c\}$. Obviously, one expects that a better approximation of the theoretically optimal chip waveform is obtained with a larger value of L. Nevertheless, numerical results in Section 2.4.1 show that for all values of β, $L \leq 5$ is enough to practically achieve the maximum MAI suppression capability of the optimal chip waveform and the carrier spacing.

Applying the constraints $X(0) = 0.5$ and $X(1) = 1$ to (2.34) gives $x_0 = 0.5$ and $\sum_{i=1}^{L} x_i = 0.5$. Furthermore, it is reasonable to require that $X(f)$ decreases monotonically over $[0, 1]$. It then follows that $X'(f) \leq 0$ and $a_1 < 0$, where $X'(f)$ is the first derivative of $X(f)$. With these constraints, *Problem 1* is now equivalent to the following optimization problem.

Problem 2: Given the transmission rate $(1/T_b)$, the total bandwidth B_T, the number of users K and the roll-off factor β, find L coefficients x_i, $i = 1, 2, \ldots, L$ and the optimal carrier spacing c, that minimize (2.33) subject to: (i) $\sum_{i=1}^{L} x_i = 0.5$; (ii) $\sum_{i=1}^{L} i x_i f^{(i-1)} \leq 0, \quad \forall\, f \in [0, 1]$; (iii) $x_1 \leq 0$ and (iv) $0 \leq c \leq 1$.

The above finite-dimensional nonlinear constrained optimization problem can be

solved numerically, for example by sequential quadratic programming routines in the MATLAB optimization toolbox [29]. Since the sequential quadratic programming cannot guarantee a global minimum, the optimization was run for many runs with different initial conditions to obtain the global minimum.

2.4.1 Results and Comparisons

To compare the performance of the optimum chip waveform with the chip waveforms of Section 2.3, consider an MC-DS-CDMA system with $K = 20$ users, $M = 4$ carriers and $F = 256$. Given the number of users, the number of carriers and the roll-off factor, different values of L (i.e., the polynomial order) were used to obtain the elementary density functions and the carrier spacing. Plotting the average MAI versus L reveals that, for all the roll-off factors considered, the asymptote of the minimum average MAI is reached practically for $L = 5$. It is also observed that, the optimal carrier spacing saturates for $L \geq 5$. Thus $L = 5$ is used in all the remaining examples of this section.

Table 2.1 provides a comparison of the average MAI performance of the optimal chip waveform and the other chip waveforms for five different values of β. Note that the carrier spacing is also optimized for each of the considered chip waveforms. Observe that, although the optimal chip waveform can reduce the MAI at any value of β, the reduction is quit marginal for small values of β. This is expected because the elementary density function can only be designed over a small frequency range $(\beta/(2T_c))$. Due to this it can be seen that the optimal carrier spacings remain almost the same for all the chip waveforms when $\beta \leq 0.5$. The optimal carrier spacing are also very close to the chip rate (i.e., $c = 1/(1+\beta)$).

The situation for large values of β is, however, very different. For example, compared to the raised cosine waveform, the optimal chip waveform can reduce the MAI by 10% at $\beta = 1.0$. The optimal carrier spacing for all the considered chip waveforms are also different from the chip rate for $\beta = 0.75$ and $\beta = 1.0$.

Fig. 2.11 plots the spectra of the optimal chip waveforms obtained for different values of roll-off factors. The coefficients of the polynomial expansions of the

Table 2.1: Average MAI performance of MC-DS-CDMA systems using different chip waveforms.

β	Waveform	Normalized MAI	c (optimal)	$c = (1/1+\beta)$ $(\Delta = 1/T_c)$
0.22	Raised cosine	4.0640e-3	0.820	0.820
	"Better than Nyquist"	4.0380e-3	0.830	
	Cosine	4.0330e-3	0.820	
	Optimum	3.9828e-3	0.825	
0.35	Raised cosine	4.1550e-3	0.740	0.741
	"Better than Nyquist"	4.1140e-3	0.740	
	Cosine	4.1050e-3	0.740	
	Optimum	4.0129e-3	0.750	
0.5	Raised cosine	4.2490e-3	0.690	0.667
	"Better than Nyquist"	4.1830e-3	0.700	
	Cosine	4.1710e-3	0.690	
	Optimum	4.0230e-3	0.710	
0.75	Raised cosine	4.3900e-3	0.620	0.571
	"Better than Nyquist"	4.2690e-3	0.650	
	Cosine	4.2570e-3	0.640	
	Optimum	4.0290e-3	0.599	
1.0	Raised cosine	4.4990e-3	0.580	0.500
	"Better than Nyquist"	4.2840e-3	0.660	
	Cosine	4.2690e-3	0.700	
	Optimum	4.0462e-3	0.956	

Table 2.2: Coefficients of the polynomial expansion of the elementary density function for different values of roll-off factor β.

β	x_1	x_2	x_3	x_4	x_5
0.22	-1.1478e-1	-9.6291e-2	-9.6303e-2	-9.6311e-2	-9.6317e-2
0.35	-2.9340e-2	-2.7905e-1	3.8559e-1	2.2831e-1	-8.0551e-1
0.5	-2.7933e-1	4.3668e-1	-1.9370e-1	-2.2205e-1	-2.4161e-1
0.75	-3.4301e-1	6.1163e-1	-2.7458e-2	-3.0746e-1	-4.3370e-1
1.0	-2.0174e-1	1.8128	-7.1452	11.467	-6.4330

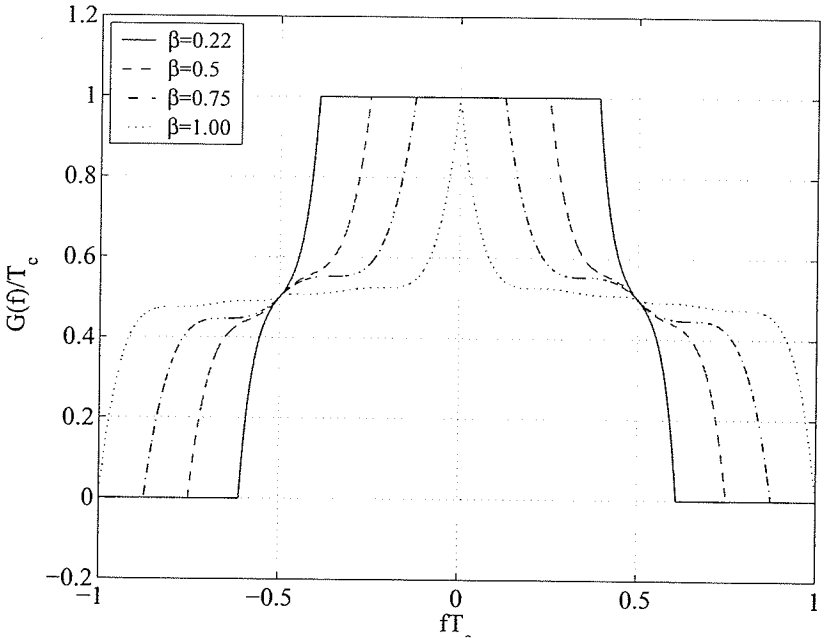

Figure 2.11: Plots of $G(f)$ for the optimal chip waveforms for different roll-off factors β.

elementary density functions for those chip waveforms are provided in Table 2.2.

In Fig. 2.12, the bit error rate (BER) performance over an AWGN channel is evaluated for MC-DS-CDMA systems employing different chip waveforms and carrier spacings with $\beta = 1.0$. By approximating the interference as a Gaussian random variable, the BER is calculated as[2] [13]

$$P_b^{\text{AWGN}} = \frac{1}{M} \sum_{l=1}^{M} Q\left(\sqrt{\overline{\text{SINR}_l}}\right) \tag{2.35}$$

where $\overline{\text{SINR}_l}$ is given in (2.30). Consistent with the average MAI performance, Fig. 2.12 shows the superiority of the proposed chip waveforms to the other schemes considered, especially at high E_b/N_0. At BER level of 10^{-5}, a gain of about 2dB and 1.5dB in E_b/N_0 can be attained by the optimal chip waveform over the space-optimized raised cosine waveform and "Better than Nyquist" waveform, respectively. Also there is a gain of about 2.5dB over the raised cosine waveform with the commonly

[2] $Q(x) = (2\pi)^{-1} \int_x^\infty \exp(-\xi^2/2) d\xi$.

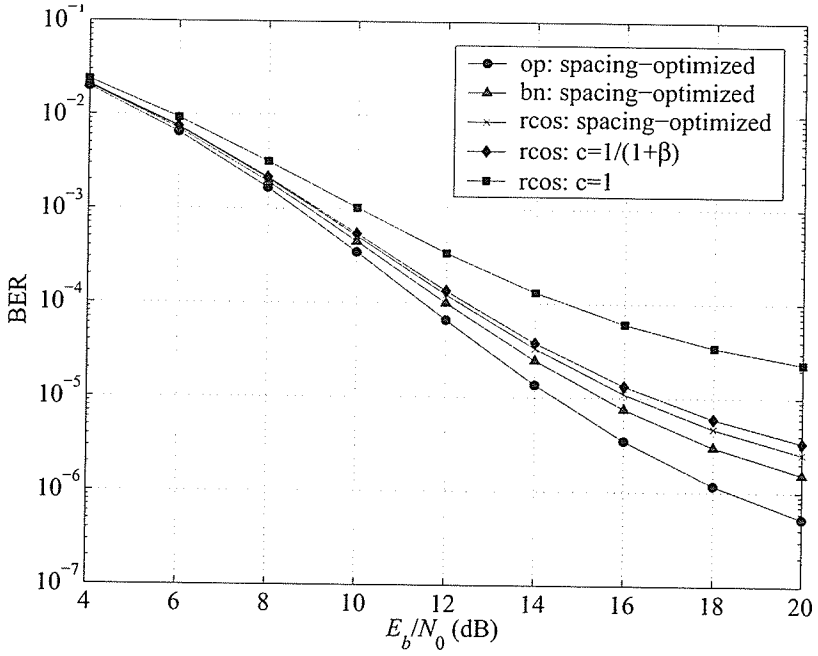

Figure 2.12: BER performance of MC-DS-CDMA systems using different chip waveforms over an AWGN channel and for $\beta = 1$: (op-Optimal, rcos-Raised cosine, bn-"Better than Nyquist").

used carrier spacing $c = 1/(1+\beta)$. Furthermore, the proposed optimal chip waveform significantly outperforms the raised cosine waveform with carrier spacing $c = 1$ (non-overlapped carriers) at any E_b/N_0 values.

Finally, Table 2.3 provides the BER performance of the above scheme over a fading channel. Here it is assumed that using $M = 4$ carriers makes each subchannel experience frequency non-selective Rayleigh fading. Note that the BER is calculated [13] as

$$P_b^{\text{fading}} = \frac{1}{2M} \sum_{l=1}^{M} \left[1 - \sqrt{\frac{\overline{\text{SINR}_l}}{2 + \overline{\text{SINR}_l}}} \right]. \tag{2.36}$$

As in the case of an AWGN channel, it can be observed again that the proposed optimal chip waveform outperforms other schemes considered. However, the performance gain is very marginal over the space-optimized "Better than Nyquist" waveform.

Table 2.3: BER performance of MC-DS-CDMA systems using different chip waveforms and carrier spacings over a fading channel: $\beta = 1.0$.

E_b/N_0 (dB)	5	15	25
Optimum	7.5928e-2	2.4466e-2	1.8224e-2
"Better than Nyquist": spacing-optimized	7.7085e-2	2.6094e-2	1.9917e-2
Raised cosine: spacing-optimized	7.7711e-2	2.6974e-2	2.0832e-2
Raised cosine: $c = 1/(1+\beta)$	7.7933e-2	2.7286e-2	2.1156e-2
Raised cosine: $c = 1$	8.1391e-2	3.2130e-2	2.6189e-2

2.5 Summary

The effect of carrier spacing and band-limited chip waveforms on the performance of MC-DS-CDMA systems has been investigated in this chapter. It is demonstrated that, there exists an optimal carrier spacing that gives the minimum MAI, for a given chip waveform and roll-off factor. Based on this conclusion, a method to jointly design the chip waveform and the carrier spacing to achieve the minimum average MAI for a band-limited MC-DS-CDMA system is presented. The optimization was simplified by approximating the elementary function with an Lth-order polynomial. It is shown that for all values of the roll-off factor, the fifth-order polynomial is good enough to practically achieve the maximum MAI suppression capability of the optimal chip waveform and the carrier spacing. The optimal elementary density functions and optimal carrier spacings were determined for various roll-off factors. The obtained waveforms were compared with the other existing chip waveforms and were shown to achieve a MAI reduction capability, especially for high values of the roll-off factor.

Chapter 3

Adaptive CI-MC-CDMA Systems

In contrast to Chapter 2, the multi-carrier CDMA system which uses frequency domain spreading, referred to as MC-CDMA, is the focus of this chapter. It is relevant to point out that in MC-CDMA systems, unlike MC-DS-CDMA systems, the chip waveform is a rectangular pulse and the carrier spacing is confined to the bit rate. That is, the carriers are orthogonal and hence there is no inter-carrier interference. It then follows that when the number of carriers and the carrier spacing are also fixed, for a given total bandwidth, the MAI in MC-CDMA systems is only determined by the set of the users' signature sequences.

To date, most MC-CDMA systems adopt signature sequences that were previously devised for DS-CDMA systems. In [30], thorough analysis and comparison of existing spreading codes, including the Hadamard-Walsh, Gold, orthogonal Gold, and Zadoff-Chu sequences are presented for MC-CDMA systems. More recently, a new family of spreading sequences, known as carrier interferometry (CI) codes, has also been introduced specifically for MC-CDMA systems [15]. The CI codes, which are of length N, have the unique feature which allows a MC-CDMA system to support N users orthogonally and, as the system demand increases, to accommodate up to an additional $N-1$ users pseudo-orthogonally. Moreover, there is no restriction on the length N of the CI codes (i.e., the length N can be any integer), making it more robust to the diverse requirements of the wireless environment.

Essentially, the CI codes are designed by appropriately varying the phases of the orthogonal carriers, while assuming a constant amplitude for all carriers. Allowing

both the amplitudes and phases of the carriers to be changed provides an additional degree of freedom to design the signature waveforms for MC-CDMA systems. While such a design still preserves all the properties of CI codes, it can provide a performance enhancement by adapting the carrier amplitudes according to the condition of the fading channel. Signature sequence adaptation in fading channels has been extensively studied for traditional DS-CDMA systems via transmitter/receiver optimization under different performance criteria [31–36]. A similar adaptation strategy is studied for MC-DS-CDMA systems in [37] by varying the carrier powers of each user.

The system of interest in this chapter is an MC-CDMA over a multipath fading channel. Given the system's total bandwidth and transmission power, the objective is to adapt the amplitudes of the orthogonal carriers according to the channel condition to optimize the system performance (i.e., the MAI is minimized). Since the phases of the sinusoidal carriers are also defined as in [15], the carrier interferometry property still applies and hence, it is appropriate to refer to the proposed MC-CDMA scheme as *adaptive carrier interferometry* MC-CDMA (ACI-MC-CDMA). For simplicity, it is assumed that there is an ideal feedback channel to transmit the updated carrier amplitudes from the receiver back to the transmitter. A minimum mean square error (MMSE) receiver is also assumed. The signal-to-interference plus noise ratio (SINR) will be used as the performance index at the output of the MMSE receiver.

The carrier amplitude adaptation is performed in the user-based mode. In user-based adaptation, the amplitude of the carriers are adapted to maximize the overall SINR, which is the sum of the SINR of all carriers. Two algorithms, namely local and global adaptation, are examined for user-based adaptation. These algorithms are implemented based on the technique presented in [36] for SC-CDMA systems.

In local adaptation, an individual user is allowed to adapt his/her own carrier amplitudes to optimize his/her own performance, without considering the performance of other users in the system. Since the signals from other users are treated as noise, the performance criterion for this adaptation strategy is the SINR of that particular user. This type of strategy is well suited for situations where each user needs to achieve

a different quality of service, as is typical in multimedia wireless communications as well as multirate communications. Although this adaptation is applicable for both uplink or downlink communications, it is more appropriate for the downlink, where other users' information is not generally available at a particular user's receiver.

In contrast, global adaptation updates each user's carrier amplitudes in order to optimize the overall system performance. Hence, the total mean square error (or equivalently, the average SINR of all users) is a suitable performance criterion. Since overall system performance is the objective in this adaptation, global adaptation is more appropriate for uplink communications, where all the users' information is generally available at the receiver. This scheme is applicable in downlink communications as well, where different groups of users' operate at different data rates.

A common problem in MC-CDMA is the problem of high peak-to-average power ratio (PAPR). High peaks in the power result from highly fluctuating envelopes, a consequence of using independently modulated carriers. This, in turn, leads to an inefficient operation of the transmit power amplifier because an increased signal dynamic range requires power amplifiers with a greater linear region of operation. It is shown in [38] that the PAPR in the downlink CI-MC-CDMA is well within tolerable levels for the power amplifiers. On the other hand, the uplink of the CI-MC-CDMA suffers from high PAPR. To reduce the uplink PAPR to acceptable levels PAPR reduction techniques are necessary. In this chapter, it will be shown that the proposed scheme eliminates the PAPR problem present in the conventional CI-MC-CDMA systems, without applying any PAPR reduction techniques.

The chapter is organized as follows. Section 3.1 describes the system model under consideration. Section 3.2 establishes the optimization problems and also provides the solutions. Section 3.3 illustrates the performance of the proposed ACI-MC-CDMA systems and compares it with that of the conventional CI-MC-C DMA systems studied in [15]. Finally, conclusions are drawn in Section 3.4.

3.1 System Model

This section describes the model of the MC-CDMA systems considered in this chapter. Assume that there are K users. Each user employs N subcarriers to transmit his/her information over a channel of bandwidth B_T. Note that different from MC-DS-CDMA, here the number of subcarriers is equal to the processing gain of the system (i.e., $M = N$). Fig. 3.1 illustrates the power spectral density of the MC-CDMA system under consideration. Note that for convenience, the carriers are indexed from 0 to $N-1$. The N subcarriers are overlapped with carrier spacing $\Delta = 1/T_b$, where T_b is the bit duration. From Fig. 3.1 it is not hard to see that the number of subcarriers N is related to B_T and T_b as

$$N = F - 1 \tag{3.1}$$

where $F = B_T T_b$ is the parameter characterizing the bandwidth-bit duration product of the system. Observe that for a fixed bit duration (i.e., fixed bit rate) the number of carriers (and hence the processing gain of the system) is limited by the total system bandwidth B_T.

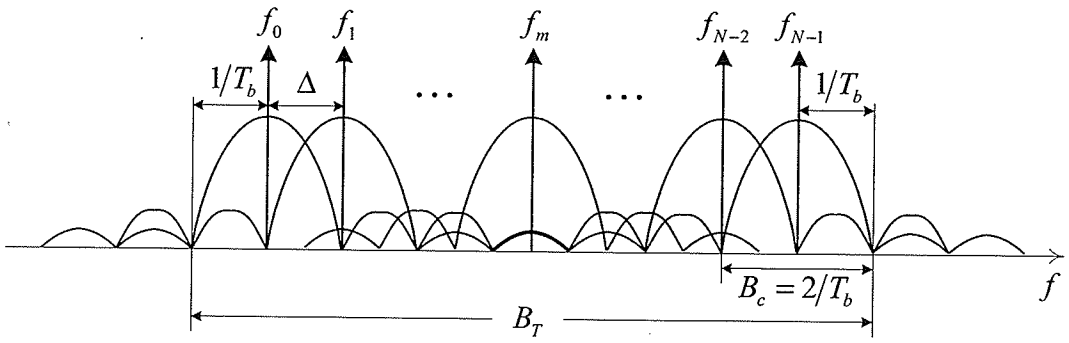

Figure 3.1: The PSD of an MC-CDMA system.

Shown in Fig. 3.2 is a baseband equivalent model of the kth user's transmitter for one possible implementation of an MC-CDMA system under consideration. The generation of an MC-CDMA signal can be described as follows. The ith bit, $b_k(i)$, is replicated into N parallel copies. The mth branch (subcarrier) of the parallel stream

is multiplied by a chip, $c_k(m) = a_{k,m}e^{jm\theta_k}$, and then modulated by the corresponding subcarrier frequency. The transmitted signal consists of the sum of the outputs of these branches.

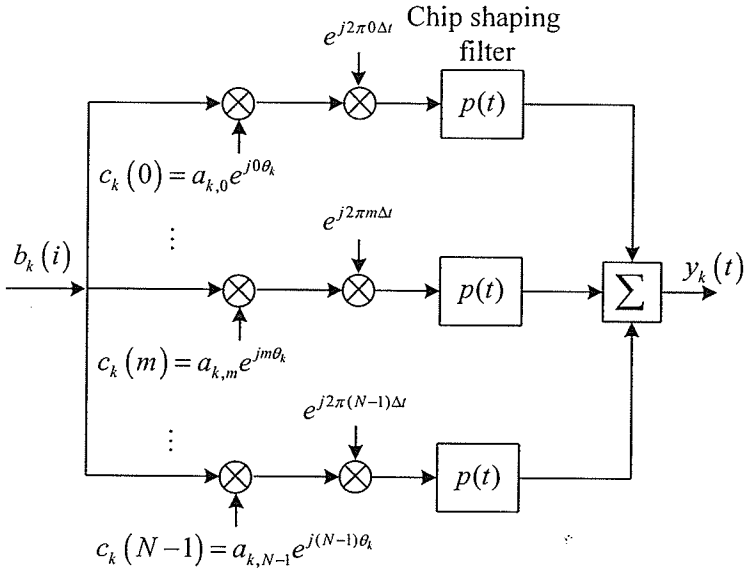

Figure 3.2: The baseband equivalent transmitter of the kth user in an MC-CDMA system.

As illustrated in Fig. 3.2, the complex baseband transmitted signal corresponding to the ith bit of the kth user is

$$y_k(t) = b_k(i)s_k(t - iT_b) \tag{3.2}$$

where $b_k(i)$ is the binary data sequence of the kth user, which is modeled as a sequence of i.i.d random variables taking values in $\{+1, -1\}$ with equal probability. For the MC-CDMA systems considered in this chapter, the signature waveform $s_k(t)$ of the kth user is constructed as follows:

$$\begin{aligned} s_k(t) &= \left[\sum_{m=0}^{N-1} a_{k,m}e^{jm(2\pi\Delta t+\theta_k)}\right] p(t) \\ &= \left[\sum_{m=0}^{N-1} s_k^{(m)}(t)\right] p(t) \end{aligned} \tag{3.3}$$

where $p(t)$ is a unit-energy rectangular chip pulse limited to $[0, T_b]$ and $s_k^{(m)}(t) = a_{k,m}e^{jm(2\pi\Delta t+\theta_k)}$. Note that the set of waveforms $\{s_k^{(m)}(t)\}_{m=0}^{N-1}$ determines how the total power of the transmitted signal is spread (or distributed) over the total bandwidth. This construction of the signature waveforms unifies several variants of spreading waveforms proposed in the literature. By setting $\theta_k = 0$ and $a_{k,m} = \pm 1$, the current spreading system becomes the MC-CDMA described in [7]. On the other hand, the carrier-interferometry MC-CDMA (CI-MC-CDMA) scheme proposed in [15] is realized by setting $a_{k,m} = 1$.

In this chapter, the phases of the signature waveforms are defined in the same way as in [15]. That is,

$$\theta_k = \begin{cases} \frac{2\pi}{N} \cdot k, & 0 \le k \le N-1 \\ \frac{2\pi}{N} \cdot k + \frac{\pi}{N}, & N \le k \le 2N-1 \end{cases} . \tag{3.4}$$

However, different from [15], here the amplitudes of the carriers $a_{k,m}$ are allowed to vary at the transmitter in accordance with the feedback information from the receiver. Therefore the proposed MC-CDMA systems are referred to as adaptive carrier-interferometry MC-CDMA (ACI-MC-CDMA) systems.

The channel under consideration is a frequency-selective Rayleigh fading channel. The number of carriers is chosen such that each carrier undergoes frequency non-selective slow Rayleigh fading. With this assumption, one can model the channel gains $h_{k,m}$, $k = 0, 1, \ldots, K-1$ and $m = 0, 1, \ldots, N-1$ as zero-mean complex Gaussian random variables. The magnitude of each channel gain is therefore Rayleigh distributed. Furthermore, although the channel gains $h_{k,m}$'s are generally correlated [15], here for simplicity it is assumed that $h_{k,m}$'s are independent and identically distributed for different k and m. Note that such a simplified channel model is also considered in [39–41].

As in [15], to make the analysis simple, the system is assumed to be synchronized. The complex baseband received signal during the ith bit duration is given by

$$r(t) = \sum_{k=0}^{K-1} b_k(i) \sum_{m=0}^{N-1} h_{k,m}a_{k,m}e^{jm(2\pi\Delta t+\theta_k)}p(t - iT_b) + n(t) \tag{3.5}$$

where $n(t)$ is additive white gaussian noise with two-sided power spectral density of $N_0/2$. For slow fading channels, the channel gains can be assumed to be invariant over the time interval of transmitter adaptation.

At the receiver of every user, the received signal is first projected onto N orthogonal carriers to obtain vector $\mathbf{r} = [r_0, \ldots, r_m, \ldots, r_{N-1}]^T$. With exact phase and carrier synchronization, the mth component of $\mathbf{r}$ is given by

$$r_m = \sum_{k=0}^{K-1} b_k(i) h_{k,m} a_{k,m} e^{jm\theta_k} + n_m \tag{3.6}$$

where n_m is a Gaussian random variable with zero mean and variance $\sigma^2 = N_0/2$. Furthermore, the vector $\mathbf{r}$ can be expressed as

$$\mathbf{r} = \sum_{k=0}^{K-1} b_k(i) \mathbf{P}_k \mathbf{H}_k \mathbf{a}_k + \mathbf{n} \tag{3.7}$$

where $\mathbf{a}_k = [a_{k,0}, \ldots, a_{k,m}, \ldots, a_{k,N-1}]^T$ is the carrier amplitude vector chosen by the kth user, $\mathbf{H}_k$ is an $N \times N$ diagonal matrix whose mth diagonal element is $h_{k,m}$, $\mathbf{P}_k$ is an $N \times N$ diagonal matrix whose mth diagonal element is $e^{jm\theta_k}$ and $\mathbf{n}$ is a Gaussian noise vector with covariance matrix $\sigma^2\mathbf{I}$, where $\mathbf{I}$ denotes the identity matrix.

The vector $\mathbf{r}$ is then fed to a receive filter in order to combine the signal components from all the N carriers to give the decision statistic. The decision statistic for the jth user is

$$Z_j = \mathbf{w}_j^H \mathbf{r} \tag{3.8}$$

where $\mathbf{w}_j = [w_{j,0}, \ldots, w_{j,m}, \ldots, w_{j,N-1}]^T$ is an N-dimensional weight vector of the receive filter of the jth user. The superscripts H and T denote the Hermitian and transpose operations, respectively. Here a minimum mean square error (MMSE) receiver is employed, and to achieve the best performance, the weight vector is designed jointly to minimize the composite mean square error [42]

$$\begin{aligned} \text{MSE} &= E\left\{\|b_j(i) - Z_j\|^2\right\} \\ &= E\left\{\left\|b_j(i) - \mathbf{w}_j^H \mathbf{r}\right\|^2\right\}. \end{aligned} \tag{3.9}$$

The optimum weight vector can be shown to be [43]

$$\mathbf{w}_j = \mathbf{R}^{-1} \mathbf{H}_j \mathbf{P}_j \mathbf{a}_j. \tag{3.10}$$

In (3.10), $\mathbf{R}$ is the received correlation matrix, defined as

$$\begin{aligned}\mathbf{R} &= \sum_{k=0}^{K-1} \mathbf{H}_k \mathbf{P}_k \mathbf{a}_k \mathbf{a}_k^H \mathbf{P}_k^H \mathbf{H}_k^H + \sigma^2 \mathbf{I} \\ &= \mathbf{R}_j + \mathbf{H}_j \mathbf{P}_j \mathbf{a}_j \mathbf{a}_j^H \mathbf{P}_j^H \mathbf{H}_j^H \end{aligned} \tag{3.11}$$

where $\mathbf{R}_j$ is the interference-plus-noise correlation matrix corresponding to the jth user. This matrix is defined as

$$\mathbf{R}_j = \sum_{\substack{k=0 \\ k \neq j}}^{K-1} \mathbf{H}_k \mathbf{P}_k \mathbf{a}_k \mathbf{a}_k^H \mathbf{P}_k^H \mathbf{H}_k^H + \sigma^2 \mathbf{I}. \tag{3.12}$$

It also can be shown that the optimal weight vector given above also maximizes the signal-to-interference-plus-noise ratio (SINR) at the output of the MMSE receiver [43], which is given by

$$\mathrm{SINR}_j = \mathbf{a}_j^H \mathbf{P}_j^H \mathbf{H}_j^H \mathbf{R}_j^{-1} \mathbf{H}_j \mathbf{P}_j \mathbf{a}_j. \tag{3.13}$$

It is obvious from (3.13) that the SINR_j achieved by the MMSE receiver filter still depends on the carrier amplitudes of the jth user. Thus, it is possible to further improve the system performance by suitably choosing the user carrier amplitudes.

3.2 Signature Waveform Adaptations

Two different adaptation strategies of the carrier amplitudes, namely local adaptation and global adaptation, are presented in this section. In local adaptation, an individual user adapts his/her carrier amplitudes without taking any other users into account. Thus, one is interested in only the desired user's performance. On the other hand, in global adaptation, the users adapt their carrier amplitudes by considering the whole system's performance. In both methods it is assumed that the channel information is available at the receiver. More specifically, in local adaptation, the receiver needs to know only the desired user's channel information. In contrast, global adaptation requires that each receiver needs to know all other users' channel information as well as their receive filters. Moreover, a centralized receiver may be used to perform a joint detection (i.e., multiuser detection) for multiple users.

Both adaptation strategies can be implemented using either the *forward-backward* or the *joint* method, which are similar to the methods presented in [36] for single carrier CDMA systems. The *forward-backward* method switches between optimizing the receiver with a fixed transmitter and optimizing the transmitter with a fixed receiver. On the other hand, in the *joint* method one jointly optimizes the receive filters and the carrier amplitudes of the user. Although both methods should give the same performance, their convergence and complexity properties are different.

The last part of this section presents two procedures for adapting the carrier amplitude vectors of a group of users (i.e., multiuser adaptation). Specifically, one procedure is performed iteratively with local or global adaptation on the assumption that that each user has his/her own receivers. The other procedure is non-iterative and can be performed using a multiuser detector.

3.2.1 Local Adaptation

The problem at hand can be formulated as follows. Assume that user j is the user of interest for performance optimization. The goal is to obtain the optimal carrier amplitude vector, $\mathbf{a}_j$, that minimizes the MSE_j (or maximizes the SINR_j) at the output of the receive filter, subject to a constraint on the transmitted power of the jth user. Since $\mathbf{P}_j\mathbf{P}_j^H = \mathbf{I}$, the transmitted power can be computed simply as $\|\mathbf{P}_j\mathbf{a}_j\|^2 = \|\mathbf{a}_j\|^2$. Let ξ_j be the power constraint of the jth user. Then the above mentioned goal can be achieved by solving the following optimization problem:

$$\begin{aligned} \min_{\mathbf{a}_j} \quad & \text{MSE}_j = E\left\{\left\|b_j(i) - \mathbf{w}_j^H\mathbf{r}\right\|^2\right\} \\ \text{subject to} \quad & \|\mathbf{a}_j\|^2 \leq \xi_j. \end{aligned} \tag{3.14}$$

The solution to the above problem can be obtained by two methods: the *forward-backward* and the *joint* methods.

In the *forward-backward* method, one first optimizes the receiver, which is given by (3.10) in the forward step and then optimizes the transmitter in the backward step. Using the Lagrange multiplier μ_j, the objective function in (3.14) is written as

$$L_j = E\left\{\left\|b_j(i) - \mathbf{w}_j^H\mathbf{r}\right\|^2\right\} + \mu_j\left(\|\mathbf{a}_j\|^2 - \xi_j\right). \tag{3.15}$$

By assuming $\mathbf{w}_j$ was optimized (and hence fixed) and setting the gradient of (3.15) with respect to the carrier amplitudes to zero, one obtains the following condition for the optimal carrier amplitude vector

$$\mathbf{a}_j = \left(\mathbf{H}_j^H \mathbf{P}_j^H \mathbf{w}_j \mathbf{w}_j^H \mathbf{H}_j \mathbf{P}_j + \mu_j \mathbf{I}\right)^{-1} \mathbf{H}_j^H \mathbf{P}_j^H \mathbf{w}_j. \tag{3.16}$$

Using the matrix inversion lemma[1] [44] and invoking the equality in the constraint, the optimal solution for $\mathbf{a}_j$ can be further simplified to

$$\mathbf{a}_j = \nu \mathbf{H}_j^H \mathbf{P}_j^H \mathbf{w}_j \tag{3.17}$$

where $\nu = \sqrt{\xi_j / (\mathbf{w}_j^H \mathbf{H}_j^H \mathbf{H}_j \mathbf{w}_j)}$ is a scalar. The iterative procedure to implement this *forward-backward* method is illustrated in the following.

- *Step 1*: The jth user's transmitter sends the 1st data symbol using the initial carrier amplitudes $\mathbf{a}_j$. The initial carrier amplitudes can be set as $a_{j,m} = 1/\sqrt{N}$ for $m = 0, 1, \cdots, N-1$.

- *Step 2*: The weight vector $\mathbf{w}_j$ of the jth user's receive filter is then determined using (3.10) based on the current carrier amplitudes $\mathbf{a}_j$.

- *Step 3*: With the weight vector $\mathbf{w}_j$ computed in Step 2, the receiver estimates the new carrier amplitudes $\mathbf{a}_j$ using (3.17).

- *Step 4*: The receiver repeats Step 2 and Step 3 until the convergence of the MSE is achieved.

- *Step 5*: Once the minimum MSE is achieved, the receiver transmits the updated carrier amplitudes $\mathbf{a}_j$ back to transmitter via the feedback channel. The transmitter uses the updated carrier amplitudes to send the subsequent data symbols.

Unlike the *forward-backward* method, which switches between the transmitter and the receiver, the *joint* method provides a closed-form solution by jointly optimizing

[1] If $\mathbf{B} = (\mathbf{A} + \mathbf{XRY})$, then $\mathbf{B}^{-1} = \mathbf{A}^{-1} - \mathbf{A}^{-1}\mathbf{X}\left(\mathbf{R}^{-1} + \mathbf{YA}^{-1}\mathbf{X}\right)^{-1}\mathbf{YA}^{-1}$.

the carrier amplitudes and the receive filter for the jth user. This optimization problem can be formulated as follows:

$$\begin{aligned} \max_{\mathbf{a}_j} \quad & \text{SINR}_j = \mathbf{a}_j^H \mathbf{P}_j^H \mathbf{H}_j^H \mathbf{R}_j^{-1} \mathbf{H}_j \mathbf{P}_j \mathbf{a}_j \\ \text{subject to} \quad & \|\mathbf{a}_j\|^2 \leq \xi_j. \end{aligned} \tag{3.18}$$

Using the method of Lagrange multiplier, the above optimization problem can be stated as

Select $\mathbf{a}_j$ to maximize

$$L_j = \mathbf{a}_j^H \mathbf{P}_j^H \mathbf{H}_j^H \mathbf{R}_j^{-1} \mathbf{H}_j \mathbf{P}_j \mathbf{a}_j + \mu_j \left(\|\mathbf{a}_j\|^2 - \xi_j \right) \tag{3.19}$$

where μ_j is the Lagrange multiplier. Maximizing with respect to $\mathbf{a}_j$ yields the following necessary condition

$$\left\{ \mathbf{P}_j^H \mathbf{H}_j^H \mathbf{R}_j^{-1} \mathbf{H}_j \mathbf{P}_j \right\} \mathbf{a}_j = \nu \mathbf{a}_j. \tag{3.20}$$

That is, the optimal $\mathbf{a}_j$ is the eigenvector of $\left\{ \mathbf{P}_j^H \mathbf{H}_j^H \mathbf{R}_j^{-1} \mathbf{H}_j \mathbf{P}_j \right\}$ that maximizes the SINR_j. In other words, $\mathbf{a}_j$ should be chosen to align with the channel having the strongest signal component and the least interference. Note that, ν is the maximum eigenvalue of the associated matrix. The above mentioned problem analogous to that encountered in beam forming [45].

Note further that, if there is no multipath interference (i.e., $\mathbf{H}_j = \mathbf{I}$), then $\mathbf{a}_j$ is simply chosen as an eigenvector corresponding to the maximum eigenvalue of $\mathbf{R}_j^{-1}$. This implies that the optimum $\mathbf{a}_j$ lies in the subspace containing the least interference and noise. A similar observation was also made for optimal spreading sequence selection in DS-CDMA in [31] and [36]. It should be pointed out that in this optimization SINR_j is used instead of MSE_j. If MSE_j is considered, then a similar necessary condition to (3.20) can be obtained, where the only difference is that $\mathbf{R}_j^{-1}$ is replaced by $\mathbf{R}^{-1}$. Since $\mathbf{R}$ depends on $\mathbf{a}_j$, the condition obtained using SINR_j is more convenient to solve.

3.2.2 Global Adaptation

In this adaptation strategy, one wishes to find the carrier amplitudes from the perspective of optimizing the performance of the system as a whole. A single user or a group of users is allowed to adapt their carrier amplitudes in order to improve the global system's performance for given transmitted powers. Since the overall system's performance is of particular interest, instead of minimizing MSE_j individually, the minimization of their sum (i.e., the total mean square error, or TMSE) shall be considered as the performance criterion. Note that, compared to local adaptation, global adaptation penalizes any additional interference to other users as a result of the change in an individual user's carrier amplitudes.

In this adaptation, one wishes to find the optimum carrier amplitude vector of the jth user by minimizing the TMSE subject to the constraint on the transmitter power and on the assumption that each user implements his/her own MMSE receiver. Hence, the optimization problem can be formulated as follows:

$$\begin{aligned} \min_{\mathbf{a}_j} \quad & \text{TMSE} = \sum_{j=0}^{K-1} \text{MSE}_j = E\left\{\left\|\mathbf{b}(i) - \mathbf{W}^H\mathbf{r}\right\|^2\right\} \\ \text{subject to} \quad & \|\mathbf{a}_j\|^2 \le \xi_j, \quad j = 0, 1, \cdots, K-1 \end{aligned} \tag{3.21}$$

where $\mathbf{b}(i) = [b_0(i), b_1(i), \cdots, b_{K-1}(i)]^T$, $\mathbf{W} = [\mathbf{w}_0, \mathbf{w}_1, \cdots, \mathbf{w}_j, \cdots, \mathbf{w}_{K-1}]$ is the $N \times K$ matrix of receive filters and $\mathbf{r}$, $\mathbf{w}_j$ are given in (3.7) and (3.10), respectively. Again, using the Lagrange multiplier method, the objective function in the above optimization problem can be written as

$$L = E\left\{\left\|\mathbf{b}(i) - \mathbf{W}^H\mathbf{r}\right\|^2\right\} + \sum_{j=0}^{K-1} \mu_j[\|\mathbf{a}_j\|^2 - \xi_j]. \tag{3.22}$$

As in local adaptation the solution for (3.22) can be obtained using, either the *forward-backward* or the *joint* method.

In the *forward-backward* method, if the receive filters are assumed to be optimized (i.e., $\mathbf{w}_j : j = 0, 1, \cdots, K-1$ is fixed), one obtains the optimal $\mathbf{a}_j$ to minimize (3.22) to be

$$\mathbf{a}_j = \left(\mathbf{P}_j^H\mathbf{H}_j^H\mathbf{W}\mathbf{W}^H\mathbf{H}_j\mathbf{P}_j + \mu_j\mathbf{I}\right)^{-1}\mathbf{H}_j^H\mathbf{P}_j^H\mathbf{w}_j. \tag{3.23}$$

As with local adaptation, one iterates updating the transmitter in (3.23) and the receiver in (3.10) until the TMSE is minimized. It should be noted, however, that each update of $\mathbf{a}_j$ should satisfy the power constraint. This can be achieved by properly adjusting the Lagrange multipliers via a numerical search algorithm.

Note that, to obtain the optimal carrier amplitude vector in (3.23), requires knowledge of the receive filters as well as the channel information of all the users. This is in contrast to the optimal carrier amplitude vector given in (3.17) in local adaptation, where only knowledge of the desired users' channel information and the receive filter is required. Furthermore, the convergence of this method is slower than the *forward-backward* method in local adaptation. This is because this method needs to process the information of all other users, as is obvious from (3.23).

As with local adaptation, the optimal carrier amplitude vector can also be obtained using the *joint* method. In this case, instead of minimizing TMSE, maximizing the total SINR is considered to be the performance criterion since the related derivation is somewhat simpler. The optimization problem can be formulated as follows:

$$\begin{aligned} \max_{\mathbf{a}_j} \quad & \text{TSNIR} = \sum_{j=0}^{K-1} \text{SINR}_j = \sum_{j=0}^{K-1} \mathbf{a}_j^H \mathbf{P}_j^H \mathbf{H}_j^H \mathbf{R}_j^{-1} \mathbf{H}_j \mathbf{P}_j \mathbf{a}_j \\ \text{subject to} \quad & \|\mathbf{a}_j\|^2 \leq \xi_j, \quad j = 0, 1, \cdots, K-1. \end{aligned} \tag{3.24}$$

The Lagrange function L is then given by

$$L = \sum_{j=0}^{K-1} \mathbf{a}_j^H \mathbf{P}_j^H \mathbf{H}_j^H \mathbf{R}_j^{-1} \mathbf{H}_j \mathbf{P}_j \mathbf{a}_j + \sum_{j=0}^{K-1} \mu_j \left(\|\mathbf{a}_j\|^2 - \xi_j \right) \tag{3.25}$$

where μ_j is the Lagrange multiplier. The derivative of L with respect to $\mathbf{a}_j$ can be obtained as follows. Observe that $\mathbf{R}_j^{-1}$ ($\mathbf{R}_j$ is defined in (3.12)) is not a function of $\mathbf{a}_j$, while $\mathbf{R}_k^{-1}$ (for $k \neq j$) can be expressed explicitly as a function of $\mathbf{a}_j$ using the matrix inversion lemma [44] as follows:

$$\begin{aligned} \mathbf{R}_k^{-1} &= \left(\mathbf{R}_{k,j} + \mathbf{H}_j \mathbf{P}_j \mathbf{a}_j \mathbf{a}_j^H \mathbf{P}_j^H \mathbf{H}_j^H \right)^{-1} \\ &= \mathbf{R}_{k,j}^{-1} - \frac{1}{1 + \mathbf{a}_j^H \mathbf{P}_j^H \mathbf{H}_j^H \mathbf{R}_{k,j}^{-1} \mathbf{H}_j \mathbf{P}_j \mathbf{a}_j} \mathbf{R}_{k,j}^{-1} \mathbf{H}_j \mathbf{P}_j \mathbf{a}_j \mathbf{a}_j^H \mathbf{P}_j^H \mathbf{H}_j^H \mathbf{R}_{k,j}^{-1} \end{aligned} \tag{3.26}$$

where

$$\mathbf{R}_{k,j} = \sum_{\substack{i=0 \\ i\neq j,k}}^{K-1} \mathbf{H}_i \mathbf{P}_i \mathbf{a}_i \mathbf{a}_i^H \mathbf{P}_i^H \mathbf{H}_i^H + \sigma^2 \mathbf{I}. \tag{3.27}$$

Therefore, the derivative of L with respect to $\mathbf{a}_j$ is given by

$$\frac{\partial L}{\partial \mathbf{a}_j} = 2\left\{1 - \sum_{\substack{k=0 \\ k\neq j}}^{K-1} \frac{\zeta_{k,k}}{(1+\zeta_{j,k})^2}\right\} \mathbf{P}_j^H \mathbf{H}_j^H \mathbf{R}_{k,j}^{-1} \mathbf{H}_j \mathbf{P}_j \mathbf{a}_j + 2\mu_j \mathbf{a}_j \tag{3.28}$$

where $\zeta_{j,k} = \mathbf{a}_j^H \mathbf{P}_j^H \mathbf{H}_j^H \mathbf{R}_{k,j}^{-1} \mathbf{H}_j \mathbf{P}_j \mathbf{a}_j$. Setting $\partial L/\partial \mathbf{a}_j = 0$ gives the following condition for the optimal carrier amplitude vector

$$\mathbf{Q}_j \mathbf{a}_j = \nu \mathbf{a}_j \tag{3.29}$$

where

$$\mathbf{Q}_j = \left\{1 - \sum_{\substack{k=0 \\ k\neq j}}^{K-1} \frac{\zeta_{k,k}}{(1+\zeta_{j,k})^2}\right\} \mathbf{P}_j^H \mathbf{H}_j^H \mathbf{R}_{k,j}^{-1} \mathbf{H}_j \mathbf{P}_j \tag{3.30}$$

and $\nu = -\mu_j$. The optimal $\mathbf{a}_j$ is, therefore, the eigenvector of matrix $\mathbf{Q}_j$ which corresponds to the maximum eigenvalue of $\mathbf{Q}_j$. Although, solving (3.29) might look straightforward, it is complicated by the fact that $\mathbf{Q}_j$ depends on $\mathbf{a}_j$ through $\zeta_{j,k}$.

Instead of solving the problem in (3.24) directly, an iterative approach suggested in [37] can be used to seek a stationary point of the Lagrange function (3.25). Specifically, at each step, update $\mathbf{a}_j$ and μ_j according to the following relationships

$$\mathbf{a}_j \leftarrow \mathbf{a}_j - \epsilon \frac{\partial L}{\partial \mathbf{a}_j} \tag{3.31}$$

$$\mu_j \leftarrow \mu_j + \epsilon \left(\|\mathbf{a}_j\|^2 - \xi_j\right) \tag{3.32}$$

where ϵ is a parameter, which can be numerically chosen so that $\mathbf{a}_j$ satisfies the power constraint at each update. A gradient descent algorithm is used to update $\mathbf{a}_j$ while a gradient ascent algorithm can be used to update μ_j. The steps in (3.31) and (3.32) are repeated until the TSINR is maximized. It should be pointed out that the computational complexity of the *joint* method in global optimization is considerably

higher than the *forward-backward* method in global optimization. In addition, there can be multiple solutions, corresponding to local optima of the objective function. Consequently, for performance comparison in Section 3.3, results are obtained only by the *forward-backward* method.

3.2.3 Multiuser Adaptation

In multiuser adaptation, a group of users are allowed to adapt their carrier amplitudes simultaneously. This can be performed iteratively by assuming that each user implements its own receiver, or non-iteratively using a multiuser detector.

The iterative update can be performed with either global or local adaptation. In both adaptation strategies, the *forward-backward* and the *joint* methods lead to two different iterative algorithms for seeking the optimum points for multiuser adaptation [36]. Assume that the users' carrier amplitude vectors are assigned initially as $\mathbf{a}_1 = \mathbf{a}_2 \cdots = \mathbf{a}_j = \cdots = \mathbf{a}_K$, with $a_{j,m} = 1/\sqrt{N}$, $j = 0, 1 \cdots, K-1$. In global adaptation, the *forward-backward* method implies that all the receive filters are optimized according to (3.10) in the forward step, followed by the optimization of the carrier amplitude vectors of all the users as in (3.23) in the backward step, and so on. This updating procedure is illustrated in Fig. 3.3-(a), where it is referred to as horizontal optimization, since all the receivers in the forward step or all the transmitters in the backward step are lined up horizontally. On the other hand, in the *joint* method, condition (3.29) can be applied successively across all users, which can be referred to as vertical or user-by-user optimization in Fig. 3.3-(b). This is because the transmitter and the receiver for a particular user are lined up vertically. Note that the TMSE must converge in either case, since it cannot increase after an update. The horizontal and vertical optimizations can also be applied by iterating the optimal conditions obtained in local adaptation across all the users. In this case it is shown in [32, 36] that the convergence to a fixed point is more difficult to establish. Due to this difficulty, this algorithm shall not be considered for multiuser adaptation in this chapter.

It can be seen from the above discussion that the iterative algorithm takes time

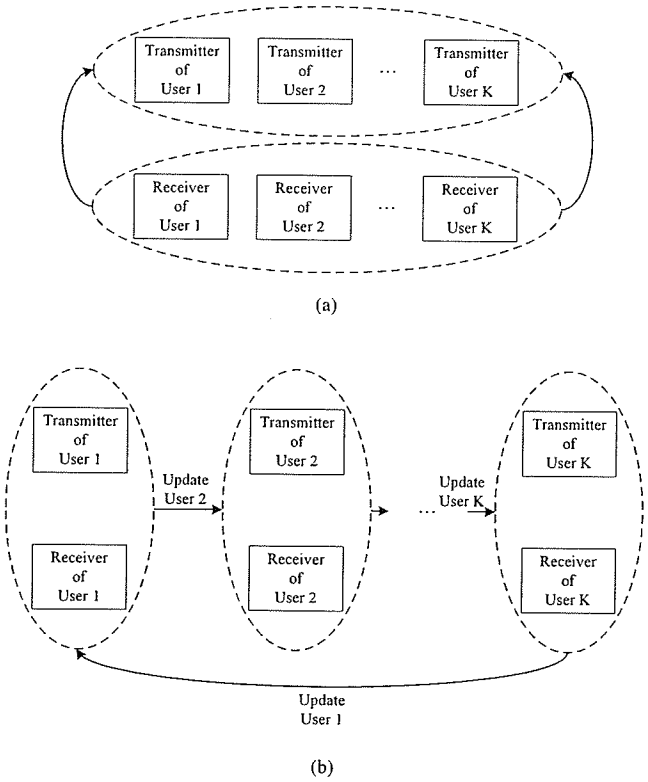

Figure 3.3: Multiuser adaptation using iterative method (a) Horizontal optimization and (b) Vertical optimization.

to converge. Also its computational complexity is quite high. For example, consider horizontal optimization. In each backward step one needs to compute the carrier amplitude vector for every user. Computing the carrier amplitude vector for a specific user is time consuming because one needs to obtain the Lagrange multiplier numerically in order to satisfy the power constraint of that particular user. Furthermore, this procedure needs to be repeated for all users.

Rather than using the horizontal or vertical iterative algorithm across all the users, one can obtain the carrier amplitude vectors of all the users in one step by performing multiuser detection and jointly optimizing the carrier amplitude vectors of all the users. This non-iterative method is described in the following. The optimization

problem now can be formulated as

$$\begin{aligned} \min_{\mathbf{A}} \quad & \text{TMSE} = E\left\{\left\|\mathbf{b}(i) - \mathbf{W}^H\mathbf{r}\right\|^2\right\} \\ \text{subject to} \quad & \|\mathbf{a}_j\|^2 \leq \xi_j, \quad j = 0, 1, \cdots, K-1 \end{aligned} \tag{3.33}$$

where $\mathbf{W} = \mathbf{R}^{-1}\mathbf{HPA}$ is the optimal weight matrix of the MMSE multiuser receiver; $\mathbf{H} = [\mathbf{H}_0, \cdots, \mathbf{H}_k, \cdots, \mathbf{H}_{K-1}]$ is an $N \times NK$ channel matrix of all users in the group; $\mathbf{P} = \text{diag}(\mathbf{P}_0, \cdots, \mathbf{P}_k \cdots, \mathbf{P}_{K-1})$ is an $NK \times NK$ block-diagonal matrix formed by grouping all the K users' carrier phases together; and $\mathbf{A} = \text{diag}(\mathbf{a}_0, \cdots, \mathbf{a}_k \cdots, \mathbf{a}_{K-1})$ is the $NK \times K$ block-diagonal matrix containing the carrier amplitudes of all the users in the group. Note that the formulation of this optimization problem is different from the problem described in (3.21).

Let $\mathbf{H} = \mathbf{U}\boldsymbol{\Sigma}\mathbf{V}^H$ be the singular-value decomposition of matrix $\mathbf{H}$, where $\mathbf{V}$ and $\mathbf{U}$ are $NK \times NK$ and $N \times N$ unitary matrices, respectively. It is assumed that the singular values ε_n are arranged in a descending order in the diagonal matrix

$$\boldsymbol{\Sigma} = \begin{bmatrix} \varepsilon_1 & & & \\ & \varepsilon_2 & & \mathbf{0} \\ & & \ddots & \\ & & & \varepsilon_N \end{bmatrix} \tag{3.34}$$

and that $\mathbf{H}$ is of full rank, i.e., $\varepsilon_n > 0$ for $n = 1, 2, \cdots, N$. For simplicity assume $K = N$. Let $\upsilon_1, \upsilon_2, \cdots, \upsilon_n, \cdots, \upsilon_N$ ($\upsilon_n > 0$; $n = 1, 2, \cdots, N$) be the eigenvalues of $\mathbf{F}^H\mathbf{F}$ arranged in descending order, where $\mathbf{F} = (\mathbf{H}^H\mathbf{H})^{1/2}\mathbf{B}/\sigma$ and $\mathbf{B} = \mathbf{PA}$. Then the optimization problem in (3.33) can be simplified to

$$\begin{aligned} \min_{\upsilon_n} \quad & \text{TMSE} = \sum_{n=1}^{N} \frac{1}{\upsilon_n + 1} \\ \text{subject to} \quad & \sum_{n=1}^{N} \frac{\upsilon_n}{\varepsilon_n^2} \leq \frac{\xi}{\sigma^2} \end{aligned} \tag{3.35}$$

where $\xi = \sum_{j=0}^{K-1} \xi_j$. The proof that the problem defined in (3.33) is equivalent to the problem defined in (3.35) is provided in Appendix A. Solving the problem in

(3.35) and combining the solution with problem defined in (3.33), the optimal carrier amplitude matrix that achieves the minimum TMSE is given by the following proposition.

Proposition 1: Given K, N, σ and $\mathbf{H}$, let $\widetilde{\mathbf{V}}$ be a $K \times K$ unitary matrix such that

$$\operatorname{diag}\left(\widetilde{\mathbf{V}}\operatorname{diag}\left(\frac{\upsilon_1}{\varepsilon_1^2}, \frac{\upsilon_2}{\varepsilon_2^2}, \cdots, \frac{\upsilon_N}{\varepsilon_N^2}\right)\widetilde{\mathbf{V}}^H\right) = \operatorname{diag}\left(\xi_1, \xi_2, \cdots, \xi_K\right). \tag{3.36}$$

Then, the optimal carrier amplitude matrix is

$$\mathbf{A} = \sigma \mathbf{P}^H \mathbf{V} \begin{bmatrix} \frac{\sqrt{\upsilon_1}}{\varepsilon_1} & & & & \\ & \ddots & & & \\ & & \frac{\sqrt{\upsilon_n}}{\varepsilon_n} & & \\ & & & \ddots & \\ & & & & \frac{\sqrt{\upsilon_N}}{\varepsilon_N} \\ & & \mathbf{0} & & \end{bmatrix} \widetilde{\mathbf{V}}^H \tag{3.37}$$

where

$$\upsilon_n = \varepsilon_n \left[\frac{\frac{\xi}{\sigma^2} + \sum_{l=1}^{N} \frac{1}{\varepsilon_l^2}}{\sum_{l=1}^{N} \frac{1}{\varepsilon_l}} \right] - 1. \tag{3.38}$$

The proof of the above proposition is given in Appendix B.

The results provided by Proposition 1 implies the following. If one thinks about the eigenvectors of the matrix $\mathbf{H}^H\mathbf{H}$ as the vectors that define a space spanned by the MC-CDMA systems having the channel matrix $\mathbf{H}$, the selection of the optimal carrier amplitude matrix $\mathbf{A}$ above chooses good channels (corresponding to large eigenvalues), while discarding the bad channels (with small eigenvalues). In the absence of fading (such as AWGN channels), the channel matrix is an identity matrix, i.e., $\mathbf{H} = \mathbf{I}$, which implies that the channel is equally good. In this case, carrier amplitudes are evenly occupied by the whole channel space (see Appendix C), which is consistent with the results obtained in [37].

In general, establishing the convergence of optimization with individual cost functions to a fixed point in the presence of multipath, remains an open problem. The

numerical results in Section 3.3, indicate that the iterative algorithm presented here generally converges to the optimal solution.

3.3 Performance Comparisons

This section illustrates the performance of the proposed ACI-MC-CDMA system and compares it with the conventional CI-MC-CDMA systems studied in [15]. The numerical results are obtained via computer simulations using MATLAB. The performance comparison is twofold. In Section 3.3.1, the system performance is evaluated based on the SINR at the output of the receiver. The relative performance of the proposed adaptation strategies is first presented and the proposed ACI-MC-CDMA performance is compared with that of conventional CI-MC-CDMA. Here both single and multiuser adaptation is considered.

As described in the beginning of this chapter, the PAPR is high for conventional CI-MC-CDMA system. Unlike the CI-MC-CDMA system, in the proposed ACI-MC-CDMA, PAPR reduction (or elimination) is achieved through the adaptation strategies that simultaneously improve the systems performance. Section 3.3.2 presents the PAPR comparison between ACI-MC-CDMA system and CI-MC-CDMA system.

3.3.1 SINR Performance

To investigate the performance of the proposed ACI-MC-CDMA systems with various adaptation algorithms presented in the previous section, consider a system with $N = 16$ carriers. The channel gains $h_{k,m}$, $k = 0, 1, \cdots, K-1$ and $m = 0, 1, \cdots, N-1$ are normalized so that the average power is unity, i.e., $E\{\|\mathbf{H}_k\|^2\} = 1$. A power constraint $\|\mathbf{a}_k\| = 1$ is set for all users $k = 0, 1, \cdots, K-1$.

First, the performance of single user adaptation is considered. Fig. 3.4 illustrates the convergence of SINR at the output of the receive filter for the first user and for different adaptation algorithms. Here the number of users in the system is $K = 8$ and the signal-to-noise ratio (SNR) is set at 16dB. The first user is assumed to be the desired user, while other users are treated as interference users. Observe that, as

the number of iterations increases, the performance of the forward-backward method in local adaptation converges to that of the joint method. Furthermore, it can be seen that the forward-backward method in global adaptation needs more iterations to converge than the local adaptation.

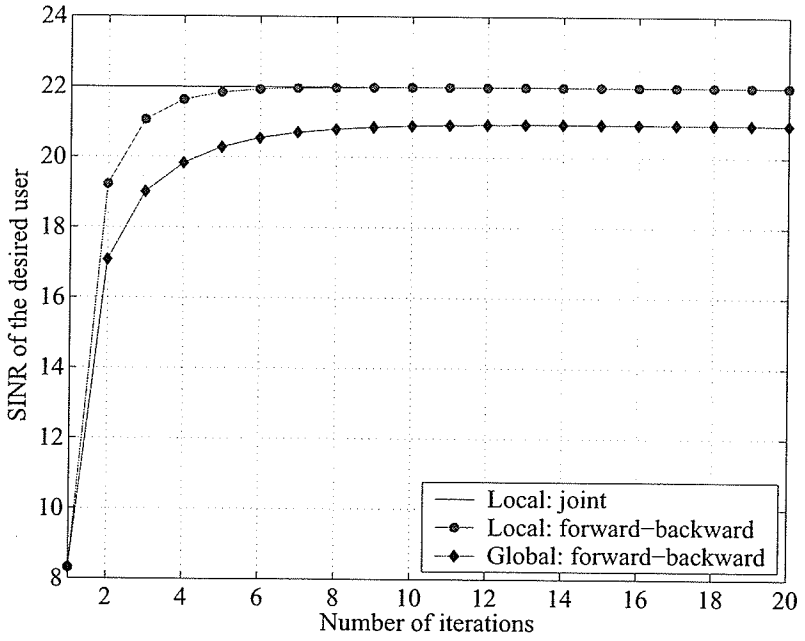

Figure 3.4: Convergence of the SINR with single user adaptation: $N = 16$, $K = 8$ and SNR = 16dB.

Figure 3.5 shows the SINR performance of the first user versus the channel SNR for the case $K = 16$. As expected, local adaptation performs better than global adaptation. This is because the global adaptation takes the performance of other users into account, which compromises the performance of the desired user. In addition, it was observed before that global adaptation needs more computation time to converge. Performance comparison of the proposed ACI-MC-CDMA and the conventional CI-MC-CDMA in [15] clearly shows that ACI-MC-CDMA outperforms CI-MC-CDMA. For example, at SNR = 10dB, local adaptation in ACI-MC-CDMA provides a gain of about 5.0dB in SINR over the conventional CI-MC-CDMA. Although the global adaptation is unable to achieve the same performance, it still offers a 4.0dB gain over the conventional CI-MC-CDMA.

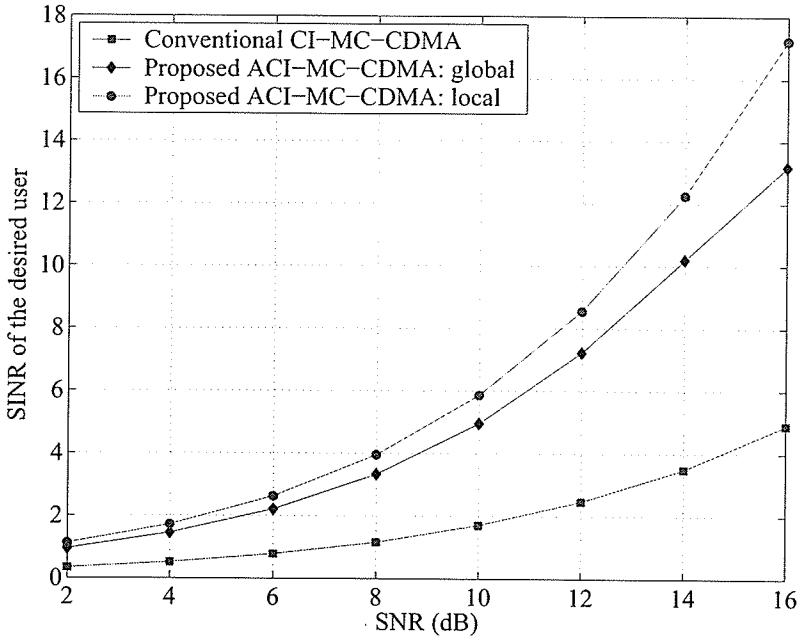

Figure 3.5: Performance for single user adaptation: $N = 16$ and $K = 16$.

Figure 3.6 also demonstrates the performance of various systems as a function of the number of users K. As the number of users increases, there is a performance degradation for all systems due to the increase in multiuser interference. Observe from this figure that the global adaptation performs very close to the local adaptation for small number of users. When K becomes larger, there is a clear performance gap between the two adaptation strategies. This again is due to the fact that global adaptation takes the performance of other users into account, which compromises the performance of the desired user.

Also observe that, the performance of the conventional CI-MC-CDMA decreases slowly when K increases up to 16. However, there is an abrupt performance degradation once K increases beyond 16. This observation is consistent with the fact that the CI codes are orthogonal when $K \leq N$, whereas the CI codes are pseudo-orthogonal for $K > N$. This observation is also in contrast to the proposed ACI-MC-CDMA where, for both the local and global adaptations, the performance degradation is more graceful when K increases.

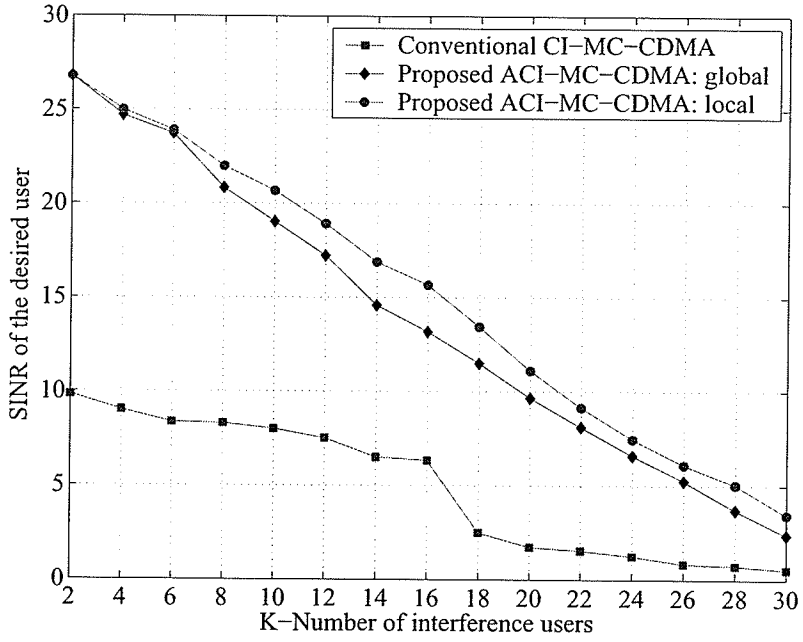

Figure 3.6: Influence of the number of interference users in single user adaptation: $N = 16$ and SNR $= 16$dB.

Finally, the performance of multiuser adaptation is presented in Fig. 3.7. Since multiuser adaptation is considered, the *average* SINR is the performance measure used in this figure. Similar to single user adaptation, a substantial performance gain is also obtained by the proposed ACI-MC-CDMA using multiuser adaptation over the conventional CI-MC-CDMA. Moreover, it can be seen from this figure that the performance of multiuser adaptation provides a substantial gain over CI-MC-CDMA. At the SNR of 12 dB this gain is in the neighborhood of $5 - 7$dB. The larger gain is given by the non-iterative method. However it should be mentioned again that the computational complexity of iterative algorithm is higher than that of the proposed non-iterative method.

In this section one has demonstrated that the proposed ACI-MC-CDMA systems outperforms the conventional CI-MC-CDMA. However, it is important to keep in mind that such performance improvement comes at the expense of a higher system complexity, which depends on the particular adaptation strategy chosen.

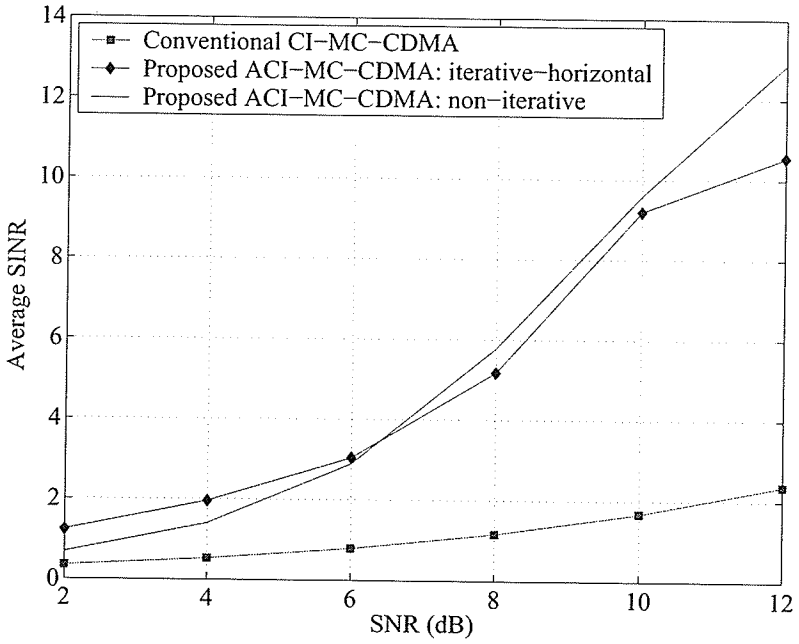

Figure 3.7: Performance for multiuser adaptation: $N = 16$ and $K = 16$.

3.3.2 PAPR Performance

This section presents the PAPR benefits of the proposed ACI-MC-CDMA systems. One common problem regarding the use of MC-CDMA with carrier interferometry codes is the high peak-to-average power ratio (PAPR) [46]. High peaks in the power result from highly fluctuating envelopes, a consequence of using independently modulated carriers. This, in turn, leads to an inefficient operation of the transmit power amplifier because an increased signal dynamic range requires power amplifiers with a greater linear region of operation.

The signal envelope compactness can be measured using the crest factor (CF) [47, 48] which relates to the PAPR as

$$CF = \sqrt{PAPR} = \frac{\|u(t)\|_\infty}{\|u(t)\|_2} \tag{3.39}$$

where $u(t)$ is the multicarrier signal, $\|u(t)\|_\infty$ corresponds to the maximum absolute value of $u(t)$ and $\|u(t)\|_2$ is the root-mean-square (RMS) value of $u(t)$. For the uplink, $u(t) = b_k(i)s_k(t) = s_k(t)$; and $u(t) = \sum_{k=0}^{K-1} b_k(i)s_k(t)$ for the downlink, where $s_k(t)$

is the signature waveform of the kth user defined in (3.3). It then follows that the PAPR of an uplink system directly depends only on the amplitudes of the carriers. On the other hand, the PAPR of a downlink system depends on the amplitudes of the carriers as well as the users' transmitted bits.

In CI-MC-CDMA systems, the amplitudes of all the carriers are the same (i.e., $a_{k,m} = 1$ for all m). Hence, the amplitude of the signature waveform of each user becomes N. This is the reason why a CI-MC-CDMA system produces a higher CF for the uplink. Although the signature waveform of an individual user has a poor CF, it is shown in [38] that, the combined signal in the downlink improves the CF tremendously. Such a reduction in the CF is due to the averaging effect of the users's random transmitted information bits. Furthermore, in [49] the CF in the downlink of a fully-loaded CI-MC-CDMA system was theoretically analyzed. It is proved in [49] that the peak behavior of a fully-loaded CI-MC-CDMA system is better than the traditional MC-CDMA.

More recently, reference [46] shows that when $K < N$, the downlink CF degrades gradually and approaches the uplink CF as K tends to 1. Furthermore, it is demonstrated that the CFs of a fully-loaded CI-MC-CDMA uplink system as well as a partially-loaded CI-MC-CDMA downlink system can be brought to very low values by applying the Schroeder's simple CF reduction technique [50].

Specifically, the CF reduction technique used in [46] introduces a phase correction into each carrier at the transmitter side. Consequently, the amplitudes of carriers are allowed to be different and can be positive or negative. This modification of the carrier amplitudes helps to reduce the amplitudes of the signature waveforms compared to that of the traditional CI-MC-CDMA, and as a direct consequence, produces a low CF.

Although the ACI-MC-CDMA system is proposed to primarily achieve a better system performance in terms of the SINR, it shall be demonstrated in this subsection that the proposed ACI-MC-CDMA possesses a second desirable properly, namely a low CF. In ACI-MC-CDMA, as explained in the previous sections, the carrier amplitudes $a_{k,m}$ are allowed to vary. Therefore, unlike CI-MC-CDMA, but similar

to the phase-corrected CI-MC-CDMA, the carriers have different amplitudes and different signs. Note, however, that rather than varying the carrier amplitudes based on a fixed (and optimal) set of Schroeder codes [50] (usually found by a computer search) as in the phased-corrected CI-MC-CDMA, the carrier amplitudes are varied adaptively in ACI-MC-CDMA according to the channel conditions.

From the above discussion, it is reasonable to predict that the CF of the proposed ACI-MC-CDMA is lower than that of the conventional CI-MC-CDMA, but it might be higher than the CF of the phase-corrected CI-MC-CDMA. Such a prediction is confirmed by the numerical results in the following.

Fig. 3.8 shows the CF levels of the uplink ACI-MC-CDMA with local adaptation over 100,000 transmissions. The results were obtained with $N = 16$ carriers and for SNR=4dB (Fig. 3.8-(a)) and SNR=16dB (Fig. 3.8-(b)). Observe from Fig. 3.8-(a) that most of the CF values stay closer to the mean CF level of 1.62 and some values exceed 2.2 (a typical acceptable CF value [46]). This can be clearly observed from Table. 3.1. However, no CF values are higher than 3.47. Similarly, for SNR=16dB, Fig. 3.8-(b) displays no CF values above 4.35 and most of the CF values stay closer to the mean CF level of 1.89. Compared to the case when SNR=4dB, the percentage of the CF values exceeding 2.2 is higher for SNR=16dB (see Table. 3.1). Although there is a small variation in CF levels between SNR=4dB and SNR=16dB, the proposed ACI-MC-CDMA generally has much lower CF values compared to the conventional CI-MC-CDMA system, where for $N = 16$ carriers the CF level is 4.00.

Table 3.1: The statistics of Uplink $\sqrt{PAPR}$ for $N = 16$.

	SNR=4dB	SNR=16dB
Mean	1.62	1.89
Variance	0.04	0.08
Maximum	3.47	4.35
Percentage that $\sqrt{PAPR} > 2.2$	1%	15%

The cdf's of CF with different adaptation strategies are illustrated in Fig. 3.9 for $N = 16$ carriers. Similar to the SINR performance, it is observed that the CF

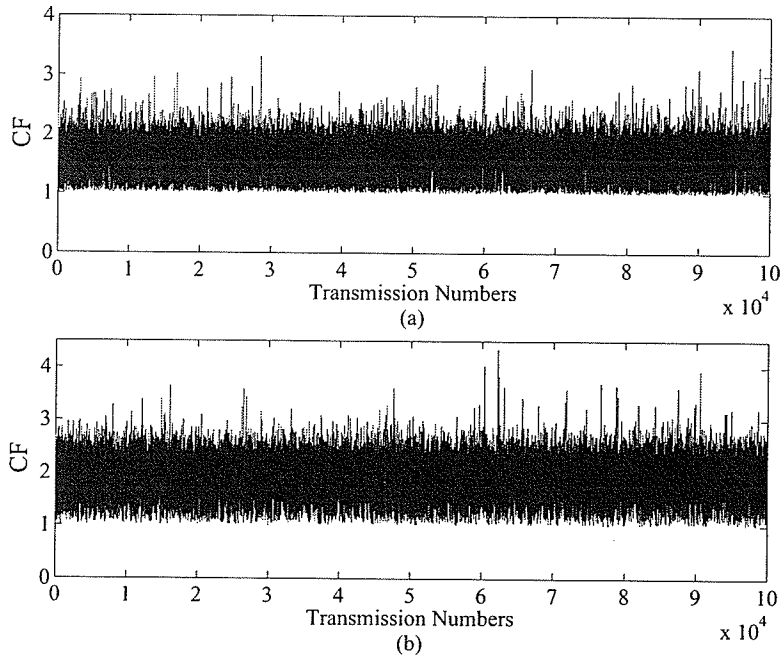

Figure 3.8: CF per transmissions with local adaptation for (a) SNR=4dB and (b) SNR=16dB: $N = 16$.

performance with the local adaptation is better than that with the global adaptation. More specifically, as can be determined from Fig. 3.9, with local adaptation, the probability that the CF $\geq$ 2.2 is less than 3% and 15% for SNR=4dB and SNR=16dB, respectively. On the other hand, with global adaptation, the probability that CF $\geq$ 2.2 is less than 10% for SNR=4dB and 40% for SNR=16dB.

Table 3.2 summarizes and compares the (mean) CF values of different MC-CDMA schemes in the uplink and for various number of carriers. The CF values of the conventional CI-MC-CDMA system can be computed analytically, while the CF values of the phase-corrected CI-MC-CDMA system are taken from [46]. Observe from Table 3.2 that the CF values of the conventional CI-MC-CDMA increases with increasing N and are the highest compared to the CF values of the other two schemes. Although the CF values of the ACI-MC-CDMA are higher than that of the phase-corrected CI-MC-CDMA, they are well within the tolerable levels of power amplifiers. Similar to the phase-corrected CI-MC-CDMA, the CF values of the ACI-MC-CDMA remain

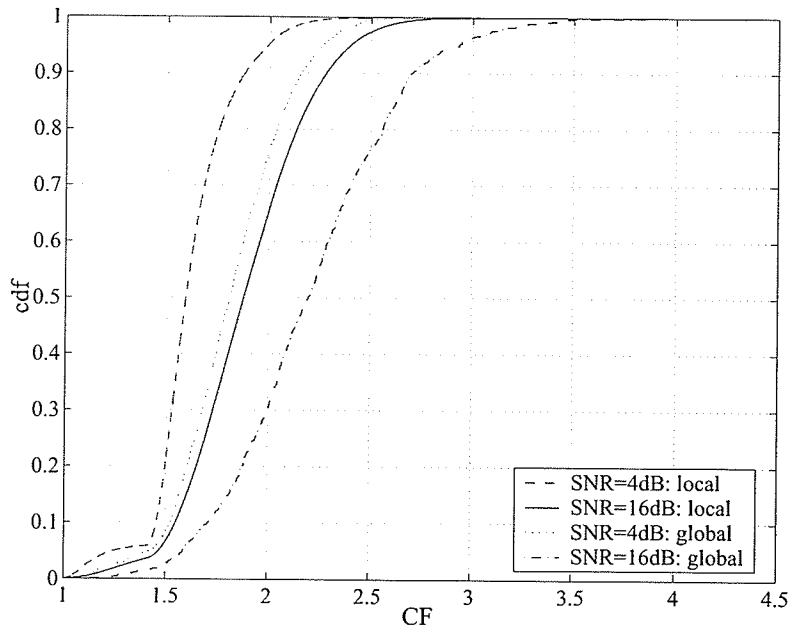

Figure 3.9: Cumulative density functions of CF with different SNRs' and different adaptation strategies: $N = 16$.

almost constant regardless of the number of carriers. But different from both the conventional and phase-corrected CI-MC-CDMA, the CF values of the ACI-MC-CDMA increase with the increasing channel SNR. This is of course the direct consequence of adapting the the carrier amplitudes in accordance with the channel condition in ACI-MC-CDMA.

3.4 Summary

Adaptive CI-MC-CDMA systems have been proposed and studied in this chapter. The novelty in the proposed systems is that the amplitudes of the subcarriers are allowed to change according to the channel conditions. Two adaptive strategies, namely local and global adaptations were presented to update the carrier amplitudes. In multiuser adaptations the proposed non-iterative algorithm performs slightly worse than the iterative algorithm at low channel signal-to-noise ratio, but it gives a considerable performance gain at high channel signal-to-noise ratio. In single user adaptation, the

Table 3.2: Uplink $\sqrt{PAPR}$ values for different number of carriers N.

N	$CF = \sqrt{PAPR}$					
	CI-MC-CDMA		ACI-MC-CDMA			
	Conventional	Phase-Corrected	Local		Global	
			SNR		SNR	
			4dB	16dB	4dB	16dB
8	2.82	1.36	1.68	1.88	1.88	2.12
16	4.00	1.37	1.62	1.89	1.82	2.21
32	5.65	1.37	1.58	1.85	1.71	2.30

local adaptive algorithm performs much better than the global adaptive algorithm. Beside having different performance, each of the considered algorithms has its own advantages and disadvantages in terms of implementation. Which adaptation strategy to use therefore depends on the particular application. More importantly, numerical results show that there is a considerable performance gain provided by the proposed ACI-MC-CDMA over the conventional CI-MC-CDMA considered in [15]. In addition to this, it has also been shown that the proposed ACI-MC-CDMA is also attractive in terms of PAPR reduction.

Chapter 4

Phase Offset Assisted MC-DS-CDMA Systems

This chapter is again devoted to MC-DS-CDMA systems. It was shown in Chapter 2 that for a given system bandwidth and transmission rate, by jointly designing the chip waveform and carrier spacing one can reduce the MAI especially for high values of roll-off factors. However, the MAI reduction is quite marginal. Furthermore, it was observed that the optimal carrier spacing (normalized carrier spacing) is close to one. This implies that the MAI induced by other users from other subcarriers is smaller than the MAI induced by the other users from the same subcarrier. The MAI induced by the other users from the same carrier, can be reasonably reduced by employing multiuser detectors at the receiver. However the correlation receiver is still the only practical solution because the complexity of multiuser detection is usually prohibitive in multi-carrier CDMA systems with a large number of users.

As in Chapter 2, a common and important performance measure for the correlation receiver is the SINR. In order to maximize the SINR, it is necessary to minimize the variance of the MAI at output of the receiver. Ideally, the MAI can be made zero by employing orthogonal signature waveforms for each user. However this limits the number of users that share the available resources. Therefore, for a given system bandwidth, the set of signature waveforms that produces a minimum MAI is desired. Finding such signature waveforms is the goal of this chapter. In order to make the analysis simpler, this chapter concentrates only on synchronous MC-DS-CDMA systems.

It is important to note that for a system with two users, when the desired user's signature waveform and the interfering user's signature waveform are exactly phase shifted by $\pi/2$ degrees, the MAI is zero. Motivated by this observation, this chapter introduces a novel construction of signature waveforms such that the cross correlations among users' signature waveforms are minimized, hence minimizing the MAI. The approach is as follows. As in conventional MC-DS-CDMA, each user simultaneously transmits the information over M carriers. However, unlike conventional MC-DS-CDMA, over each carrier, the user's data is spread by the user's specific spreading code and the spread data is transmitted with a carrier having a carefully chosen phase offset to ensure that the overall cross correlations among the users' signature waveforms are minimized. Hence the proposed system is called phase offset assisted MC-DS-CDMA. Two phase offset assisted systems, namely carrier-based and user-based, are introduced.

In carrier-based phase offset, a carefully chosen phase offset is introduced in each carrier to minimize the MAI. In this scheme, it is found that there are only $2M$ phase offsets available, M the number of carriers in the system. Therefore, when the total number of users in the system less than twice the number of carriers, for each user a different phase offset can be assigned. However, when the total number of users in the system exceeds $2M$, the same phase offset needs to be assigned to several users. This scheme is shown to have a MAI reduction of about 50% compared to the conventional MC-DS-CDMA systems. Additionally, it reduces the PAPR problem present in the conventional MC-DS-CDMA systems. The MAI performance, however, is not uniform among the carriers.

By contrast, in user-based phase offset, each user is assigned a different phase offset where, unlike carrier-based phase offset the same phase offset is used in all the carriers. The advantage of this assignment is that the MAI performance is uniform over all the carriers and also over all users. This approach also reduces the MAI by 50%, compared to conventional MC-DS-CDMA systems. However, unlike carrier-based phase offset, this system does not have any PAPR benefit.

The proposed approach improves the system performance in an additive white

Gaussian channel for both downlink and uplink. However, in fading channels, the performance improvement is only for the downlink, not the uplink communication. This is because the fading channel's phase response is completely random in uplink communication. Therefore at the receiver when phase correction is performed on the desired user signal, it does not simultaneously correct the phases of the interference users' signals. On the other hand, for downlink communications, i.e., transmissions from the base station to the terminals, a terminal receives interfering signals designated for other users through the same channel as the desired user's signal. Thus, there is only one set of amplitudes and phases describing the channel for all users' signals. This implies that when phase correction is applied on the desired user signal at the receiver, the phase of the interfering users' signals will also be corrected. This is the main reason why the proposed system performs better than the conventional MC-DS-CDMA system [10] over fading channels for the downlink.

The remainder of this chapter is organized as follows. The next section introduces the system model for the phase offset assisted MC-DS-CDMA system. The phase offset assignment methods, are described in Section 4.2 and Section 4.3. Section 4.4 presents the tradeoff between carrier-based and user-based phase offset systems. Finally, the chapter summary is provided in Section 4.5.

4.1 System Model

Consider a band-limited MC-DS-CDMA system in downlink with M carriers and K users. Different from Chapter 2, this chapter considers the system to be synchronous with a fixed carrier spacing, $\Delta = B_c$, between the adjacent carriers. That is, the subcarriers do not overlap. Hence, there will be no inter-carrier interference. The corresponding power spectral density of the system is shown in Fig. 4.1. Then, according to Fig. 4.1, the system's total bandwidth and the bandwidth of the subcarrier are related by

$$B_T = MB_c. \tag{4.1}$$

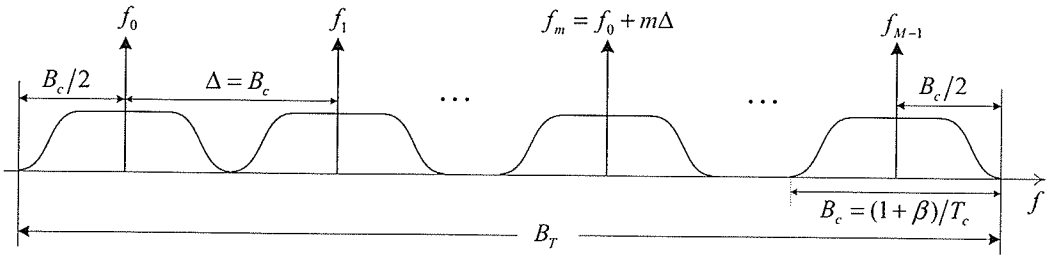

Figure 4.1: The PSD of a band-limited phase offset assisted MC-DS-CDMA system.

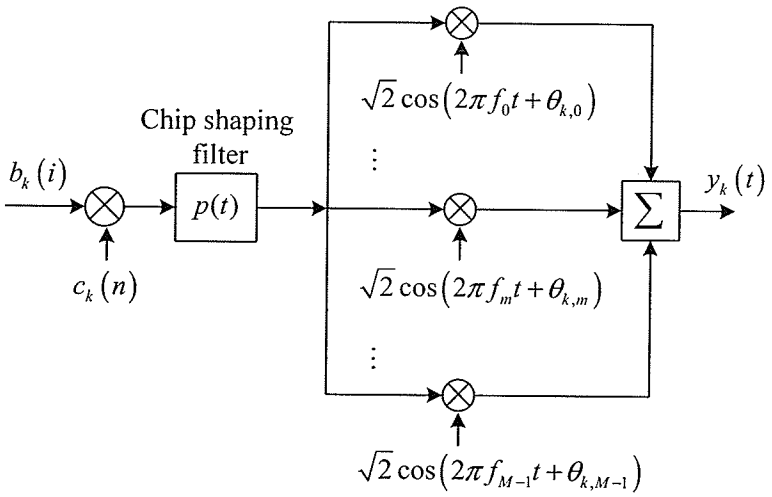

Figure 4.2: The transmitter of the kth user in an phase offset assisted MC-DS-CDMA system.

The transmitter of the kth user is shown in Fig. 4.2, which is similar to the one described in [10]. At the transmitter, each user's bit, $b_k(i) \in \{+1, -1\}$, with bit duration T_b, is copied into M parallel branches, where each branch corresponds to a different subcarrier frequency. Note that, here one transmits the same bit on all the subcarriers, whereas in chapter 2, one transmitted different bits on different subcarriers. At each branch, $b_k(i)$ is spread first by a spreading sequence $\mathbf{c}_k = \{c_k(0), \ldots, c_k(N-1)\}$ of length N. Similar to Chapter 2, this chapter also considers the spreading sequences to be random spreading sequences. Moreover, for a bit duration T_b, there are N chips. Thus, $T_b = NT_c$. Using this relationship and (4.1), for fixed B_T and T_b, the number

of carriers M and the processing gain N of the proposed system is related by

$$N = \frac{F}{(1+\beta)M} \tag{4.2}$$

where $F = B_T T_b$.

After spreading, the signal is modulated by a subcarrier with a carefully chosen phase offset $\theta_{k,m}$. The transmitted signal which corresponds to the ith data symbol of the kth user is

$$y_k(t) \;=\; \sqrt{2E_c}b_k(i)s_k(t),\; -\infty \leq t \leq \infty \tag{4.3}$$

where E_c is the energy per chip. The effective signature waveform of the kth user, $s_k(t)$, is constructed as follows:

$$s_k(t) = \sum_{n=0}^{N-1} c_k(n)p(t-nT_c) \sum_{m=0}^{M-1} \cos\left(2\pi f_m t + \theta_{k,m}\right). \tag{4.4}$$

In (4.4), $f_m = f_0 + m\Delta$ is the mth subcarrier frequency. The chip waveform $p(t)$ is band-limited to $[-B_c/2, B_c/2]$ and satisfies the Nyquist criterion. Furthermore it is assumed that $\int_{-\infty}^{\infty} |p(t)|^2 dt = 1$.

Observe from (4.4) that the signature waveform of a specific user is described by the number of carriers M, the processing gain N, the shape of the chip waveform $p(t)$, the carrier spacing Δ and the phase offset $\theta_{k,m}$. Thus, the present framework gives a great flexibility to design the users' signature waveforms. The present construction of signature waveforms unifies several variants of signature waveforms proposed to date. By setting $\theta_{k,m} = 0$, the current system becomes the conventional MC-DS-CDMA proposed in [10]. On the other hand, by setting $N = 1$ and $c_k(n) = 1$, i.e., no spreading in time domain, it reduces to the frequency domain spreading system, known as CI-MC-CDMA described in [15]. Moreover, the traditional SC-CDMA systems corresponds to $\Delta = 0$, $\theta_{k,m} = 0$ and $M = 1$.

Assuming that the channel is slow varying frequency-selective Rayligh fading as

described in Chapter 2, the received signal can be written as

$$r(t) = \sqrt{2E_c}\sum_{k=0}^{K-1} b_k(i)\sum_{n=0}^{N-1} c_k(n)p(t-nT_c) \cdot \sum_{m=0}^{M-1} \alpha_m \cos\left(2\pi f_m t + \theta_{k,m} + \varphi_m\right) + n(t) \quad (4.5)$$

where $n(t)$ is additive white Gaussian noise with two-sided power spectral density of $N_0/2$. Observe that, different from Chapter 2, the fading amplitude, $\alpha_{k,m} = \alpha_m$, $\forall\ k$ and phase of the mth subchannel, $\varphi_{k,m} = \varphi_m$, $\forall\ k$. This is because, here the channel is considered only for downlink. The fading amplitudes are assumed to be i.i.d.

The receiver structure of the proposed system is illustrated in Fig. 4.3 for user k. Each branch consists of a chip-matched filter, a correlator and a combiner with weights. The output of the chip-matched filter is sampled every T_c seconds and then correlated with the corresponding time domain spreading sequence. The correlated outputs of all the branches are combined to generate the decision statistic. Here the maximal ratio combiner [10], which maximizes the SINR at the input of the comparator, is used to determine the weight vector $\mathbf{w}_k = [w_{k,0}, \ldots, w_{k,m}, \ldots, w_{k,M-1}]$.

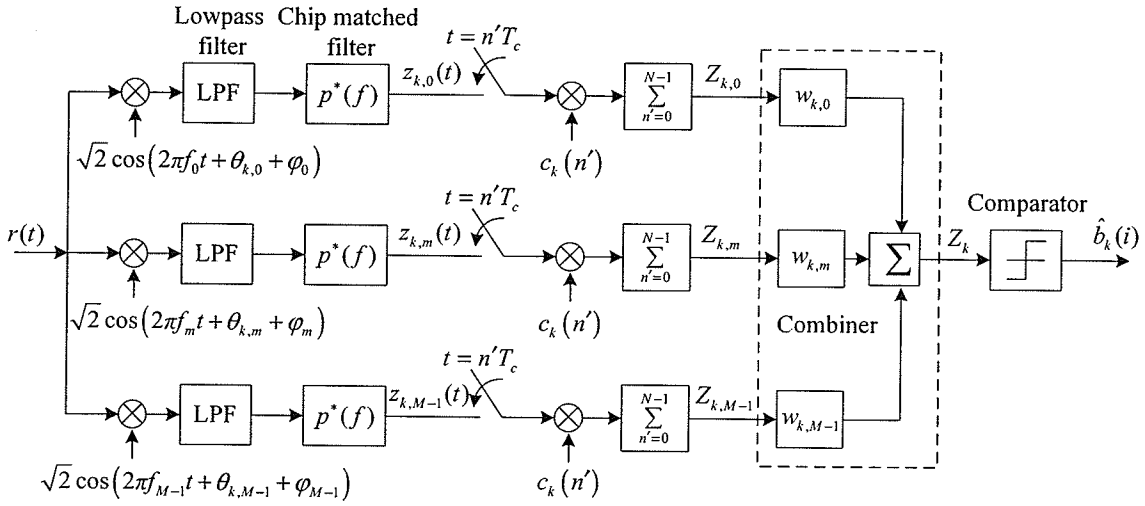

Figure 4.3: The receiver of the kth user in an phase offset assisted MC-DS-CMDA system.

4.1.1 Interference Analysis

Consider the detection of symbol $b_k(i)$ of the kth user when the carrier, phase, code and symbol are assumed to be perfectly synchronized. The signal at the output of the chip-matched filter on the mth branch, $z_{k,m}(t)$, in Fig 4.3 can be written as

$$\begin{aligned} z_{k,m}(t) &= \sqrt{E_c}\alpha_m \sum_{j=0}^{K-1} b_j(0)\cos(\theta_{j,m}-\theta_{k,m}) \sum_{n=0}^{N-1} c_j(n)g(t-nT_c)+\eta(t) \\ &= d_{k,m}(t)+i_{k,m}^{(2)}(t)+\eta(t) \end{aligned} \tag{4.6}$$

where

$$d_{k,m}(t) = \sqrt{E_c}\alpha_m b_k(i) \sum_{n=0}^{N-1} c_1(n)g(t-nT_c) \tag{4.7}$$

is the desired user signal and

$$i_{k,m}^{(2)}(t) = \sqrt{E_c}\alpha_m \sum_{\substack{j=0 \\ j\neq k}}^{K-1} b_j(i)\cos(\theta_{j,m}-\theta_{k,m}) \sum_{n=0}^{N-1} c_j(n)g(t-nT_c) \tag{4.8}$$

is the multiple access interference from other users ($j \neq k$) from the same carrier. The function $\eta(t)$ is defined by (2.13) while $g(t)$ is defined by (2.12). Note that, different from the matched filter output defined in (2.10), here the interference from the other users ($j \neq k$) from the other subcarriers and the interference from the other subcarriers of the desired user is zero, because the subcarriers do not overlap.

The correlator output $Z_{k,m}$ for the desired symbol $b_k(i)$ can be written as

$$Z_{k,m} = \sum_{n'=0}^{N-1} c_1(n')z_{k,m}(n'T_c) = D_{k,m}+I_{k,m}+\eta. \tag{4.9}$$

In (4.9),

$$D_{k,m} = \sum_{n'=0}^{N-1} c_1(n')d_{1,l}(n'T_c) = \sqrt{E_c}b_k(i)\alpha_m \tag{4.10}$$

$$I_{k,m} = \sqrt{E_c}\alpha_m \sum_{\substack{j=0 \\ j\neq k}}^{K-1} b_j(0) \sum_{n=0}^{N-1} c_j(n)c_k(n)\cos(\theta_{j,m}-\theta_{k,m}) \tag{4.11}$$

and

$$\eta = \sum_{n'=0}^{N-1} c_1(n')\eta(n'T_c). \tag{4.12}$$

Note that the property $g(n' - n)T_c = 0$ for $n' \neq n$, has been used to obtain the expressions in (4.10) and (4.11). The superscript index (2) of the multiple access interference $I_{k,m}^{(2)}$ in (4.9) has been removed for simplicity.

Taking into account the randomness of the spreading sequences, the mean of $Z_{k,m}$ conditioned on $b_k(i)$ and α_m is given by $E\{Z_{k,m}|b_k(i), \alpha_m\} = N\sqrt{E_c}b_k(i)\alpha_m$. As usual, assuming $I_{k,m}$ and η are uncorrelated and have zero means, the variance of $Z_{k,m}$ conditioned on $b_k(i)$ and α_m can be written as

$$\text{var}\{Z_{k,m}|b_k(i), \alpha_m\} = \text{var}\{I_{k,m}\} + \text{var}\{\eta\} \tag{4.13}$$

where, the variance due to the AWGN component can be shown to be $\text{var}\{\eta_{k,m}\} = NN_0/2$ and the MAI variance (variance of $I_{k,m}$) is

$$\text{var}\{I_{k,m}\} = E\{I_{k,m}^2\} = NE_c\alpha_m^2\widehat{I}_{k,m} \tag{4.14}$$

where

$$\widehat{I}_{k,m} = \sum_{\substack{j=0 \\ j\neq k}}^{K-1} \cos^2(\theta_{j,m} - \theta_{k,m}). \tag{4.15}$$

Observe that the MAI variance defined in (4.14) depends on the phase offsets through $\widehat{I}_{k,m}$.

Finally, the decision statistic for the symbol $b_k(i)$ is generated by passing the correlator output signals into the combiner and it is given by

$$Z_k = \sum_{m=0}^{M-1} w_{k,m}Z_{k,m} \tag{4.16}$$

where $w_{k,m}$ is the combiner gain of the mth subcarrier. With maximal ratio combining, each branch weight coefficient can be determined separately as [10]

$$w_{k,m} = \frac{E\{Z_{k,m}|b_k(i), \alpha_m\}}{\text{var}\{Z_{k,m}|b_k(i), \alpha_m\}}. \tag{4.17}$$

Then, using the results in [10], the SINR at the input of the comparator in Fig 4.3 can be written as

$$\text{SINR} = \frac{E\{Z_k|\boldsymbol{\alpha}\}}{\text{var}\{Z_k|\boldsymbol{\alpha}\}} = \sum_{m=0}^{M-1} \frac{E_c\alpha_m^2}{\text{var}\{Z_{k,m}|b_k(i),\alpha_m\}} \tag{4.18}$$

where $\boldsymbol{\alpha} = \{\alpha_0,\ldots,\alpha_m,\ldots,\alpha_{M-1}\}$. Define the average energy of the bit $\overline{E}_b \equiv MNE_cE\{\alpha_m^2\} = MNE_c\lambda$ and the average signal-to-noise ratio $\overline{\text{SNR}} \equiv \overline{E}_b/N_0$. Then substituting (4.9) onto (4.18), the average SINR of the desired user can be written as

$$\overline{\text{SINR}} = N\sum_{m=0}^{M-1}\left[\widehat{I}_{k,m} + MN\left(\frac{2\overline{E}_b}{N_0}\right)^{-1}\right]^{-1}. \tag{4.19}$$

Again note that, the $\overline{\text{SINR}}$ in (4.19) clearly depends on the phase offsets through the parameter $\widehat{I}_{k,m}$. On the other hand, the average SINR of the conventional MC-DS-CDMA [10], $\overline{\text{SINR}}_C$, can be obtained as

$$\overline{\text{SINR}}_C = NM\left[(K-1) + MN(2\overline{\text{SNR}})^{-1}\right]^{-1}. \tag{4.20}$$

4.2 Carrier-Based Phase Offset System

In this scheme, for each user, the system assigns a different phase offset in each subcarrier. For convenience, define the phase offset of the mth subcarrier for the kth user as $\theta_{k,m} = m\theta_k$. Now the problem is, how to find the $\theta_{k,m}$ such that the cross correlations among the users' signature waveforms are minimized, hence minimizing the MAI. Thus the problem at hand can be formulated as follows.

Problem 1: Consider an MC-DS-CDMA system equipped with a correlation receiver in each subchannel. Given the transmission rate $(1/T_b)$, the total bandwidth B_T (or equivalently F), the number of users K and the number of carriers M, find the optimal phase offset, $\theta_{k,m} = m\theta_k$, or equivalently θ_k such that the cross correlations among the users' signature waveforms are minimized.

Since the phase offset of each user is allowed to vary with each carrier, it is a difficult task to find the optimal phase offsets which minimize the sum cross correlation among the users' effective signature waveforms. Therefore one looks at the following

alternative. Consider the cross correlation between the kth user's effective signature waveform $s_k(t)$ and the jth user's effective signature waveform $s_j(t)$. From appendix D this cross correlation can be shown to be a time-phase correlation function

$$\rho_{k,j} = \widetilde{\rho}_{k,j} \cdot \left[\frac{\sin\left(\frac{M\Delta\theta_{k,j}}{2}\right)}{\sin\left(\frac{\psi_{k,j}}{2}\right)} \cdot \cos\left(\frac{(M-1)\Delta\theta_{k,j}}{2}\right) \right]. \tag{4.21}$$

In (4.21), the time cross correlation function is defined as $\widetilde{\rho}_{k,j} = \sum_{n=0}^{N-1} c_k(n)c_j(n)$ and the phase correlation function is $\left[\frac{\sin\left(\frac{M\Delta\theta_{k,j}}{2}\right)}{\sin\left(\frac{\Delta\theta_{k,j}}{2}\right)} \cdot \cos\left(\frac{(M-1)\Delta\theta_{k,j}}{2}\right) \right]$, where $\Delta\theta_{k,j} = \theta_k - \theta_j$. Since the cross correlation between the users' signature waveforms is defined by the product of time and phase cross correlation functions, one has great flexibility to design the system by choosing the spreading sequences and the phase offsets. Note that this flexibility is not available in the existing multi-carrier CDMA or SC-CDMA systems. For these systems the cross correlation is defined either by the time or the phase correlation function. For example, the cross correlation for conventional MC-DS-CDMA, MC-CDMA and SC-CDMA is defined by the time correlation function. For CI-MC-CDMA [15], the phase correlation function determines the cross correlation between the users' signature waveforms.

It is obvious from (4.21), if one uses the orthogonal spreading sequences, the time correlation function becomes zero and hence $\rho_{k,j} = 0$. However, as mentioned before, due to the limitation orthogonality imposes on the number of users, one is not interested in orthogonal spreading sequences. Nevertheless, with real binary sequences, the expression (4.21) can be made zero by setting the phase correlation function to zero. That is,

$$\left[\frac{\sin\left(\frac{M\Delta\theta_{k,j}}{2}\right)}{\sin\left(\frac{\Delta\theta_{k,j}}{2}\right)} \cdot \cos\left(\frac{(M-1)\Delta\theta_{k,j}}{2}\right) \right] = 0. \tag{4.22}$$

There exist $2(M-1)$ zeros due to the phase correlation function:

- $(M-1)$ equally-spaced zeros at $\Delta\theta_{k,j} = (2\pi l/M)$, $l = 1, 2, \ldots, M-1$ resulting from the $\sin(\cdot)/\sin(\cdot)$ term.
- $(M-1)$ equally-spaced zeros at $\Delta\theta_{k,j} = (2l+1)\pi/(M-1)$, $l = 1, 2, \ldots, M-1$ as a result of $\cos(\cdot)$ term.

This implies that for a given signature waveform $s_k(t)$ there exist $2(M-1)$ orthogonal signature waveforms $s_j(t)$. The existence of the first set of $(M-1)$ equally-spaced zeros indicates that a system can support M orthogonal signature waveforms (and, hence, M orthogonal users) by selecting the phase offsets as $\{\theta_k = \frac{2\pi}{M} \cdot k;$ $k = 0, 1, \ldots, M-1\}$. The existence of the second set of zeros indicates that there exists an additional set of M signature waveforms, which are orthogonal to one an other within the set, but pseudo-orthogonal to the first set. Then one can select the phase offsets for the second set as $\{\theta_k = \frac{2\pi}{M} \cdot k + \Delta\theta; k = 0, 1, \ldots, M-1\}$. Hence, one needs to select $\Delta\theta$ such that the cross correlation between the two sets of signature waveforms is minimal. From [38], select $\Delta\theta = \pi/M$, which makes the second set equidistance from the first set. Similar observations were also made for CI-MC-CDMA in [15] while analyzing the cross correlation between the users' signature waveforms.

From the above analysis, it can be seen that there are only $2M$ phase offsets are available. Therefore, when the total number of users in the system $K \leq 2M$, for each user a different phase offset will be assigned. However, when the total number of users in the system becomes more than $2M$ (i.e., $K > 2M$), a same phase offset needs to be assigned to several users. Note that here each user signal is identified by assigning a different spreading sequence. In this case the MAI will be not minimum. Thus, the phase offset of the kth user can be written as

$$\theta_k = \frac{2\pi}{M} \cdot (k \bmod M) + \Delta\theta \tag{4.23}$$

where

$$\Delta\theta = \begin{cases} 0, & (k \bmod 2M) = 0, 1, \ldots, M-1 \\ \frac{\pi}{M}, & (k \bmod 2M) = M, M+1, \ldots, 2M-1 \end{cases}. \tag{4.24}$$

With the phase offsets defined, consider the MAI performance of the proposed system. As seen from (4.14), the MAI variance depends on the spreading sequences and the phase offsets through the parameter $\widehat{I}_{k,m}$. Furthermore, it is shown that the systems' $\overline{\text{SINR}}$ also depends on $\widehat{I}_{k,m}$. Therefore, it is reasonable to evaluate the MAI performance by evaluating $\widehat{I}_{k,m}$. Recall from Section (4.1) that the parameter $\widehat{I}_{k,m}$ of

the proposed system is

$$\widehat{I}_{k,m} = \sum_{\substack{j=0 \\ j\neq k}}^{K-1} \cos^2\left(m\left(\theta_j - \theta_k\right)\right)$$
$$= \frac{K}{2} - 1 + \frac{1}{2}\sum_{j=0}^{K-1} \cos\left(2m\left(\theta_j - \theta_k\right)\right). \quad (4.25)$$

Note that, $\theta_l = 0$ for $l = 0, \cdots, K-1$ for the conventional MC-DS-CDMA proposed in [10]. Thus $\widehat{I}_{k,m} = K - 1$, for conventional MC-DS-CDMA.

Fig. 4.4 illustrates the MAI variation, $\widehat{I}_{k,m}$, over different carriers and for different numbers of users in the system. In this figure $k = 0$ is considered to be the desired user and the number of carriers in the system is $M = 8$. Note that for simplicity, the total number of carriers in the system is considered as $M = 8$. However it can be any value. It can be observed that the MAI is the same as that of the conventional MC-DS-CDMA proposed in [10] for the 0th carrier, regardless of the number of users K. However, when the total number of users $K < 2M$, for all other carriers, except the $(M/2)$th carrier, the MAI is approximately equal to $K/2 - 1$. For the $(M/2)$th carrier, the MAI is again same as that of 0th carrier (i.e.,$\widehat{I}_{k,M/2} = K - 1$). Note that this problem only occurs when the number of carriers in the system is even. Also observe that when the total number of users in the system is a multiple of two times the number of carriers the MAI is exactly $\widehat{I}_{k,m} = K/2 - 1$ for $m = 1, \ldots, M-1$ and $\widehat{I}_{k,m} = K - 1$ for $m = 0$. Hence, from these observations it can be seen that the MAI is not uniform over the carriers. The proposed system, however, considerably reduces the MAI compared to the conventional MC-DS-CDMA systems proposed in [10].

Assuming the 0th user as the desired user, the average MAI, $\widehat{I}_k = \sum_{m=0}^{M-1} \widehat{I}_{k,m}$, is given in Table 4.1. Again it shows that the proposed system considerably reduces the MAI compared to the conventional MC-DS-CDMA. However, the percentage of MAI reduction varies with K. Table 4.2 lists the average MAIs, for different desired users for $K = 6$ and $K = 8$ with $M = 8$. It can be observed that the average MAI performance of the carrier-based MC-DS-CDMA system is not uniform over all the users except when the number of users is the same as that of the number of carriers, i.e., $K = M$.

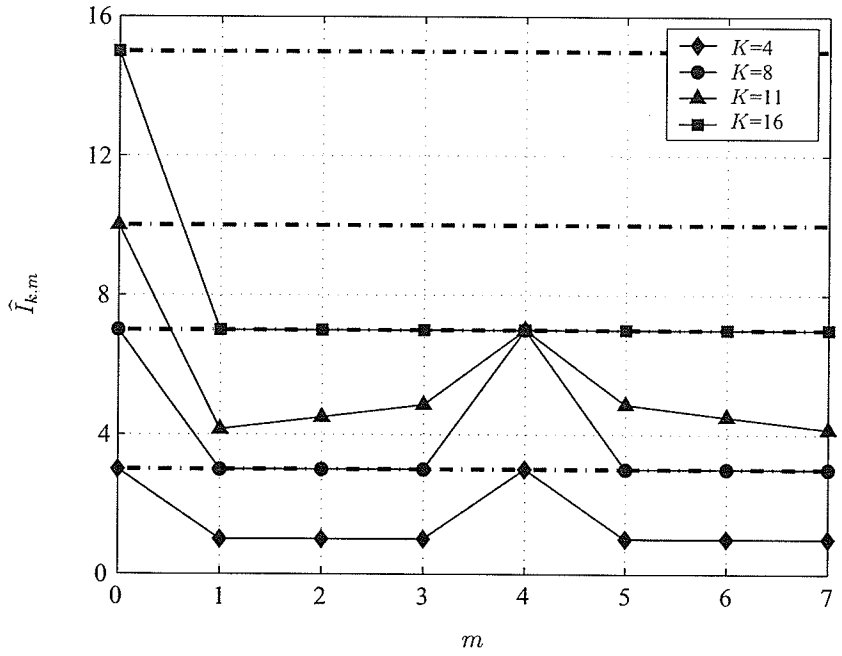

Figure 4.4: MAI variation of the carrier-based phase offset (solid curves) and conventional (dash curves) MC-DS-CDMA systems over the carriers.

Fig. 4.5 shows $\overline{\text{SINR}}$ versus $\overline{E}_b/N_0$ for different numbers of users in the system. The results were obtained with a bandwidth-bit duration product $F = B_T T_b = 256$, $M = 8$ and $\beta = 1$. It can be observed that the proposed system considerably outperforms the conventional MC-DS-CDMA system [10]. For example, at $\overline{\text{SNR}} = 20$dB, compared to the conventional MC-DS-CDMA, the proposed system performance is improved by 3dB, 2.5dB and 2.5dB when $K = 8$, $K = 16$ and $K = 32$, respectively. Also observe that the performance of the proposed system with $K = 16$, $K = 32$ and $K = 64$ is quite close to the performance of the conventional MC-DS-CDMA with $K = 8$, $K = 16$ and $K = 32$, respectively. From these observations it can be concluded that the proposed system reduces the MAI by nearly 50%.

Table 4.3 lists the SINRs at the receiver output for different desired users at three $\overline{\text{SNR}}$. Note that the difference among SINRs is quite small for low $\overline{\text{SNR}}$. However, for higher $\overline{\text{SNR}}$s, this difference increases.

Table 4.1: $\widehat{I}_0$ of carrier-based phase offset and conventional MC-DS-CDMA system with variable K: $M = 8$.

K	Proposed	Conventional	Improvement
4	1.5	3.0	50.0%
8	4.0	7.0	42.0%
16	8.0	15.0	46.0%
32	17.0	31.0	45.0%
64	35.0	63.0	44.4%

Table 4.2: $\widehat{I}_k$ of carrier-based phase offset MC-DS-CDMA system for $K = 6$ and $K = 8$ with $M = 8$.

k	0	1	2	3	4	5	6	7
$K = 6$	3.0	3.0	2.5	2.5	3.0	3.0	-	-
$K = 8$	4.0	4.0	4.0	4.0	4.0	4.0	4.0	4.0

4.3 User-Based Phase Offset System

Similar to the carrier-based phase offset scheme, this scheme also assigns a different phase offset for each user . However, unlike carrier-based phase offset, the same phase offset is used in all the subcarriers (i.e., $\theta_{k,m} = \theta_k$ for $m = 0, \cdots, M-1$). Thus an alternative objective, namely to minimize the average MAI variance at the outputs all correlation receivers is considered here. The total average MAI variance is defined by

$$\begin{aligned} J = \frac{1}{M}\sum_{k=0}^{K-1}\sum_{m=0}^{M-1} E\left\{\text{var}\{I_{k,m}\}\right\} &= E_c\lambda \sum_{k=0}^{K-1}\sum_{\substack{j=0 \\ j\neq k}}^{K-1} \cos^2\left(\theta_j - \theta_k\right) \\ &= E_c\lambda\left[\sum_{k=0}^{K-1}\sum_{j=0}^{K-1} \cos^2\left(\theta_j - \theta_k\right) - K\right] \\ &= E_c\lambda\left[\text{TSC} - K\right] \end{aligned} \tag{4.26}$$

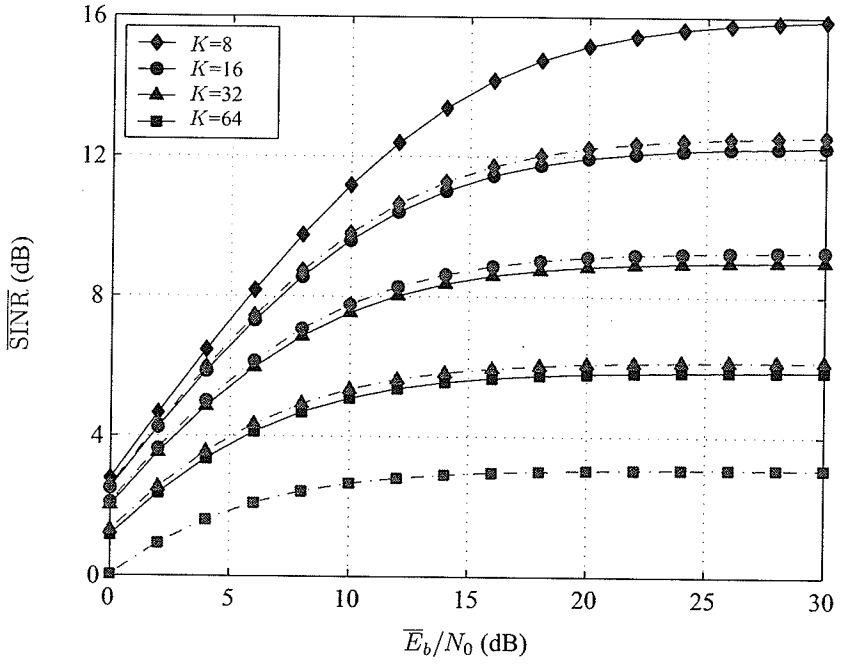

Figure 4.5: $\overline{\text{SINR}}$ performance of carrier-based phase offset (solid curves) and conventional MC-DS-CDMA (dash curves) systems with different numbers of users: $N = 16$ and $M = 8$.

where TSC is defined as the total squared correlation of the proposed system and it is given by

$$\begin{aligned} \text{TSC} &= \sum_{k=0}^{K-1} \sum_{j=0}^{K-1} \cos^2(\theta_j - \theta_k) \\ &= \frac{K^2}{2} + \frac{1}{2} \sum_{k=0}^{K-1} \sum_{j=0}^{K-1} \cos\left(2(\theta_j - \theta_k)\right). \end{aligned} \tag{4.27}$$

Minimizing J ensures an average performance level over all users, which is again in contrast to the carrier-based phase offset system. Furthermore, it is obvious that the MAI performance is also uniform over all the subcarriers. It is seen from (4.26) that, when the number of users K and number of carriers are fixed, minimizing J is equivalent to minimizing TSC. Thus, for given K and M, the optimal set of phase offsets is the one that minimizes TSC. Observe that for conventional MC-DS-CDMA systems considered in [10], TSC $= K^2$, since $\theta_j = 0$ for $j = 0, \cdots, K-1$.

In order to find a set of phase offsets $(\theta_0, \theta_1, \cdots, \theta_{K-1}) \in (0, 2\pi)$ that achieves a

Table 4.3: $\overline{\text{SINR}}$ (in dB): carrier-based phase offset MC-DS-CDMA system with $K = 6$, $M = 8$ for different $\overline{\text{SNR}}$.

User Index (k)	$\overline{\text{SNR}}$=8dB	$\overline{\text{SNR}}$=16dB	$\overline{\text{SNR}}$=32dB
0	9.92	14.67	16.74
1	9.92	14.67	16.74
2	10.11	15.35	18.03
3	10.11	15.35	18.03
4	9.92	14.67	16.74
5	9.92	14.67	16.74

minimum for the TSC, one puts the gradient of the TSC to zero, i.e.,

$$\begin{aligned}\frac{\partial \text{TSC}}{\partial \theta_k} &= \sum_{\substack{j=0 \\ j\neq k}}^{K-1} \sin\left(2\left(\theta_j - \theta_k\right)\right) \\ &= \cos\left(2\theta_k\right) \sum_{j=0}^{K-1} \sin\left(2\theta_j\right) - \sin\left(2\theta_k\right) \sum_{j=0}^{K-1} \cos\left(2\theta_j\right) \\ &= 0 \ \ \forall \ k. \end{aligned} \tag{4.28}$$

It can be seen from (4.28), in order to make $\partial \text{TSC}/\partial \theta_k = 0$, that

$$\sum_{j=0}^{K-1} \sin\left(2\theta_j\right) = \sum_{j=0}^{K-1} \cos\left(2\theta_j\right) = 0. \tag{4.29}$$

It is immediately found that (4.29) is satisfied when the phase offset $\theta_k = \frac{2\pi}{K} \cdot k$, $\forall \ k$. Indeed, for these phase offsets one obtains that $\partial \text{TSC}/\partial \theta_k = 0$, for $k = 0, \cdots, K-1$. At $\theta_k = \frac{2\pi}{K} \cdot k$, the second derivative of TSC with respect to θ_k is

$$\begin{aligned}\frac{\partial^2 \text{TSC}}{\partial \theta_k^2} &= 2\left[1 - \sin\left(2\theta_k\right) \sum_{j=0}^{K-1} \sin\left(2\theta_j\right) - \cos\left(2\theta_k\right) \sum_{j=0}^{K-1} \cos\left(2\theta_j\right)\right] \\ &= 2 \geq 0 \quad k = 0, \cdots, K-1. \end{aligned} \tag{4.30}$$

Therefore, it can be concluded that when $\theta_k = \frac{2\pi}{K} \cdot k$ for $k = 0, \cdots, K-1$ the TSC

is minimum. Substituting $\theta_k = \frac{2\pi}{K} \cdot k$ onto (4.27) yields the minimum TSC,

$$\begin{aligned}
\text{TSC} &= \frac{K^2}{2} + \frac{1}{2}\sum_{k=0}^{K-1}\sum_{j=0}^{K-1}\cos\left(\frac{4\pi}{K}\cdot(j-k)\right) \\
&= \frac{K^2}{2} + \underbrace{\frac{1}{2}\sum_{k=0}^{K-1}\cos\left(\frac{-4\pi}{K}\cdot k + \frac{2\pi}{K}\cdot(K-1)\right)\frac{\sin(2\pi)}{\sin\left(\frac{2\pi}{K}\right)}}_{=0} \\
&= \frac{K^2}{2}.
\end{aligned} \tag{4.31}$$

It then follows that the proposed user-based phase offset MC-DS-CDMA system attains a 50% TSC reduction over the conventional MC-DS-CDMA system. Now with $\theta_k = \frac{2\pi}{K} \cdot k$ and random spreading sequences the interference parameter of mth carrier defined in (4.15) simplifies to

$$\begin{aligned}
\widehat{I}_{k,m} &= \frac{K}{2} - 1 + \frac{1}{2}\sum_{j=0}^{K-1}\cos\left(\frac{4\pi}{K}(j-k)\right) \\
&= \frac{K}{2} - 1 + \underbrace{\frac{1}{2}\cos\left(\frac{-4\pi}{K}\cdot k + \frac{2\pi}{K}\cdot(K-1)\right)\frac{\sin(2\pi)}{\cos\left(\frac{2\pi}{K}\right)}}_{=0} \\
&= \frac{K}{2} - 1.
\end{aligned} \tag{4.32}$$

Note that the $\widehat{I}_{k,m}$ is same for all carriers in user-based phase offset MC-DS-CDMA. Moreover, because $\widehat{I}_{k,m}$ is not a function of θ_k, it follows that the MAI performance is uniform for all the users. This is not the case for carrier-based MC-DS-CDMA phase offset (see equation (4.25)).

Table. 4.4 compares the average $\widehat{I}_k$ performance of the proposed user-based phase offset MC-DS-CDMA system over the conventional MC-DS-CDMA system. Again it shows that the proposed user-based phase offset MC-DS-CDMA system reduces the MAI by $65\% - 50\%$ compared to the conventional MC-DS-CDMA systems. It follows further from (4.19) that, for user-based phase offset MC-DS-CDMA system, the average SINR is the same for every user and it is given by

$$\overline{\text{SINR}} = MN\left[\frac{K}{2} - 1 + MN\left(\frac{2\overline{E}_b}{N_0}\right)^{-1}\right]^{-1}. \tag{4.33}$$

Table 4.4: $\widehat{I}_k$ of user-based phase offset and conventional MC-DS-CDMA systems: $M = 8$.

K	Proposed	Conventional	Improvement
4	1.0	3.0	66.7%
8	3.0	7.0	57.1%
16	7.0	15.0	53.3%
32	15.0	31.0	51.6%
64	31.0	63.0	50.7%
128	63.0	127.0	50.3%

Observe from (4.33) and (4.20) that $\overline{\text{SINR}} > \overline{\text{SINR}}_C$, which confirms that the proposed system outperforms the conventional MC-DS-CDMA [10].

The $\overline{\text{SINR}}$ performance of both the user-based phase offset and the conventional MC-DS-CDMA systems is illustrated in Fig. 4.6. The performance curves of the user-based phase offset system with $K = 16$, $K = 32$ and $K = 64$ completely overlap those for conventional system with $K = 8$, $K = 16$ and $K = 32$, respectively. These observations imply that the user-based phase offset systems improve the system performance exactly by 50% compared to that of the conventional system.

4.4 Tradeoff between Carrier-Based and User-Based Phase Offset Systems

This section discusses the tradeoff between carrier-based and user-based phase offset MC-DS-CDMA systems.

The carrier-based offset system introduces a different phase offset in each carrier for a particular user. Consequently, the MAI performance is not uniform for all the carriers as can be clearly observed from Fig. 4.4. In contrast, the user-based phase offset system assigns the same phase offset in all the carriers for a particular user. As a direct consequence, it produces uniform MAI for all the carriers. Furthermore, from Tables 4.1 and 4.2 it can be observed that the average MAI performance of user-based phase offset system is better than that of the carrier-based phase offset system.

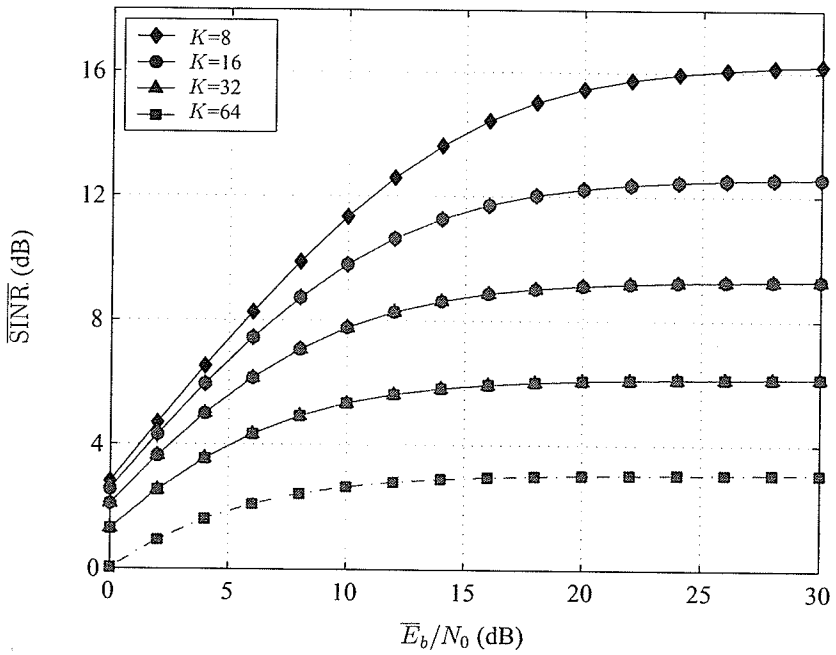

Figure 4.6: $\overline{\text{SINR}}$ performance of user-based phase offset (solid curves) and conventional MC-DS-CDMA (dash curves) systems with different numbers of users: $N = 16$ and $M = 8$.

Although the average MAI performance of the user-based phase offset system is better than that of the carrier-based phase offset system, both systems have the same SINR performance for low $\overline{E}_b/N_0$. However, for higher $\overline{E}_b/N_0$, the user-based phase offset system performance is slightly better than the carrier-based phase offset system. This can be clearly seen from Figs. 4.5 and 4.6. Indeed one can conclude that both systems have the same SINR performance.

Since a different phase offset is assigned for the different carriers in a carrier-based phase offset system, the transmitter and receiver structure becomes more complex than the user-based offset system. Additionally, the available number of phase offsets in the carrier-based phase offset system is limited by M the total number of carriers in the system. When $K > M$, same offset is assigned to several users. Indeed, the base station needs to monitor the users entering and leaving the system. This severely complicates their application in systems with a dynamically changing number of users. While implementation of carrier-based phase offset is quite complicated, it has the

advantage over user-based phase offset of having a low PAPR.

In chapter 3 it has been stated that the PAPR of a system can be measured using the crest factor (CF). In this chapter where one is only interested in downlink communications, the CF of the system is defined as

$$\mathrm{CF} = \sqrt{\mathrm{PAPR}} = \frac{\| \sum_{k=0}^{K} b_k(i) u_k(t) \|_\infty}{\| \sum_{k=0}^{K} b_k(i) u_k(t) \|_2} \tag{4.34}$$

where $u_k(t)$ is defined as

$$u_k(t) = c_k(n) p(t - nT_c) \sum_{m=0}^{M-1} \cos\left(2\pi f_m t + \theta_{k,m}\right). \tag{4.35}$$

Note that in (4.35) the chip waveform $p(t)$ is a band-limited chip waveform. In order to evaluate the PAPR of the systems, the chip waveform is assumed to be a square-root raised cosine waveform. The expression for a square-root raised cosine is given by [51]

$$p(t) = \frac{4\beta}{\pi} \frac{\cos[(1+\beta)\pi t/T_c] + T_c \sin[(1-\beta)\pi t/T_c]/(4\beta t)}{1 - (4\beta t/T_c)^2} \tag{4.36}$$

where β $(0 \leq \beta \leq 1)$ is the roll-off factor.

Specifically, in carrier-based phase offset systems, a different phase offset is assigned to each carrier for a particular user. This ensures that when a specific user carriers add coherently, other user carriers do not add coherently. This can be seen in Fig. 4.7-(a) to (c). Fig. 4.7-(a) represents the envelope of the first user; Fig. 4.7-(b) represents the envelope of the second user; and Fig. 4.7-(c) overlays all envelopes of all $2M$ users in the time domain. The envelope of the composite signal is a linear combination of these $2M$ waveforms; a signal with a low PAPR. However, when $K > 2M$ the PAPR increases, because the same offset will be assigned to several users.

Especially, it can be observed from Fig. 4.7-(a) to (c) that when $u_k(t)$ reaches its maximum $u_j(t)$ (where $k \neq j$) is at a very low value. Hence, constructive combining of all K signal energies at any one moment in time is not possible because peaks in signal energies are evenly spread over the chip time. Such an observation cannot be expected in user-based phase offset systems, because the same phase offset is used

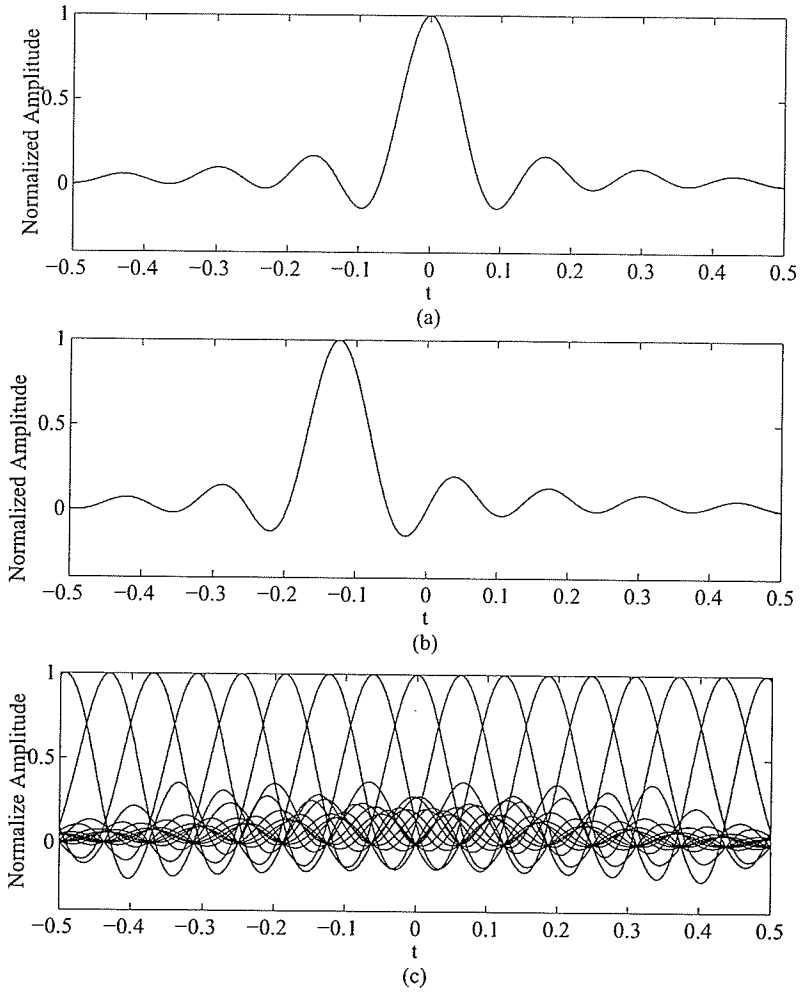

Figure 4.7: The carrier-based phase offset MC-DS-CDMA systems' transmitted envelope signals of (a) User 1 (b) User 2 and (c) All $2M$ users : $M = 8$, $\beta = 1$.

in all the carriers for a particular user. Furthermore, the CF level of the downlink depends on the binary antipodal information bits of the users (see (4.35)), $b_k(i)$, equally likely to be $+1$ or -1. Due to the averaging effect of the users' random transmitted information bits, it is reasonable to predict that the CF level of the carrier-based phase offset system is lower than that of the user-based phase offset and the conventional MC-DS-CDMA system. Such a prediction is confirmed by the numerical results presented next.

Fig. 4.8 illustrates the CF levels across 10,000 transmissions for carrier-based phase offset (Fig. 4.8-(a)), user-based phase offset (Fig. 4.8-(b)) and conventional

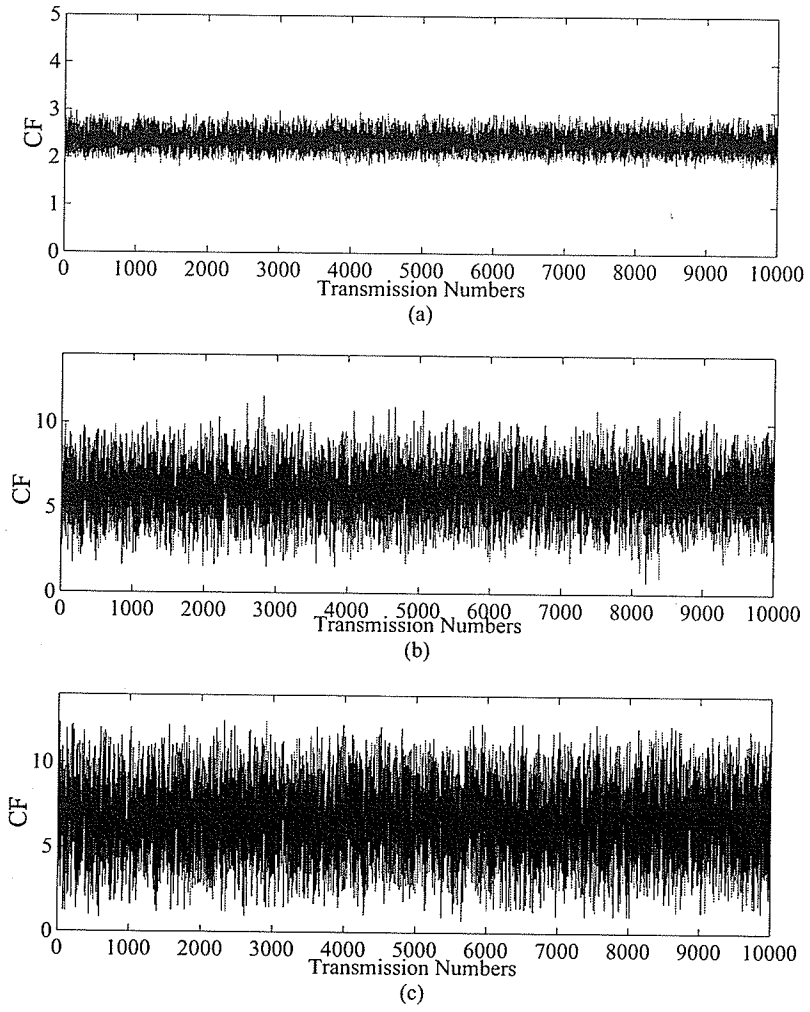

Figure 4.8: CF per transmissions for (a) Carrier-based phase offset (b) User-based phase offset and (c) Conventional MC-DS-CDMA system: $K = 8$, $M = 8$ and $\beta = 1.0$.

MC-DS-CDMA system (Fig. 4.8-(c)). The results were obtained with $K = 8$ users, $M = 8$ carriers and for $\beta = 1.0$. Observe from Fig. 4.8-(a) that most of CF values stay close to the mean CF level of 2.37 and that no CF values are higher than 3.03. On the other hand, referring to Figs. 4.8-(b) and 4.8-(c), user-based phase offset and conventional system's CF levels can be characterized as being more erratic. For the user-based phase offset system, 4.8-(b) displays a mean CF level of 6.7 and consistently reach levels that exceed 3, with some CF levels exceeding 10. The conventional system, 4.8-(c) displays a mean CF level of 6.7.

Finally, assuming $M = 8$ carriers, the cumulative density functions (cdf) of CF as a function of K the number of users are illustrated in Fig. 4.9, Fig. 4.10 and Fig. 4.11 for the different systems. As seen from Fig. 4.9, the CF level increases with increasing K. This is because when $K > 2M$, the same phase offset is assigned to several users. Furthermore, observe that, the CF level with $K = 128$ converges to that of the CF level with $K = 64$. On the other hand, it can be determined from Fig. 4.10 and Fig. 4.11, the CF level of user-based phase offset and conventional MC-DS-CDMA systems are almost indistinguishable. Moreover the CF level remains the same for all values of K. Although the CF level of carrier-based phase offset system increases, as K increases, these levels are much lower than the CF level of user-based phase offset and conventional MC-DS-CDMA systems.

4.5 Summary

Two phase offset MC-DS-CDMA systems, namely carrier-based and user-based phase offset systems have been proposed for the downlink in this chapter. In carrier-based phase offset, each user is assigned a different phase offset in each subcarrier, whereas in users-based phase offset, each user is assigned a different phase offset, however, the same offset is used in all the subcarriers. Although the MAI performance is not uniform over all the subcarriers in carrier-based offset systems, the SINR performance of carrier-based phase offset systems is all most same as that of the user-based phase offset systems. In particular, it has been shown that, compared to the conventional MC-DS-CDMA system, both the proposed phase offset assisted MC-DS-CDMA systems reduce the MAI by 50%. In addition to this, it has also been shown that when using carrier-based phase offset MC-DS-CDMA system, no PAPR problems arise.

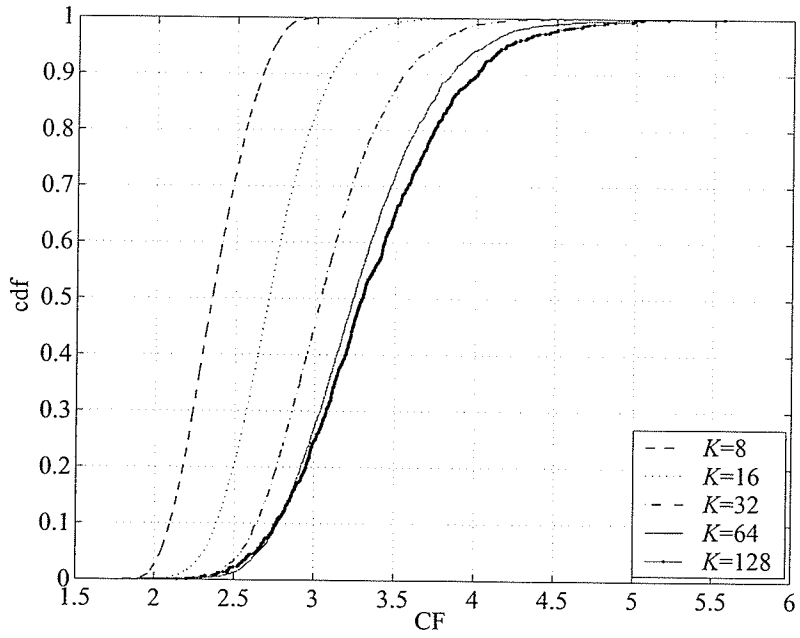

Figure 4.9: Cumulative density functions of CF with different Ks' for carrier-based phase offset MC-DS-CDMA systems: $M = 8$ and $\beta = 1.0$.

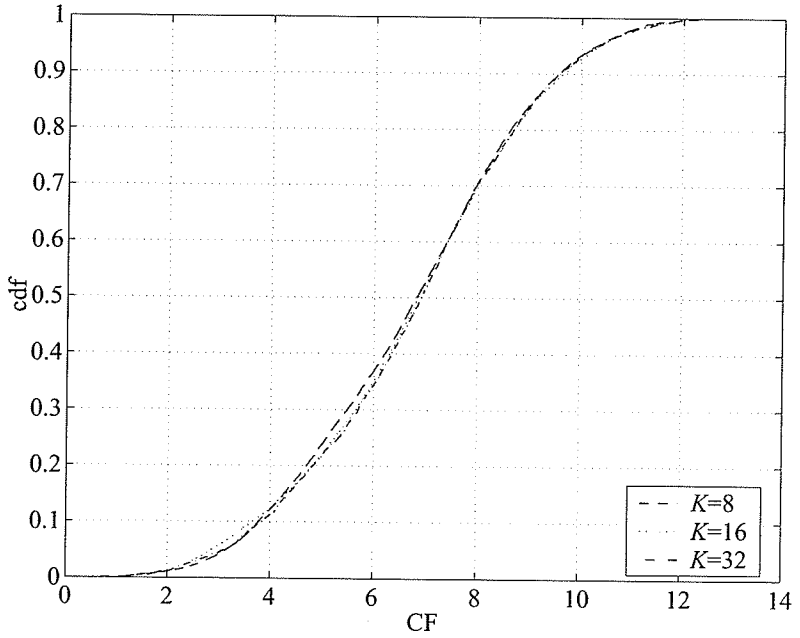

Figure 4.10: Cumulative density functions of CF with different Ks' for user-based phase offset MC-DS-CDMA systems: $M = 8$ and $\beta = 1.0$.

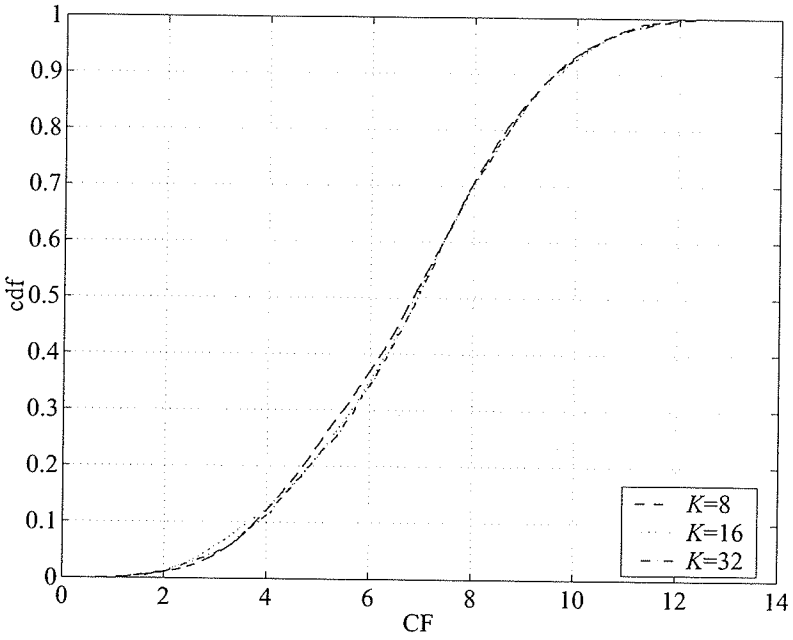

Figure 4.11: Cumulative density functions of CF with different Ks' for conventional MC-DS-CDMA systems: $M = 8$ and $\beta = 1.0$.

Chapter 5

Conclusions and Suggestions for Further Study

5.1 Conclusions

This dissertation is mainly devoted to develop techniques for multiple access interference reduction in multi-carrier CDMA systems under a given system bandwidth and transmission rate. Both the multi-carrier CDMA systems known as MC-DS-CDMA and MC-CDMA have been considered. For asynchronous band-limited MC-DS-CDMA systems, a method to jointly design the chip waveform and the carrier spacing to minimize the MAI was presented. The chip waveform was considered to be a Nyquist signaling pulse. A polynomial was used to synthesize the elementary density function, which characterizes the band-limited chip waveform. It was observed that the MAI performance of jointly optimized chip waveform and the carrier spacing is essentially that of the commonly used raised cosine waveform with optimized carrier spacing. As a practical matter, the raised cosine chip waveform for band-limited MC-DS-CDMA system is satisfactory.

An adaptive carrier interferometry scheme was proposed for MC-CDMA system to reduce the MAI. Here it was assumed that there exists a feedback channel between the receiver and the transmitter. The novelty in the proposed system is that the amplitudes of the carriers are allowed to change according to the channel conditions. In order to update the carrier amplitudes, two adaptive strategies: local and global adaptations were introduced. It was shown that, in single user adaptation, the local

adaptive algorithm performs better than the global adaptive algorithm. Furthermore, it was demonstrated that in multiuser adaptation, the proposed non-iterative algorithm performs slightly worse than the iterative algorithm at low channel SNR, but it gives a considerable performance gain at high channel SNR. More importantly, it was demonstrated that the proposed ACI-MC-CDMA system considerably outperformes the conventional CI-MC-CDMA considered in [15]. In addition to this, it was also shown that the proposed ACI-MC-CDMA is also attractive in terms of PAPR reduction.

A phase offset assisted MC-DS-CDMA system was proposed for a synchronous downlink system. Two phase offset systems, namely carrier-based phase offset and user-based phase offset, were introduced. It was shown that, although both the systems reduce the MAI by 50% compared to the conventional MC-DS-CDMA system [10], the carrier-based phase offset system is more complex than the user-based phase offset system. However, it was demonstrated that the carrier-based phase offset system eliminates the PAPR problems characteristic of user-based phase offset and conventional MC-DS-CDMA system.

In this thesis the benefits of the proposed schemes (ACI-MC-CDMA, phase offset assisted MC-DS-CDMA) were demonstrated by using some specific cases to make the analysis simple. However, it should be mentioned that the proposed schemes will offer the same benefits for any number of carriers and users in the system. In the case of ACI-MC-CDMA, there is no restriction on the number of carriers (i.e., length of the spreading sequence) because the proposed system satisfy the CI code property. Furthermore, in the phase offset assisted scheme, the number of carriers will not affect the system performance. Therefore, the selection of number of carriers depends on the technology and the channels conditions. For example, in cdma2000, only four carriers have been used in the downlink.

5.2 Suggestion for Future Study

In this dissertation, the optimal carrier spacing and the chip waveform is jointly designed for the family of Nyquist signaling waveforms. Because of Nyquist signaling

waveforms, it has been observed that the elementary density function can only designed over a small frequency range. As in [20], the design of the chip waveforms becomes more flexible, if the condition on the chip waveform to be a Nyquist signaling pulse is removed. However, in this case one needs to account for the interchip interference in the design. Therefore, joint design of optimal chip waveform and carrier spacing for MC-DS-CDMA systems with arbitrary band-limited chip waveforms remains to be studied.

The adaptive carrier interferometry MC-CDMA systems proposed in this dissertation has, for simplicity, assumed that there is an ideal feedback channel to transmit the updated carrier amplitudes from the receiver back to the transmitter. Although significant performance gains seem possible through such an adaptation, the value of such an approach should be closely examined considering such system issues as limited feedback bandwidth availability, fading channels, and time-varying interference. For instance, the channel conditions and interference may change faster than the feasible transmitter update rate. This would essentially negate any potential performance gains. Furthermore, data traffic in multimedia cellular networks and ad hoc wireless networks is anticipated to be highly asymmetric. Also it will be a challenging topic to study is the convergence and tracking properties of proposed algorithms.

It may be interesting to develop some adaptation algorithms similar to that proposed for SC-CDMA systems [36, 52] which reduce the bandwidth requirement in the feedback channel by requiring only a minimum amount of information to be fed back from the receiver, thus making the adaptive structure more feasible for practical systems. It may be also instructive to explore the tradeoff offered by the proposed adaptation with realistic impairments and limitations, and investigate ways to making this tradeoff more favorable. One interesting topic is the effect of finite feedback bandwidth on the performance of the adaptation algorithms.

Appendix A

Proof That Problem in (3.33) is Equivalent to Problem in (3.35)

With the optimal weight matrix $\mathbf{W} = \mathbf{R}^{-1}\mathbf{HPA}$, the TMSE can be simplified to

$$\text{TMSE} = \text{tr}\left\{\mathbf{I} - \tilde{\mathbf{A}}^H\mathbf{R}^{-1}\tilde{\mathbf{A}}\right\} \tag{A.1}$$

where $\mathbf{R} = \tilde{\mathbf{A}}\tilde{\mathbf{A}}^H + \sigma^2\mathbf{I}$ is the receiver correlation matrix and $\tilde{\mathbf{A}} = \mathbf{HPA}$. Note that

$$\begin{aligned}
\tilde{\mathbf{A}}^H\mathbf{R}^{-1}\tilde{\mathbf{A}} &= \tilde{\mathbf{A}}^H\left[\tilde{\mathbf{A}}\tilde{\mathbf{A}}^H + \sigma^2\mathbf{I}\right]^{-1}\tilde{\mathbf{A}} \\
&= \mathbf{B}^H\mathbf{H}^H\left[\mathbf{HBB}^H\mathbf{H}^H + \sigma^2\mathbf{I}\right]\mathbf{HB} \\
&= \frac{\mathbf{B}^H\mathbf{H}^H}{\sigma}\left[\frac{\mathbf{HB}}{\sigma}\frac{\mathbf{B}^H\mathbf{H}^H}{\sigma} + \mathbf{I}\right]^{-1}\frac{\mathbf{HB}}{\sigma} \\
&= \mathbf{I} - \left[\mathbf{I} + \frac{\mathbf{B}^H\mathbf{H}^H\mathbf{HB}}{\sigma^2}\right]^{-1} \\
&= \mathbf{I} - \left[\mathbf{I} + \mathbf{F}^H\mathbf{F}\right]^{-1}
\end{aligned} \tag{A.2}$$

where the relationship $\mathbf{X}^H[\mathbf{XX}^H + \mathbf{I}]^{-1}\mathbf{X} = \mathbf{I} - [\mathbf{I} + \mathbf{X}^H\mathbf{X}]^{-1}$ is invoked in (A.2) and, recall that, $\mathbf{B} = \mathbf{PA}$ and $\mathbf{F} = (\mathbf{H}^H\mathbf{H})^{1/2}\mathbf{B}/\sigma$. Substituting (A.2) into (A.1) yields

$$\text{TMSE} = \text{tr}\left\{\left[\mathbf{I} + \mathbf{F}^H\mathbf{F}\right]^{-1}\right\}. \tag{A.3}$$

Furthermore, the constraint stated in (3.21) can be also written in terms of matrix $\mathbf{F}$ as follows

$$\begin{aligned}
\text{diag}\left[\mathbf{A}^H\mathbf{A}\right] &= \text{diag}\left[\sigma^2\mathbf{F}^H[\mathbf{H}^H\mathbf{H}]^{-1}\mathbf{F}\right] \\
&\leq [\xi_0, \cdots, \xi_j, \cdots, \xi_{K-1}]
\end{aligned} \tag{A.4}$$

where the operator diag[·] takes the diagonal elements of a matrix to form a row vector. Furthermore, the inequality is interpreted as element-by-element comparison. Hence, one can reformulate the optimization problem in (3.21) in terms of matrix $\mathbf{F}$ as

$$\begin{aligned} \min_{\mathbf{A}} \quad & \text{TMSE} = \text{tr}\left\{\left[\mathbf{I}+\mathbf{F}^H\mathbf{F}\right]^{-1}\right\} \\ \text{subject to} \quad & \text{diag}\left[\sigma^2\mathbf{F}^H[\mathbf{H}^H\mathbf{H}]^{-1}\mathbf{F}\right] \leq [\xi_0,\cdots,\xi_j,\cdots,\xi_{K-1}]. \end{aligned} \tag{A.5}$$

Next, considered a related optimization problem with a weaker constraint

$$\begin{aligned} \min_{\mathbf{A}} \quad & \text{TMSE} = \text{tr}\left\{\left[\mathbf{I}+\mathbf{F}^H\mathbf{F}\right]^{-1}\right\} \\ \text{subject to} \quad & \text{tr}\left\{\sigma^2\mathbf{F}^H[\mathbf{H}^H\mathbf{H}]^{-1}\mathbf{F}\right\} \leq \xi \end{aligned} \tag{A.6}$$

where $\xi = \sum_{j=1}^{K}\xi_j$. With the singular value decomposition $\mathbf{H} = \mathbf{U}\boldsymbol{\Sigma}\mathbf{V}^H$ in (3.34), one has the following spectral decomposition of matrix $\left[\mathbf{H}^H\mathbf{H}\right]^{-1}$,

$$\left[\mathbf{H}^H\mathbf{H}\right]^{-1} = \mathbf{V}\text{diag}\left[\frac{1}{\varepsilon_1^2},\frac{1}{\varepsilon_2^2},\cdots,\frac{1}{\varepsilon_N^2},0,\cdots,0\right]\mathbf{V}^H \tag{A.7}$$

where the eigenvalues $\frac{1}{\varepsilon_1^2},\frac{1}{\varepsilon_2^2},\cdots,\frac{1}{\varepsilon_N^2}$ are arranged in an ascending order. To proceed on need to make use of the following result, the proof of which can be found in [53] (p. 249).

Lemma 1: Suppose $\mathbf{X}$ and $\mathbf{Y}$ are two Hermitian $N\times N$ matrices. Arrange the eigenvalues x_i of $\mathbf{X}$ in a descending order and the eigenvalues y_i of $\mathbf{Y}$ in an ascending order. Then

$$\text{tr}\{\mathbf{XY}\} \geq \sum_{i=1}^{N} x_i y_i. \tag{A.8}$$

Let $\upsilon_1,\upsilon_2,\cdots,\cdots,\upsilon_N$, $(\upsilon_n > 0, n = 1,2,\cdots,N)$ be the eigenvalues of $\mathbf{F}^H\mathbf{F}$ arranged in descending order, and apply this lemma to $\text{tr}\left\{\mathbf{F}^H[\mathbf{H}^H\mathbf{H}]^{-1}\mathbf{F}\right\}$. One has

$$\text{tr}\left\{\mathbf{F}^H[\mathbf{H}^H\mathbf{H}]^{-1}\mathbf{F}\right\} = \text{tr}\left\{[\mathbf{H}^H\mathbf{H}]^{-1}\mathbf{F}\mathbf{F}^H\right\} \geq \sum_{n=1}^{N}\frac{\upsilon_n}{\varepsilon_n^2}. \tag{A.9}$$

Performing a similar spectral factorization gives

$$\text{TMSE} = \text{tr}\left\{\left[\mathbf{I}+\mathbf{F}^H\mathbf{F}\right]^{-1}\right\} = \sum_{n=1}^{N}\frac{1}{\upsilon_n+1}. \tag{A.10}$$

Therefore, the optimization problem reduces to

$$\begin{aligned} \min_{\upsilon_n} \quad & \text{TMSE} = \sum_{n=1}^{N} \frac{1}{\upsilon_n + 1} \\ \text{subject to} \quad & \sum_{n=1}^{N} \frac{\upsilon_n}{\varepsilon_n^2} \leq \frac{\xi}{\sigma^2}. \end{aligned} \tag{A.11}$$

Appendix B

The Proof of Proposition 1

To solve the optimization problem in (A.11), form the Lagrange function

$$L = \sum_{n=1}^{N} \frac{1}{\upsilon_n + 1} + \mu \left(\sum_{n=1}^{N} \frac{\upsilon_n}{\varepsilon_n^2} - \frac{\xi}{\sigma^2} \right) \tag{B.1}$$

where μ is the Lagrange multiplier. Taking the derivative with respect to υ_n and setting it to zero yields

$$\upsilon_n = \pm \frac{\varepsilon_n}{\sqrt{\mu}} - 1. \tag{B.2}$$

Since $\upsilon_n > 0$, one selects

$$\upsilon_n = \frac{\varepsilon_n}{\sqrt{\mu}} - 1. \tag{B.3}$$

Selecting the Lagrange multiplier to satisfy the power constraint, the optimal eigenvalues can be found from (B.3) as

$$\upsilon_n = \varepsilon_n \left[\frac{\frac{\xi}{\sigma^2} + \sum_{l=1}^{N} \frac{1}{\varepsilon_l^2}}{\sum_{l=1}^{N} \frac{1}{\varepsilon_l}} \right] - 1. \tag{B.4}$$

Then, it is not hard to see that the following choice of $\mathbf{F}$ attains the minimum TMSE

$$\mathbf{F} = \mathbf{V} \begin{bmatrix} \sqrt{\upsilon_1} & & & & \\ & \ddots & & & \\ & & \sqrt{\upsilon_n} & & \\ & & & \ddots & \\ & & & & \sqrt{\upsilon_N} \\ & & \mathbf{0} & & \end{bmatrix} \widetilde{\mathbf{V}}^H. \tag{B.5}$$

In (B.5) $\mathbf{V}$ is an $NK \times NK$ unitary matrix which can be obtained from (A.7) and $\widetilde{\mathbf{V}}$ is a $K \times K$ unitary matrix which can be constructed to satisfy the constraint

$$\operatorname{diag}\left(\widetilde{\mathbf{V}}\operatorname{diag}\left(\frac{\upsilon_1}{\varepsilon_1^2}, \frac{\upsilon_2}{\varepsilon_2^2}, \cdots, \frac{\upsilon_N}{\varepsilon_N^2}\right)\widetilde{\mathbf{V}}^H\right) = \operatorname{diag}\left(\xi_0, \xi_1, \cdots, \xi_{K-1}\right). \tag{B.6}$$

Therefore, with $\mathbf{A} = \sigma\mathbf{P}^H\left[\mathbf{H}^H\mathbf{H}\right]^{-\frac{1}{2}}\mathbf{F}$, the original optimization problem in (3.33) can be solved as indicated in (3.37).

Appendix C

The Solution to the Optimization Problem in (3.35) for the Case of AWGN Channels

In the absence of multipath, the channel matrix is an identity matrix, i.e., $\mathbf{H} = \mathbf{I}$. In this case the optimization problem in (A.6) reduces to

$$\begin{aligned} \min_{\mathbf{A}} \quad & \text{TMSE} = \text{tr}\left\{\left[\mathbf{I} + \frac{\mathbf{A}^H\mathbf{P}^H}{\sigma}\frac{\mathbf{P}\mathbf{A}}{\sigma}\right]^{-1}\right\} \\ \text{subject to} \quad & \text{tr}\left[\mathbf{A}^H\mathbf{A}\right] \leq \xi. \end{aligned} \tag{C.1}$$

As seen before, the constraint is equivalent to

$$\text{tr}\left[\mathbf{A}^H\mathbf{A}\right] = \text{tr}\left[\mathbf{A}\mathbf{A}^H\right] = \sum_{n=1}^{N} \upsilon_n \leq \xi \tag{C.2}$$

where υ_n, $n = 1, 2, \cdots, M$ are the eigenvalues of $\mathbf{A}^H\mathbf{A}$. Performing the same spectral factorization, the TMSE can be written as

$$\begin{aligned} \text{TMSE} &= \text{tr}\left\{\left[\mathbf{I} + \frac{\mathbf{A}^H\mathbf{P}^H}{\sigma}\frac{\mathbf{P}\mathbf{A}}{\sigma}\right]^{-1}\right\} \\ &= \sum_{n=1}^{N} \frac{1}{(1/\sigma^2)\upsilon_n + 1}. \end{aligned} \tag{C.3}$$

Now the problem is to find N positive eigenvalues $\{\upsilon_1, \cdots, \upsilon_n, \cdots, \upsilon_N\}$ that minimize $\sum_{n=1}^{N}(\upsilon_n\sigma^{-2} + 1)^{-1}$, subject to $\sum_{n=1}^{N}\upsilon_n = \xi$. The Lagrange method can be used to show that the optimal eigenvalues are simply equal to ξ/N, i.e., $\upsilon_1 = \upsilon_2 = \cdots = \upsilon_N = \xi/N$.

Thus, the minimum TMSE is obtained when $\mathbf{A}^H\mathbf{A}$ is a scalar times the identity matrix, or equivalently,

$$\mathbf{A}^H\mathbf{A} = \mathbf{S}\Lambda\mathbf{S}^H = \mathbf{S}\left[(\xi/N)\mathbf{I}_{N\times N}\right]\mathbf{S}^H \tag{C.4}$$

where $\mathbf{S}$ can be constructed to satisfy the following constraint

$$\mathrm{diag}\left(\mathbf{S}\left[(\xi/N)\mathbf{I}_{N\times N}\right]\mathbf{S}^H\right) = \mathrm{diag}\left(\xi_1, \xi_2, \cdots, \xi_K\right). \tag{C.5}$$

Given $\mathbf{S}$ one can construct the carrier amplitude matrix $\mathbf{A}$ as follows:

$$\mathbf{A} = \sigma\mathbf{P}^H\mathbf{V}\begin{bmatrix}(\sqrt{\xi/N})\mathbf{I}_{N\times N} \\ \\ \mathbf{0}_{NK-N\times NK-N}\end{bmatrix}\mathbf{S}^H \tag{C.6}$$

where $\mathbf{V}$ is an $NK\times NK$ unitary matrix constructed such that the columns of matrix $\mathbf{A}$ are orthogonal and have norm squared equal to $\xi_1, \xi_2, \cdots, \xi_K$.

Appendix D

Derivation of the Cross Correlation between the Effective Signature Waveforms

The cross correlation between kth user's signature waveform $s_k(t)$ and jth user's signature waveform $s_j(t)$ can be written as

$$\rho_{k,j} = \int_{-\infty}^{\infty} s_k(t)s_j(t)dt \tag{D.1}$$

where $s_k(t)$ is defined by (4.4). Substituting for $s_k(t)$ and $s_j(t)$, $\rho_{k,j}$ can be written as

$$\rho_{k,j} = \sum_{n=0}^{N-1}\sum_{n'=0}^{N-1} c_k(n)c_j(n') \sum_{m=0}^{M-1}\sum_{m'=0}^{M-1} \int_{-\infty}^{\infty} \cos\left(2\pi f_m t + m\theta_k\right) \cos\left(2\pi f_{m'} t + m'\theta_j\right) p(t - nT_c)p(t - n'T_c)dt. \tag{D.2}$$

Ignoring the high frequency terms and considering the fact that the subcarriers do not overlap, (D.2) can be simplified as

$$\rho_{k,j} = \sum_{n=0}^{N-1}\sum_{n'=0}^{N-1} c_k(n)c_j(n') \int_{-\infty}^{\infty} p(t - nT_c)p(t - n'T_c)dt \cdot \sum_{m=0}^{M-1} \cos\left(m\left(\theta_k - \theta_j\right)\right). \tag{D.3}$$

Using the Nyquist and unit-energy properties of $p(t)$ (D.3) can be further simplified as

$$\begin{aligned}
\rho_{k,j} &= \sum_{n=0}^{N-1} c_k(n)c_j(n) \int_{-\infty}^{\infty} p^2(t - nT_c)dt \cdot \sum_{m=0}^{M-1} \cos\left(m\left(\theta_k - \theta_j\right)\right) \\
&= \widetilde{\rho}_{k,j} \sum_{m=0}^{M-1} \cos\left(m\left(\theta_k - \theta_j\right)\right) \\
&= \widetilde{\rho}_{k,j} \cdot \left(\frac{\sin\left(\frac{M\Delta\theta_{k,j}}{2}\right)}{\sin\left(\frac{\psi_{k,j}}{2}\right)} \cdot \cos\left(\frac{(M-1)\Delta\theta_{k,j}}{2}\right) \right)
\end{aligned} \tag{D.4}$$

where $\widetilde{\rho}_{k,j} = \sum_{n=0}^{N-1} c_k(n)c_j(n)$ and $\Delta\theta_{k,j} = \theta_k - \theta_j$.

References

[1] R. L. Pickholtz, L. B. Milstein, and L. Schillig, "Spread spectrum for mobile communications," *IEEE Transactions on Vechicular Technology*, vol. 40, pp. 313–322, May 1991.

[2] A. J. Viterbi, *Principles of Spread Spectrum Communication.* Addison-Wesley, 1995.

[3] TIA TR45.5, *The CDMA2000 ITU-R RTT Candidate Submission.*, June 1998.

[4] S. W. Weinstein and P. M. Ebert, "Data transmission by frequency division multiplexing using the discrete fourier transform," *IEEE Transactions on Communications*, vol. 19, pp. 628–634, Oct. 1971.

[5] S. Hara, "Overview of multicarrier CDMA," *IEEE Communications Magazine*, pp. 126–133, Dec. 1997.

[6] A. Chouly, A. Brajal, and S. Jourdan, "Orthogonal multicarrier techniques applied to direct sequence spread spectrum CDMA systems," in *Proc. IEEE Global Telecommunications Conference GLOBECOM '93*, (Houston, U.S.A), pp. 1723 –1728, Nov. 1993.

[7] N. Yee, J. P. Linnartz, and G. Fettweis, "Multi-carrier CDMA in indoor wireless radio networks," in *Proc. IEEE International Symposium on Personal, Indoor and Mobile Radio Communications '93*, (Yokohama, Japan), pp. 109–113, Sep. 1993.

[8] S. Hara and R. Prasad, "DC-CDMA, MC-CDMA and MT-CDMA for mobile multi-media communications," in *Proc. IEEE VTC '96*, (Atlanta, U.S.A), pp. 1106–1110, April 1996.

[9] V. M. DaSilva and E. S. Sousa, "Multicarrier orthogonal CDMA signals for quasi-synchronous communication systems," *IEEE Journal on Selected Areas in Communications*, vol. 12, pp. 842 –852, June 1994.

[10] S. Kondo and L. B. Milstein, "Performance of multicarrier DS-CDMA systems," *IEEE Transactions on Communications*, vol. 44, pp. 238 –246, Feb. 1996.

[11] E. A. Sourour and M. Nakagawa, "Performance of orthogonal multicarrier CDMA in a multipath fading channel," *IEEE Transactions on Communications*, vol. 44, pp. 356 –367, March 1996.

[12] H. H. Nguyen and E. Shwedyk, "On carrier spacing in multucarrier CDMA system," in *Proc. IEEE Canadian Conference on Electrical and Computer Engineering*, (Winnipeg, Canada), pp. 1216–1220, May 2002.

[13] H. H. Nguyen, "Effect of chip shaping on the performance of band-limited multicarrier CDMA systems," in *IEEE Transactions on Vehicular Technology*, vol. 54, pp. 1022–1029, May 2005.

[14] K. Fazel, "Performance of CDMA/OFDM for mobile communication system," in *Proc. IEEE International Conference on Personal Communications ICUPC'93*, (Ottawa, Canada), pp. 975–979, Oct. 1993.

[15] B. Natarajan, C. R. Nassar, M. Michelini, and Z. Wu, "High-performance MC-CDMA via carrier interferometry codes," *IEEE Transactions on Vehicular Technology*, vol. 50, pp. 1344–1353, Nov. 2001.

[16] L. Vandendorpe, "Multitone spread spectrum multiple access communications system in a multipath Rician fading channel," *IEEE Transactions on Vehicular Technology*, vol. 44, pp. 327 –337, May 1995.

[17] Y. H. Kim, I. Song, H. G. Kim, and J. Lee, "Design and performance analysis of a convolutionally coded overlapping multicarrier DS-CDMA system," *IEEE Transactions on Vehicular Technology*, vol. 49, pp. 1950–1967, Sep. 2000.

[18] S. M. Elnoubi and A. El-Beheiry, "Effect of overlapping between successive carriers of muticarrier CDMA on the performance in a multipath fading channel," *IEEE Transactions on Communications*, vol. 49, pp. 769–773, May 2001.

[19] L.-L. Yang and L. Hanzo, "Performance of generalized multicarrier DS-CDMA over Nakagami-m fading channels," *IEEE Transactions on Communications*, vol. 50, pp. 956 –966, June 2002.

[20] W. Gao, J. H. Cho, and J. S. Lehnert, "Chip waveform design for DS/SSMA systems with aperidoic random spreading sequences," *IEEE Transactions on Wireless Communications*, vol. 1, pp. 37–45, Jan. 2002.

[21] T. F. Wong, T. M. Lok, and J. S. Lehnert, "Asynchronous multiple-access interference suppression and chip waveform selection with aperiodic random sequences," *IEEE Transactions on Communications*, vol. 47, pp. 103–114, Jan. 1999.

[22] M. A. Landolsi and W. E. Stark, "DS-CDMA chip waveform design for minimal interference under bandwidth, phase and envelope constraints," *IEEE Transactions on Communications*, vol. 47, pp. 1737–1746, Nov. 1999.

[23] H. H. Nguyen, "Performance of multicarrier DS-CDMA systems with time-limited chip waveforms," *Canadian Journal of Electrical and Computer Engineering (Special Issue on Advances in Wireless Communications and Networking)*, vol. 29, pp. 23–29, Jan./April 2004.

[24] K. W. Yip and T. S. Ng, "Effects of carrier frequency accuracy on quasi-synchronous, multicarrier DS-CDMA communications using optimized sequences," *IEEE Journal on Selected Areas in Communications*, vol. 17, pp. 1915–1923, Nov. 1999.

[25] E. Geraniotis and B. Ghaffari, "Performance of binary and quaternary direct-sequence spread-spectrum multiple-access systems with random signature sequences," *IEEE Transactions on Communications*, vol. 39, pp. 713–724, May 1991.

[26] N. C. Beaulieu, C. C. Tan, and M. O. Damen, "A Better than Nyquist Pulse," *IEEE Communications Letters*, vol. 5, pp. 367–368, Sep. 2001.

[27] N. C. Beaulieu and M. O. Damen, "Parametric construction of nyquist-i pulses," *IEEE Transactions on Communicatins*, vol. 12, pp. 2134 – 2142, Dec. 2004.

[28] A. M. Tonello and A. Assalini, "Improved Nyquist pulses," *IEEE Communications Letters*, vol. 2, pp. 87 – 89, Feb. 2004.

[29] T. Coleman, M. A. Branch, and A. Grace, *Optimization Toolbox*. Natick, MA: The MathWorks Inc., 2000.

[30] B. M. Popović, "Spreading sequence for multicarrier CDMA systems," *IEEE Transactions on Communications*, vol. 47, pp. 918–926, June 1999.

[31] T. M. Lok and T. F. Wong, "Transmitter adaptation in multicode DS-CDMA systems," *IEEE Journal on Selected Areas in Communications*, vol. 19, pp. 69–82, Jan. 2001.

[32] S. Ulukus and R. D. Yates, "Iterative construction of optimum signature sequence sets in synchronous CDMA systems," *IEEE Transactions on Information Theory*, vol. 47, pp. 1989–1998, July 2001.

[33] O. Kaya and S. Ulukus, "Jointly optimal power and signature sequence allocation for fading CDMA," in *Proc. IEEE Global Telecommunications Conference GLOBECOM '03*, (San Francisco, USA), pp. 1872–1876, Dec. 2003.

[34] L. Gao and T. F. Wong, "Power control and spreading sequence allocation in a CDMA forward link," *IEEE Transactions on Information Theory*, vol. 51, pp. 1407–1413, Aug. 2004.

[35] P. Viswanath and V. Anantharam, "Optimal sequences and sum capacity of synchronous CDMA systems," *IEEE Transactions on Information Theory*, vol. 45, pp. 1984 – 1991, Sept. 1999.

[36] G. S. Rajappan and M. L. Honig, "Signature sequence adaptation for DS-CDMA with multipath," *IEEE Journal on Selected Areas in Communications*, vol. 20, pp. 384–395, Feb. 2002.

[37] T. M. Lok and T. F. Wong, "Transmitter and receiver optimization in multicarrier CDMA sytems," *IEEE Transactions on Communications*, vol. 48, pp. 1197–1207, July 2000.

[38] B. Natarajan, *Carrier Interferometry for Next Generation CDMA and TDMA Wireless Systems: A Multicarrier Framework.* PhD thesis, Colorado State University, 2002.

[39] J. G. Andrews and T. H. Y. Meng, "Performance of multicarrier CDMA with succesive interference cancellation in a multipath fading channel," *IEEE Transactions on Communications*, vol. 52, pp. 811–822, May 2004.

[40] J. Jang and K. B. Lee, "Effect of frequency offset on MC/CDMA system performance," *IEEE Communications Letters*, vol. 3, pp. 196–198, July 1999.

[41] M. Abdel-Hafez, Z. Li, and M. Latva-aho, "On frequency domain equalization for MC-CDMA in Nakagami fading channels," *EUROPEAN Transactions on Telecommunications*, vol. 15, pp. 7–13, 2004.

[42] S. L. Miller and B. J. Rainbolt, "MMSE detection of multicarrier CDMA," *IEEE Journal on Selected Areas in Communications*, vol. 18, pp. 2356–2362, Nov. 2000.

[43] S. Verdu, *Multiuser Detection.* Cambridge University Press, 1 ed., 1998.

[44] R. A. Horn and C. R. Johnson, *Matrix Analysis.* Cambridge, UK: Cambridge University Press, 1999.

[45] Y. Pan, K. Letaief, and Z. Caott, "MIMO/OFDM with adaptive interleaved beamforming and power allocation for high-capacity wireless access," in *Proc. IEEE Vehicular Technology Conference VTC'04*, pp. 1906–1910, 2004.

[46] B. Natarajan and C. R. Nassar, "Crest factor reduction in MC-CDMA employing carrier interferometry codes," *EURASIP Journal on Wireless Communications and Networking*, vol. 2, pp. 374–379, 2004.

[47] B. M. Popović, "Synthesis of power efficient multitone signals with flat amplitude spectrum," *IEEE Transactions on Communications*, vol. 39, pp. 1031–1033, July 1991.

[48] E. V. D. Ouderaa, J. Schoukens, and J. Renneboog, "Peak factor minimization of input and output signals of linear systems," *IEEE Transactions on Instrumentation and Measurments*, vol. 37, pp. 207–212, June 1988.

[49] G. Wunder and K. G. Paterson, "Crest-factor analysis of carrier interferometry MC-CDMA and OFDM systems," in *International Symposium on Information Theory*, (Chicago, USA), July 2004.

[50] M. R. Schroeder, "Synthesis of low-peak-factor signals and binary sequences with low autocorrelation," *IEEE Transactions on Information Theory*, vol. 16, pp. 85–89, 1970.

[51] E. A. Lee and D. G. Messerschmitt, *Digital Communications.* Boston, MA: Kluwer Academic, 2 ed., 1994.

[52] L. Gao and T. F. Wong, "Power control and spreading sequence allocation in a CDMA forward link," *IEEE Transactions on Information Theory*, vol. 50, pp. 105–124, Jan. 2004.

[53] A. W. Marshall and I. Olkin, *Inequalities: Theory of Majorization and Its Applications.* New York, USA: Academic Press Inc., 1 ed., 1979.